Odoribacter splanchnicus mitigates *Salmonella*-induced gut inflammation and its associated pathogenesis via its secreted bacteriocin

Dipasree Hajra[1], Debapriya Mukherjee [1#], Rhea Vij [1#], Raju S Rajmani [2], Venkatareddy Dadireddy[3], Deepakash Das[4], Tanweer Hussain[4], Mahipal Ganji[3], Utpal Tatu [3], Chakravortty D [1,5 *]

[1]Department of Microbiology and Cell Biology, Indian Institute of Science

[2]Centre of Infectious Disease Research, Indian Institute of Science, Bangalore, India

[3]Department of Biochemistry, Indian Institute of Science, Bangalore, India

[4]Department of Developmental Biology and Genetics, Indian Institute of Science, Bangalore, India

[5]Adjunct Faculty, School of Biology, Indian Institute of Science Education and Research, Thiruvananthapuram

*Corresponding author: Prof. Dipshikha Chakravortty

#Equal Contribution

Email: dipa@iisc.ac.in

Tel. No. 0091 80 22932842

Abstract

Foodborne pathogens pose a major global health hazard, worsened by drug-resistant strains. Therefore, designing novel therapeutic strategies is crucial. Here, we identified the protective role of gut-commensal *Odoribacter splanchnicus* (OS) against *Salmonella* in mice by promoting colonization resistance, preserving gut barrier integrity, and preventing acute inflammation and biofilm formation. *In vitro,* both live *O. splanchnicus* (OS) and their culture supernatant inhibited *Salmonella* biofilm formation, intracellular proliferation in human intestinal cells, and virulence gene expression. Further, our results depicted that OS's protective role acts over a broad spectrum as it confers protection against Gram-positive, *Listeria*

monocytogenes and Gram-negative, *Salmonella* Typhimurium. Notably, OS conferred protection even when administered post-infection in mice, highlighting its therapeutic potential. Using several biochemical and proteomics approaches, we characterized key OS-secreted molecules that limit intracellular *Salmonella* and *Listeria* replication in human intestinal epithelial cells by regulating key virulence effectors and flagella. Collectively, our study establishes OS as the broad-spectrum protective agent against *Salmonella* and *Listeria* infections, with promising therapeutic potential.

Keywords: *Salmonella* pathogenesis, **Gut vascular barrier permeability**, **inflammation**, **inter-species bacterial regulation**, ***Listeria***, ***Odoribacter splanchnicus***, **gut commensal**, **biofilm, flagella**

Teaser

***O. splanchnicus* as an antidote to foodborne bacterial infections**

Main Text

Introduction

The existence of the gut vascular barrier (GVB) acts as a protective barrier against the entry of microorganisms into systemic blood circulation (1, 2). Enteric pathogens such as *Salmonella enterica* can cross the mucus and intestinal epithelial barrier, ultimately leading to GVB damage and systemic dissemination (1). The gut microbiota aids in the maintenance of the intestinal epithelial barrier by the production of several metabolites such as Short-chain fatty acids (SCFAs), indoles, and polyphenol metabolites that contribute to epithelial barrier integrity and turnover by regulating the expression of Tight-junction (TJ) genes (3). Additionally, these SCFAs have the potential to exert anti-inflammatory properties by regulating cytokine production, mucosal immune cell migration, and secretion of antimicrobial peptides (AMPs) by intestinal epithelial cells and macrophages (4-6).

53 Our previous study reported an incidence of increased *Salmonella* dissemination in blood, liver,
54 and spleen upon SIRT1 and SIRT3 inhibition owing to the increased inflammatory response
55 (7, 8). SIRT1, a NAD+-dependent nuclear deacetylase, and the mitochondrial counterpart
56 SIRT3, mediates an immune-metabolic shift in the infected host during *Salmonella* infection
57 progression and maintains a replication niche for the pathogen. In the systemic mice model of
58 *Salmonella* infection, both SIRT1 and SIRT3 have been reported to regulate *Salmonella*
59 dissemination to secondary sites of infection such as the MLN, liver, and spleen via the
60 bloodstream. SIRT1 inhibitor (EX-527) and SIRT3 inhibitor (3TYP)-treated mice cohorts
61 exhibited enhanced bacterial dissemination, and organ loads due to heightened production of
62 inflammatory arsenals such as ROS, IL-1β, and IL-6 (7). Therefore, in this study, we have
63 additionally assessed the effect of OS treatment under SIRT1 and SIRT3 inhibitor-treated
64 conditions to mimic aggravated inflammatory conditions during *Salmonella* infection.

65 *Salmonella* enters the body through the ingestion of contaminated food and water, resisting the
66 acidic stomach pH with acid tolerance response (ATR) genes, and finally reaches the lumen of
67 the small intestine(9). The pathogen gains entry into the non-phagocytic epithelial cells via
68 *Salmonella* Pathogenicity Island-1 (SPI-1) effectors to breach the intestinal barrier (10). Once
69 traversing through the mucosal lining of the gut epithelium, it reaches the lamina propria (10).
70 In the lamina propria, *Salmonella* encounters various host immune cells like neutrophils,
71 macrophages, and dendritic cells. Macrophages, dendritic cells, and neutrophils are responsible
72 for successful dissemination throughout the body through the reticulo-endothelial system
73 (RES) to the secondary organs such as Mesenteric Lymph Node (MLN), liver, and spleen(10).
74 *Salmonella* relies on the SPI-2 secretion for its intracellular and intravacuolar life by injecting
75 various virulence factors into the host cell cytosol (11, 12).

Here, in the present study, we aim to understand whether colonization with the gut commensal, *Odoribacter splanchnicus* (OS) could ameliorate *Salmonella*-induced inflammation and pathogenic dissemination. OS, belonging to the order Bacteroidales, is a common member of the human intestinal microbiota. *Bacteroidetes* is one of the major commensal phyla dominating the healthy mouse as well as the human gut (13). A decrease in *Odoribacter* abundance has been linked to different microbiota-associated diseases, such as non-alcoholic fatty liver disease, cystic fibrosis, and inflammatory bowel disease (IBD)(14). A recent report indicated the ability of OS and its effectors transported in Outer membrane vesicles (OMVs) to exhibit anti-inflammatory effects on the gut epithelium(14). Further, OS has been implicated in conferring resistance against colitis and colorectal cancer(15). This led us to hypothesize that *O. splanchnicus* might ameliorate the inflammatory disease conditions associated with *Salmonella* infection and dissemination.

Our study shows that OS colonization promotes colonization resistance of *Salmonella*, and systemic dissemination even under aggravated inflammatory responses such as SIRT1 or SIRT3-inhibited conditions. OS ameliorates acute *Salmonella*-induced inflammation and its associated pathogenesis by promoting colonization resistance, resulting in decreased *Salmonella* invasion of gut tissue, the preservation of tight junctions, and GVB maintenance. Further, we demonstrate that not only live OS but its culture supernatant inhibits *Salmonella in vitro* biofilm formation, intracellular proliferation in human intestinal cells, and virulence gene expression. Subsequently, our results depict that the specific protective role of OS acts over a broad spectrum as it confers protection against both flagellated Gram-positive, *Listeria monocytogenes* and Gram-negative, *Salmonella* Typhimurium. Furthermore, OS conferred protection even after its administration to mice post-establishment of infection highlighting its therapeutic potential. Subsequently, we identified the key OS-secreted bacteriocin protein responsible for limiting intracellular *Salmonella* and *Listeria* replication in human intestinal

101 cells by regulating virulence genes such as flagella. Overall, our study implicates the broad-
102 spectrum protective role of OS in mitigating foodborne infections caused by *Salmonella* and
103 *Listeria* pathogenesis.

104 **Results**

105 ***O. splanchnicus* hinders *Salmonella* burden and its systemic dissemination**

106 To denote the role of OS in *Salmonella* pathogenesis, we colonized C57BL/6 mice with 10^5
107 CFU of OS 1 day prior to *Salmonella* infection via the oral route and validated the colonization
108 by undertaking OS 16S rRNA qPCR analysis (Fig 1, A-B). OS pre-colonized mice showed
109 decreased susceptibility to *Salmonella* infection in comparison to the non-colonized mice
110 cohort which succumbed to death by day 9 post-infection (p.i.). Contrastingly, 100% of the OS
111 colonized mice were alive even at day 11 post *Salmonella* infection (Fig 1, C). *Salmonella*
112 colonization of the feces and intestinal tissue and dissemination to the MLN, blood, and liver
113 were reduced upon OS pre-colonization (Fig 1, D-K). OS non-colonized mice exhibited
114 increased weight loss percentage upon *Salmonella* infection and OS pre-colonization prevented
115 weight loss (Fig 1, H). Our previous findings revealed increased bacterial dissemination owing
116 to heightened inflammatory responses in the case of SIRT1 and SIRT3 knockdown or inhibitor-
117 treated conditions(7). Therefore, in this study, we intended to examine whether OS could exert
118 its protective role against *Salmonella* infection even in the case of aggravated inflammatory
119 conditions such as in the case of SIRT1 (EX-527) or SIRT3 (3TYP) inhibited conditions. Our
120 result suggests that even in aggravated conditions of inflammation and *Salmonella*
121 dissemination under SIRT1 or SIRT3 inhibitory conditions, OS could prevent *Salmonella*
122 organ burden and dissemination (Fig 1,H-K).

123 ***O. splanchnicus* colonization ameliorate the acute *Salmonella-induced* inflammation and**
124 **its associated pathogenesis**

125 Heightened inflammatory responses facilitate *Salmonella* dissemination in mice(7). Thus, we
126 hypothesized that OS gut colonization might ameliorate the *Salmonella*-induced inflammation.
127 ELISA-mediated IL-6 serum quantification revealed reduced IL-6 production upon *S.*
128 Typhimurium (STM) infection in the OS colonized mice group to the non-colonized cohort
129 (Fig 2, A). The reduced IL-6 production upon OS colonization was even observed in elevated
130 inflammatory conditions of SIRT1 or SIRT3 inhibition. To combat the enteric pathogen
131 challenge, the host employs one of its major defence arsenals, that is, the production of
132 antimicrobial peptides (AMPs)(16, 17). STM infection induces enhanced mRNA expression of
133 AMPs in mice with respect to the uninfected control as per previous literature findings (17).
134 We found that OS colonization in mice resulted in the downregulation of several AMP genes
135 such as Lysozyme-C1 precursor, Angiogenin-4 precursor, CCL20, Beta-defensin-4 and
136 Regenerating-islet-derived 3 beta-precursor (Fig 2, B). Mucus lining serves as another crucial
137 barrier against the entry of enteric pathogens(18). However, enteric pathogens adopt several
138 strategies to circumvent this barrier to reach the underlying epithelium(19). To assess the mucin
139 layer dynamics upon the *Salmonella* challenge, we assessed MUC2 expression in the ileal
140 tissues of OS colonized versus non-colonized mice groups. Our result depicted enriched MUC2
141 expression in the OS non-colonized mice cohort compared to the colonized cohort (Fig.2, C).
142 The increase in the mucus lining upon *Salmonella* infection could be one of the host defense
143 mechanisms to bolster the barrier and exclude pathogens(20). As per previous literature, the
144 rate of mucin production is modulated by several stimuli including inflammatory cytokines
145 (21), vasoactive antimicrobial peptides, and other innate and adaptive immune responses (18).
146 Germ-free mice depict a reduced number of goblet cells, and mucin storage granules(22) as
147 well as reduced expression of AMPs(23). The haematoxylin eosin-stained intestinal sections
148 suggested increased intestinal tissue damage with irregularly organized villi, necrotic
149 submucosa layer, and detached intestinal cells in all the STM-infected non-OS-colonized

150 cohorts. However, OS pre-colonization restored the intestinal tissue architecture in all the mice
151 cohorts (Fig 2, D).

152 ***O. splanchnicus* restricts *Salmonella*-mediated GVB damage by promoting tight junction**
153 **gene expression**

154 *Salmonella* breaches the gut vascular barrier (GVB) by inducing tight junction disruption.
155 *Salmonella* like other food-borne antigens enters into the Mesenteric Lymph Node (MLN) by
156 accessing the lymphatics and subsequently gains entry into the liver via the bloodstream(24).
157 The translocation of the pathogen across the blood endothelial cells is governed by the integrity
158 of the GVB(1). The GVB refers to the endothelial barrier and the microvasculature
159 characterized by the elaborate framework of the junctional complexes (1). The GVB
160 architecture is maintained by several tight junctions and adherens junction proteins that control
161 paracellular trafficking(25, 26). Other cell types associated with the microvasculature of the
162 GVB forming a vascular unit includes pericytes and fibroblasts(27). PV-1 (plasmalemma-
163 vesicle associated protein-1) expression is a marker of GVB damage and heightened PV-1
164 expression denotes EC permeability(28, 29). Our data depict heightened PV-1 marker
165 expression alongside reduced tight junction protein mRNA expression such as *Tjp1* and
166 *Claudin5* upon *Salmonella* infection correlating with the previously observed increased
167 bacterial dissemination in blood and liver (Fig. 3, A-B, Fig. S1, A; Fig. 1 I-K). CD34, an
168 endothelial marker lining the blood vessels (30, 31), is induced upon OS colonization in
169 *Salmonella*-infected mice intestines indicative of intact vasculature (Fig. 3, B-D, Fig.S1, B).
170 On the contrary, OS mice cohorts exhibited reduced CD34 expression in secondary sites of
171 dissemination such as the liver, suggesting toward reduced vasculature (Fig.S1, C). Therefore,
172 OS pre-colonization attenuates the *Salmonella* dissemination by exhibiting reduced PV-1
173 protein expression and promoting tight junction protein expression (Fig. 3, A-D). Angiogenesis
174 is one of the processes that facilitate bacterial dissemination. Previous studies in

175 *Mycobacterium marinum* have shown that transcriptional induction of pro-angiogenic markers
176 like *Vegfa* contributes to increased bacterial burden and dissemination(32). In our study, OS
177 pre-colonization in the gut resulted in reduced expression of the pro-angiogenic *Vegfa* in the
178 infected liver tissues, which coincided with the reduced *S*. Typhimurium burden in the
179 bloodstream and liver (Fig S1, D). Together, our results depict the ability of OS to suppress
180 angiogenesis. OS could exert its angiogenesis inhibitory effects even in instances of aggravated
181 dissemination conditions like in the case of SIRT1 and SIRT3 inhibitor treatment in mice.
182 Previous literature suggested reduced expression of *Axin2,* a β catenin target gene, upon
183 wildtype *Salmonella* infection, even after Wnt3a stimulation suggesting that *Salmonella* affects
184 the GVB by inhibiting canonical Wnt signalling (1). Here, our results suggest that OS pre-
185 colonization restores the *Salmonella*-triggered attenuated Wnt signalling response with
186 increased Axin2 expression in the *Salmonella*-infected intestinal tissues (Fig. S1, E). The
187 integrity of the infected mice gut was estimated by the gut permeability assay using FITC-
188 Dextran (Fig. 3, E). Our results indicate increased gut vascular permeability upon *Salmonella*
189 challenge which declined upon OS pre-colonisation, implicating the ability of OS to prevent
190 gut barrier disruption.

191 **_O. splanchnicus_ culture supernatant restricts _Salmonella_ biofilm formation and**
192 **intracellular proliferation in human intestinal cells**

193 To delineate the mechanism behind the protective role of OS against *Salmonella* pathogenesis,
194 we performed *Salmonella* infection studies in human intestinal epithelial cell line Caco-2 in
195 the presence of OS. The intracellular survival assay suggested decreased STM invasion and
196 subsequently attenuated intracellular replication within the infected Caco-2 cells upon co-
197 infection with live OS and in the presence of OS culture supernatant (Fig 4, A-B). However,
198 STM co-infection with fixed OS showed percent invasion and intracellular replication like that
199 of STM infection (Fig 4, A-B). Together, these results hinted at the presence of some secreted

200 inhibitory components in the OS culture supernatant that has the propensity to limit STM
201 infection. The reduced invasion and proliferation of STM within Caco-2 cells in presence of
202 OS was subsequently validated in immunofluorescence studies, wherein STM showed a
203 significant reduction in invasion at 2hr p.i. and intracellular proliferation at 16hr p.i. in case of
204 OS co-infection (Fig 4, C-D). Similar results were obtained upon infection with the human-
205 restricted serovar *S.* Typhi (STY) to the Caco-2 cells wherein OS and its supernatant attenuated
206 STY invasion and intracellular replication (Fig. 4, E-F). Further, we assessed the *in vitro* growth
207 of the STM in co-culture conditions with OS or in the presence of OS culture supernatant in
208 anaerobic conditions to mimic the microaerophilic or hypoxic environment of the gut or in
209 aerobic culture conditions. We observed no significant delay *in vitro* growth of STM at its
210 initial lag to log phase of its growth in the presence of OS supernatant or with live OS under
211 anaerobic culture conditions (Fig S2, A-B). In aerobic growth conditions as well, *Salmonella*
212 growth remained unperturbed even in the presence of OS or its culture supernatant (Fig S2, C-
213 D). Several previous studies have corroborated the ability of commensal bacterial culture
214 supernatants to inhibit colonization and the biofilm formation of several pathogens. For
215 instance, a commensal bacterium, *Staphylococcus epidermis*, could inhibit biofilm formation
216 and nasal colonization of its pathogenic counterpart, *Staphylococcus aureus* (33). Moreover,
217 biofilm formation is also regulated at the interspecies level. Indole is an inter-species biofilm
218 regulator that decreases *E. coli* biofilm formation and facilitates biofilm formation of
219 pseudomonads (34). STM forms biofilm to colonize the host, evade host defence arsenals and
220 antibiotics, persist during chronic infections, and transmit to new hosts (35, 36). We, therefore,
221 examined the biofilm pellicle strength and biofilm formation of STM via crystal violet staining
222 on the solid-liquid interface in the presence or absence of live, PFA-fixed-OS or OS culture
223 supernatant by inoculating STM in biofilm-inducing media with low salinity. STM exhibited
224 biofilm formation defect in the presence of live OS or OS supernatant (Fig 4, G). However, the

225 STM biofilm inhibitory property of OS was diminished upon treatment with paraformaldehyde
226 (PFA)-fixed OS (Fig 4, G). Further, qPCR-mediated gene expression studies of *Salmonella*
227 biofilm genes revealed decreased expression of genes regulating biofilm (*csgD*, *csgA*, *bapA*)
228 under treatment with live OS or its culture supernatant (Fig.4, H-J). Flagella-mediated
229 attachment and several virulence factors such as SPI-1 and SPI-2 genes are responsible for
230 *Salmonella* pathogenesis and its biofilm formation (37-39). Therefore, we evaluated a few of
231 the *Salmonella* flagellar and SPI-1 and SPI-2 gene expression in the presence or absence of OS
232 or its culture supernatant via quantitative real-time PCR. Our results depicted attenuated
233 expression of flagellar gene (*fliC*), SPI-1 (*sipC*) and SPI-2 (*pipB2*) genes both in the presence
234 of live OS and its spent media but not in presence of PFA fixed-OS (Fig. 4, K-M). The loss in
235 *Salmonella* flagellar motility was further validated via TEM imaging wherein OS or its
236 supernatant reduced the flagella formation of *Salmonella* considerably (Fig.4, N). Together,
237 our results implicate the ability of OS to inhibit STM biofilm formation via active secretion of
238 certain inhibitory molecules in the supernatant.

239 ***O. splanchnicus* inhibitory effect on *Salmonella* is specific as *Enterococcus faecalis*,**
240 **another gut resident microbe, fail to inhibit *Salmonella* intracellular proliferation or**
241 **biofilm formation**

242 The resident gut microbes provide colonization resistance against invading pathogens by
243 deploying several mechanisms, including the production of inhibitory molecules, nutrient
244 competition, maintenance of the intestinal epithelial integrity, immune activation, and via the
245 deployment of bacteriophages (40, 41). To understand whether our observed inhibitory trait of
246 OS against *Salmonella* is due to a common colonization restriction phenomenon of gut
247 microbes via competitive inhibition, or it is a specific phenomenon, we evaluated the role of
248 another gut resident microbe, *Enterococcus faecalis* on *Salmonella* intracellular replication in
249 human intestinal epithelial cells and *Salmonella* biofilm formation. *Enterococcus sp.* belong to

250 the phylum of Firmicutes in the family Enterococcaceae. Approximately, 10^6-10^7 *Enterococcus*
251 *sp*. reside in the human intestine with major abundance of *E. faecalis* (10^5-10^7 CFU/gm feces)
252 and *E. faecium* (10^4-10^5/gm feces) (42). *E. faecalis*, *E. faecium*, *Bifidobacterium sp*.
253 *Lactobacillus sp.,* and *E. coli* colonize the gut of healthy breastfed infants during the initial 7-
254 10 days post birth (43). Our intracellular survival assay data showed no defect in *Salmonella*
255 invasion or intracellular replication capability in Caco-2 cells in presence or absence of *E.*
256 *faecalis*, its culture supernatant or PFA-fixed *E. faecalis* (Fig. S3, A-B). Moreover, *E. faecalis*
257 or its *E. faecalis* supernatant did not inhibit *Salmonella* biofilm formation (Fig. S3, C).
258 Together, our results suggest the inability of *E. faecalis* to inhibit *Salmonella* invasion,
259 intracellular proliferation or its *in vitro* biofilm formation, thereby highlighting the specificity
260 of OS in restricting *Salmonella* pathogenesis.

261 ***O. splanchnicus* confers protection against another foodborne pathogen *Listeria***
262 ***monocytogenes***

263 To understand whether OS exerts a common broad-spectrum protection or colonization
264 resistance against other foodborne pathogens such as *Listeria monocytogenes*, we orally
265 infected 6-8-week-old C57Bl/6 mice with 10^8 CFU of *L. monocytogenes* (LM) 1 day post
266 colonization with 10^5 CFU of *O. splanchnicus* for organ burden evaluation via oral gavage. For
267 survival study, mice were orally gavaged with 10^9 CFU of *L. monocytogenes*. OS-colonized
268 mice exhibited increased survival rates upon LM challenge compared to the non-colonized
269 mice cohort (Fig. 5, A). In line with the survival data, the increased bacterial burden was
270 observed in the blood, feces, intestinal tissue, MLN, spleen and liver alongside enhanced
271 percent loss in mice body weight in the case of *Listeria* infection in non-colonized mice group
272 with respect to OS-precolonized- mice group (Fig. 5, B-J). In a similar line to *Salmonella*
273 infection, OS mitigated host antimicrobial response with reduced expression of antimicrobial
274 peptide transcripts and Muc2 production during LM infection amounting to reduced intestinal

275 tissue damage. Further, OS promoted tight junction functions during *Listeria* infection with
276 reduced expression of GVB damage marker, *PV-1* and angiogenesis marker, *Vegf* expression
277 (Fig. S4, A-E). Moreover, OS colonization could restrict the *in vivo Salmonella* and *Listeria*
278 biofilm within the spleens of the infected mice cohorts as opposed to the non-colonized mice
279 cohorts (Fig.S4, F-G). We estimated the biofilm or the communities of bacterial cells within
280 the spleen tissue via Calcofluor white staining (44). Calcofluor white stains the biofilm matrix
281 or extracellular polymeric substances (EPS) comprised of cellulose (44, 45) and
282 exopolysaccharides that help in the adherence of the bacterial cells. This is the first study
283 demonstrating biofilm-like bacterial colonies of *Salmonella* or *Listeria* secreting EPS in
284 spleens. Like *Salmonella*, *in vitro* culture of *Listeria* with OS or its culture supernatant led to a
285 loss in flagella as evidenced via the TEM imaging (Fig.S4, H). Since flagella is one of the
286 factors facilitating biofilm formation and invasion, OS could inhibit both *Salmonella* and
287 *Listeria* colonisation and biofilm formation. Similar to *Salmonella* infection, OS colonization
288 enhanced CD34 expression in *Listeria*-infected mice intestines and reduced CD34 expression
289 in the *Listeria*-infected liver (Fig. S4, I-J). Further, LM exhibited attenuated intracellular
290 proliferation within human intestinal Caco-2 cells upon live OS or OS supernatant treatment
291 (Fig. 6). Altogether, this result hints at the potency of OS to act broadly against Gram-positive
292 and Gram-negative bacteria.

293 **The protective role of *O. splanchnicus* against *Salmonella* Typhimurium and *Listeria***
294 ***monocytogenes* persists even on administration post-establishment of infection**

295 Next, we sought to examine whether the protective role of OS against *Salmonella* and *Listeria*
296 is sustained when the infection has been fully developed and whether it can serve as a treatment
297 regimen against foodborne diseases. Our results indicate the protective ability of OS against
298 both foodborne pathogens in their intestinal phase of infection when administered at 1-day
299 post-infection (dpi) as depicted by lower pathogen loads in all the organs and blood along with

300 reduced percent weight loss at 5th-day post-*Salmonella* or *Listeria* challenge in the OS-
301 administered (1-dpi) cohort when compared to the untreated cohorts (Fig. 7,A-K, Fig. S5, A-
302 C). Although the protective ability of OS persists even upon establishment of infection when
303 administered at 3rd-day post-*Salmonella* or *Listeria* challenge as indicated by reduced organ
304 loads and percent weight loss in the OS-colonized cohorts, the extent of protection is lower
305 compared to its administration at 1-dpi (Fig. 7, L-W, Fig. S5, D-S), Further, the OS challenge
306 at 1-dpi reduced the mice's susceptibility to the *Salmonella* and *Listeria* challenge(Fig. 7, L,R).
307 However, administration of OS at 3-dpi delayed the death of the *Salmonella* and *Listeria*-
308 infected mice cohorts by 1 day (Fig. 7, L,R). In line with the survival and organ burden data,
309 OS treatment at both 1st and 3rd dpi reduced both *Salmonella* and *Listeria*-induced GVB
310 damage with reduced PV-1 expression, mucin, AMPs, and *Vegf* expression, alongside
311 promoting tight junction protein (*Tjp1* and *Claudin5*) and *Axin2* expression (Fig. S5, D-M).
312 However, OS administration at 3-dpi conferred less protection than at 1-dpi as indicated by the
313 protein expression profiles of Muc2, PV-1, and tight junction protein ZO-1 (Fig. S5, R-S).
314 Moreover, the hematoxylin- eosin-stained intestinal sections revealed reduced intestinal tissue
315 damage with restoration in the villi architecture in the 1- and 3-dpi OS-administered mice
316 cohorts compared to the non-OS-treated groups (Fig.7, X).

317 Moreover, OS colonization could restrict the *in vivo Salmonella* and *Listeria* biofilm within the
318 spleens of the infected mice cohorts as opposed to the non-colonized mice cohorts both when
319 administered at 1-day and 3-day post-pathogen challenge. (Fig.7, Y-Z). Additionally, OS
320 colonization mitigated gut vascular permeability during *Salmonella* and *Listeria* challenges as
321 indicated by reduced FITC-dextran fluorescence units in the plasma both upon pre or post-OS
322 colonization (Fig. S5, T).

323 Furthermore, OS alleviated *Salmonella*-induced intestinal inflammation with reduced IL-1β
324 production in the infected intestinal tissues both upon pre-colonization and post-colonization
325 at 1-dpi (Fig. S6).

326 **Characterization of the inhibitory active molecule within *O. splanchnicus* culture**
327 **supernatant**

328 Our results suggested that not only live OS but also its spent culture supernatant could inhibit
329 *Salmonella* invasion and intracellular proliferation in intestinal human epithelial cells.
330 Moreover, the OS and its supernatant could inhibit STM biofilm formation *in vitro.* This
331 inhibitory effect disappeared upon co-culture with paraformaldehyde-fixed-OS indicating the
332 presumable role of certain inhibitory microbial products secreted by metabolically live OS. To
333 delineate the nature of the secreted molecule/s, we subjected the supernatant to various
334 conditions such as high temperature, divalent cationic chelator, EDTA, and protease (proteinase
335 K), and subsequently assessed the biofilm formation (Fig. 8, A-C). Our biofilm assay suggested
336 that the active molecule is resistant to EDTA treatment and is stable at higher temperatures
337 (Fig. 8, A-B). Nevertheless, the active molecules within the fraction were sensitive to the
338 proteinase K treatment, suggesting the possibility of being protein in nature (Fig. 8, C). SDS-
339 PAGE of the OS supernatant revealed the size of the differential proteins with respect to the
340 media control ranged below 65kDa. (Fig. 8, D). Concentration-dependent estimation of the
341 biofilm activity of the supernatant revealed that the active molecules retain their activity at a
342 minimal concentration of 0.4% v/v (Fig. 8, E). We further fractionated the supernatant using
343 an Amicon 3k MWCO and 10k MWCO ultra filter device (Fig. 8, F-G). We found that the
344 active molecule/s is/ are higher than 3kDa cut-off range eliminating the role of small molecules
345 and ions (Fig. 8, F-G). A summary of the conditions tested for active molecule characterisation
346 and their effective outcome has been summarized in Fig. 8, H. Subsequently, we subjected the
347 culture supernatant to gel filtration chromatography (Fig. S7, A). Out of all the fractions tested,

348 around 24 fractions showed a biofilm inhibitory role. These 24 fractions were further subjected
349 to a titration experiment to zero down upon the three fractions with the highest inhibitory
350 activity (A82,A83,A84) (S7, B-D). The gel filtration standard curve run suggested that the
351 active molecules fall in the size range of <60kDa and >3kDa (Fig. S7, A). These three fractions
352 along with the total concentrated supernatant (serving as positive control) and fractions with
353 no or least inhibitory activity (serving as negative control-A31,B12) were ultimately subjected
354 to Reverse Phase LC-MS mass spectrometry. Upon analysis of the proteomics dataset (Fig. S7,
355 E), we obtained 364 proteins showing enrichment in the positive fractions. Among the 364
356 proteins, 74 proteins exhibited known or predicted function as per UniProt and STRING
357 database and 11 proteins were linked to antibacterial, bacteriostatic, flagella, and biofilm
358 regulation based on data curation and literature survey (Table-S1). We selected bacteriocin
359 proteins exhibiting direct association with antibacterial activity for further analysis. These
360 proteins include bacteriocins (A0A412WSU3 and A0A412WSS0) which are antimicrobial
361 peptides that can kill or inhibit closely related or unrelated bacterial strains(46, 47). We purified
362 the bacteriocins via ammonium sulphate precipitation followed by gel filtration
363 chromatography to obtain a single fraction comprising of bacteriocins with close-range
364 molecular weight (6.6 kDa and 7.156kDa, respectively) (Fig. S8).

365 ***O. splanchnicus*-derived purified peptide, bacteriocin, limits both *Salmonella* and *Listeria***
366 **pathogenesis *in vitro***

367 Treatment of the Caco-2 cells with the purified bacteriocin inhibited STM, STY, and LM
368 invasion and fold proliferation without compromising host-cell viability (Fig. 9, A-D).
369 Additionally, the purified bacteriocin treatment inhibited STM biofilm formation in a dose-
370 dependent manner alongside reduced transcript level expression of *Salmonella* biofilm
371 regulatory genes (Fig. S9, A-D). Moreover, bacteriocin treatment (10µg/ml) attenuated
372 *Salmonella* virulence gene expression such as SPI-1 gene- *sipC*, SPI-2 gene-*pipB2,* and

373 flagellar gene *fliC* (Fig. S9, E-G). Subsequently, TEM imaging revealed a complete loss of
374 *Listeria* flagella upon treatment with the OS-derived bacteriocin in contrast to *Salmonella*
375 which retained few flagella even on bacteriocin treatment (Fig. 9, E-H). Furthermore, the
376 motility assay demonstrated a significant swimming defect of *Listeria* and *Salmonella* upon
377 treatment with either OS supernatant or bacteriocin to the untreated control (Fig. 9, I-J).
378 Overall, our study depicts the novel role of OS-derived bacteriocin in limiting *Salmonella* and
379 *Listeria* invasion and pathogenesis by regulating virulence effectors such as SPI-1, SPI-2
380 genes, biofilm regulatory genes, and flagella.

381 **DISCUSSION**

382 *Salmonella* gains access to the systemic sites by traversing the gut intestinal barrier via utilizing
383 several routes. Its primary site of entry is the distal ileum wherein it induces the SPI-1 Type
384 Three Secretion System (T3SS) effector proteins to facilitate its uptake. After its initial entry
385 into the enterocytes and M-cells overlying the Peyer's patches, *Salmonella* colonizes the
386 draining MLN and eventually disseminates to the liver and spleen via the circulating
387 lymphatics and the bloodstream (48). *Salmonella* uptake by M cells facilitates its stealthy entry
388 via avoidance of the mucus barrier. Additionally, the presence of flagella allows them to propel
389 through the viscous mucus and activate the immune responses(18). The onset of systemic
390 dissemination coincides with GVB disruption and loss of tight-junction protein expression (1).
391 Several reports have suggested the protective role of gut commensals in maintaining gut
392 epithelial health against food-borne pathogen insults. *E. coli* provide colonization resistance
393 against STM in the presence of a specific microbial consortium by limiting galactitol wherein
394 *Lachnospiraceae* consume the free sugar, conferring colonization resistance (49). Moreover,
395 *E. coli* contribute to colonization resistance by competing with *S.* Enteritidis for aerobic
396 respiration (50). Similarly, the commensal *Klebsiella michiganensis* retention or transmission
397 provided colonization resistance to Enterobacteriaceae by exhibiting nutrient competition (51).

398 In this study, we report the broad-spectrum protective role of the gut commensal of
399 bacteroidales order *O. splanchnicus* that limits *Salmonella* and *Listeria* invasion, pathogenesis,
400 and systemic dissemination by promoting colonization resistance and regulating virulence
401 effectors such as SPI-1, SPI-2, flagella, and biofilm regulatory genes. Additionally, not only
402 OS but its culture supernatant could exert its inhibitory effect on *Salmonella* invasion and
403 intracellular proliferation in intestinal human epithelial cells. Moreover, the OS and its
404 supernatant could inhibit STM biofilm formation by regulating flagella formation. This STM
405 biofilm inhibitory effect was however lost upon co-culture with paraformaldehyde-fixed-OS
406 indicating the presumable role of certain inhibitory microbial products secreted by
407 metabolically live OS. Further, our studies identified OS-produced bacteriocins responsible for
408 restricting intracellular replication of *Salmonella* and *Listeria* in intestinal epithelial cells by
409 regulating bacterial virulence arsenals such as biofilm regulatory genes, SPI-1, SPI-2 genes,
410 and flagellar machinery. However, the presence of flagella on *Salmonella* post bacteriocin
411 treatment hints towards the possibility of other secreted accessory molecules within the OS
412 supernatant and warrants future research. Due to the proteinaceous nature of the bacteriocin,
413 oral administration experiments in mice were aborted. Previous studies have suggested that
414 bacteriocin expression by commensal bacteria can influence gut niche competition and
415 bacteriocin delivery can serve as an effective therapeutic strategy to eliminate colonization of
416 multi-drug resistant bacteria in the gastrointestinal tract without disrupting the indigenous
417 microbiota (52, 53). Several studies have highlighted the role of commensal-produced
418 bacteriocins. Bacteriocin-producing *Streptococcus salivarius* has been shown to effectively
419 target the CRC-causing pathogen *Fusobacterium nucleatum* in a model of the human distal
420 colon(54). *Lactobacillus plantarum* bacteriocin has been linked to intestinal and systemic
421 improvements in diet-induced obese mice and confers epithelial barrier integrity (55). Further

422 studies show that a class IIa bacteriocin, Pediocin PA-1, has an anti-bacterial effect against *L.*
423 *monocytogenes* (56).

424 This study provides evidence about inter-species regulation of gut colonization in maintaining
425 gut homeostasis and protecting against several invading foodborne pathogens. Moreover, the
426 long-term protective ability conferred by OS during pre-or post-infection colonization to mice
427 against broad-spectrum foodborne pathogens such as *Salmonella* and *Listeria* highlights its
428 therapeutic potential as a prebiotic for prophylaxis or post-infection treatment option, paving
429 the way for future therapeutic interventions to thwart food-borne infections.

430 **Materials and Methods**

431 **Bacterial Strains and Culture Conditions**

432 *Salmonella* enterica serovar Typhimurium (STM) strain ATCC 14028S, STM ATCC 14028S
433 constitutively expressing mCherry (pFPV25.1-mCherry-Amp^R, RFP), laboratory stock of
434 *Enterococcus faecalis* MTCC 439 (Ef), *Listeria monocytogenes* MTCC 657 (LM) expressing
435 mCherry and *Odoribacter splanchnicus* (OS) strain NCTC 10825 [1651/6] from ATCC were
436 used in this study. 4% paraformaldehyde-fixed-OS was used as killed bacteria control. The
437 STM, LM, and Ef bacterial strain was grown overnight in LB broth at 37 ^{0}C under 160 rpm
438 shaking conditions. OS was cultured in anaerobic condition in tryptic soy broth at 37ºC for 48-
439 72h after its revival from glycerol stock.

440 **Preparation of Cell-free Bacterial Culture Supernatant**

441 The overnight grown OS culture in tryptic soy broth was centrifuged at 10,000rpm for 10 min
442 and the supernatant was harvested. The collected supernatant was further subjected to another
443 two rounds to centrifugation to remove any residual cells. The supernatant was subsequently
444 filtered using a 0.2 µm filter and stored at − 20˚C.

445 **Animal Experiments**

446 The animal experiments were conducted in accordance with the approved guidelines of the
447 institutional animal ethics committee at the Indian Institute of Science, Bangalore, India
448 (Registration No: 48/GO/ReRcBiBt-S/Re-L/99/CPCSEA). All procedures involving the use of
449 animals were performed according to the Institutional Animal Ethics Committee (IAEC)-
450 approved protocol (CAF/Ethics/853/2021). 6–8 weeks old adult C57BL/6 male mice were used
451 in this study (bred, housed, and provided (purchased) by Central Animal Facility, Indian
452 Institute of Science, Bangalore). After one day of OS colonization (10^5 CFU/mice via oral
453 gavage), the mice were infected with 10^6 (organ burden) CFU or 10^8 CFU (for assessing
454 survival) of *S.* Typhimurium, and 10^8 (organ burden) or 10^9 (survival) CFU of *L.*
455 *monocytogenes* via oral gavage. The colonization of *O. splanchnicus* was confirmed via RT-
456 qPCR mediated quantitation of OS 16S rRNA from the mice fecal (3 fecal pellets harvested
457 from the intestine and resuspended in Trizol) and ileal samples at 6th day post-OS colonization.
458 Infected mice were subjected to intraperitoneal injection of either 1 mg/kg body weight of
459 SIRT1 inhibitor EX-527 (Sigma-Aldrich), or SIRT3 inhibitor 3TYP (Selleck Chemical) or
460 vehicle control alone on every alternate day. For post-infection OS administration studies, OS
461 was orally administered (10^5 CFU/ mice) post 1 or 3dpi. 5-day post-infection, mice were
462 euthanized, dissected out, and blood and organs were harvested. The bacterial organ load was
463 enumerated by plating the tissue homogenates on *Salmonella-Shigella* (SS) agar plates for
464 *Salmonella* or LB plates containing 50µg/ml of Ampicillin for LM. The harvested tissues and
465 the fecal samples were collected in protein lysis buffer and TRIzol (Takara) for protein and
466 RNA extraction respectively and were stored at -80ºC. For calculating percentage survival, the
467 infected mice cohorts were monitored till fatality and fatalities were reported.

468 **Blood collection and serum preparation**

469 Blood collection was performed on the 5th day post-infection via cardiac puncture post-
470 euthanization of the mouse. The collected blood was allowed to clot by incubating the vials at
471 room temperature for 45 minutes. After allowing the standing time of 45 mins, centrifugation
472 was performed at 2000g for 15 minutes in a refrigerated centrifuge. Following the
473 centrifugation, the clear, yellowish supernatant was transferred to an autoclaved microfuge tube
474 and stored at -80ºC till further downstream processing.

475 **ELISA**

476 Cytokines in mice serum were quantified according to the manufacturer's instructions(12, 57).
477 Briefly, 96-well ELISA plates of IL-6 ELISA kit (BD Bioscience- Cat No-555240) were coated
478 overnight with capture antibody at 4°C. Following day, plates were washed with 0.1% Tween-
479 20 containing PBS and blocked with 10% FBS for 1 h. Following blocking, wells were washed
480 and incubated with 50µl of serum samples in duplicates for 2 h at room temperature.
481 Subsequently, plates were washed and incubated with detection antibody and enzyme reagent
482 for 1 h at room temperature (BD Bioscience). TMB (Sigma) was used as a substrate and
483 reactions were stopped with 2 N H_2SO_4.

484 For the estimation of IL-1β, pre-coated ELISA (SARD Biosciences-Cat:SB-EKM1085) plates
485 of IL-1β ELISA kit were used, and ELISA was performed as per the manufacturer's protocol.
486 The ileal tissues were harvested in phosphate-buffered saline solution and homogenized using
487 gentleMACS homogenizer. The homogenized tissue samples were centrifuged to collect cell-
488 free supernatant and the cell-free supernatant was subjected to ELISA for cytokine estimation.

489 Absorbance was measured at 450 nm wavelength in Tecan Plate reader and the concentration
490 of cytokines were interpolated from a standard curve.

491 **Quantitative Real Time PCR**

Total RNA was isolated from the ileal section of the intestinal tissues or feces harvested in TRIzol (Takara) as per manufacturer's protocol. RNA was quantified using Nano Drop (Thermo-Fischer scientific). Integrity of isolated RNA was detected by performing 2% agarose gel electrophoresis. 3 µg of total isolated RNA was subjected to DNaseI (Thermo Fischer Scientific) treatment at 37°C for 1 hr followed by heat inactivation at 75°C in the presence of 5mM concentration of EDTA for 10 mins. The mRNA was reverse transcribed to cDNA using oligo $(dT)_{18}$ primer, random hexamer primer, buffer, dNTPs and reverse transcriptase (Takara) as per manufacturer's protocol. The expression profile of target gene was evaluated using specific primers (Table-S2) by using SYBR green RT-PCR master mix (Takara) in Applied Biosystems (Quantstudio 5) or BioRad Real time PCR instrument. β-actin was used as an internal control for mammalian genes and for bacterial genes 16S rRNA was used. All the reaction was setup in 384 well plate with three replicates for each sample.

Western blotting

The harvested tissue samples were lysed in ice-cold RIPA buffer (50 mM Tris-Cl, pH 8.0, 150 mM NaCl, 5mM EDTA, 1% NP-40, 1 % Sodium deoyxycholate, 1% SDS) containing protease inhibitor cocktail (Roche). Total protein was estimated using Bradford reagent (BioRad). Protein samples were denatured in **Laemmli SDS loading buffer** at 95ºC for 10 min and then subjected to separation on 12% SDS-PAGE gels followed by transfer onto activated 0.45µm PVDF membrane. Finally, the membrane was blocked with 5% skimmed milk in TBST (Tris Buffered Saline containing 0.1% Tween-20) and probed with appropriate primary (Table-S3) and secondary HRP-conjugated antibodies. The blots were developed using ECL substrate (Bio-Rad) using a Chemidoc (BioRad). All densitometric analysis was performed using ImageJ software.

Immunohistochemistry

The harvested tissues were fixed in 4% paraformaldehyde, embedded in paraffin and 5 µm thick paraffin sections were collected on poly-lysine coated glass slides. The sectioned tissue samples were deparaffinized using standard protocol. Briefly, the slides containing the paraffinized tissues were immersed in xylene for 10 minutes and this step was repeated twice. After the xylene treatment, the tissues were subjected to absolute alcohol treatment for 5 minutes twice, followed by 95% and 70% alcohol treatment for 5 minutes. The slides were rinsed in water followed by boiling step in water for 2 minutes and then dried. Primary antibody staining of the deparaffinized sections was performed with specific primary antibody in the presence of a permeabilizing agent, 0.01% saponin (Sigma) dissolved in 2.5% BSA containing PBS at 4°C for overnight. Following wash with PBS, sections were stained with appropriate secondary antibody tagged with fluorochrome for 1 hr at RT. This was followed by DAPI staining and mounting. For in vivo estimation of biofilm, deparaffinized tissue samples were stained with Calcofluor White (Sigma) stain for 20 min at RT. All immunofluorescence images were obtained using Zeiss multi-photon 880 microscope and were analyzed using ZEN black 2012 software.

Haematoxylin and Eosin Staining

The harvested ileal tissues were collected and fixed using 3.5% paraformaldehyde. The fixed liver was then dehydrated using a gradually increasing concentration of ethanol and embedded in paraffin. 5µm sections were collected on coated plates. Sections were further rehydrated and then stained with hematoxylin and eosin. Images were collected in a Leica microscope.

The scoring of the pathological changes is graded as 0-4; for each of the pathological lesions (Severe/ marked -4; Moderate -3; mild -2; Minor/minimum -1; No pathology -0) considering the intestinal inflammation and associated villi injury as described previously (58, 59).

Cell Culture

541 Human colorectal adenocarcinoma cell line Caco-2 were maintained in Dulbecco's Modified
542 Eagle's Media (DMEM) (Lonza) and supplemented with 10% FCS (Fetal calf serum, Gibco)
543 and 1% non-essential amino acid solution (Sigma Aldrich) at 37ºC temperature in the presence
544 of 5% CO_2 in humidified incubator. Prior to each experiment, cells were seeded into 24 well
545 or 6 well plate as per requirement at a confluency of 60%.

546 **Intracellular proliferation or gentamicin protection assay**

547 Caco-2 epithelial were infected with 3 to 4 h old log phase *S*. Typhimurium (STM) or *Listeria*
548 *monocytogenes* (LM) or *S.* Typhi (STY) bacterial culture, STM (or LM or STY) with *O.*
549 *splanchnicus*, STM (or LM or STY) in presence of *O. splanchnicus* supernatant and STM along
550 with PFA-fixed OS at an MOI of 10. For attachment of bacteria to the cells, tissue culture plates
551 were subjected to centrifugation at 600xg for 5 min and incubated at 37 ^{0}C humified incubator
552 with 5% CO_2 for 25 min. Following infection of the cells with STM at an MOI of 10, cells were
553 treated with DMEM (Sigma) + 10% FBS (Gibco) containing 100 µg/ml gentamicin for 1 hr.
554 Subsequently, the gentamicin concentration was reduced to 25 µg/ml and maintained until the
555 specified time point. Post 2hr and 16hr post-infection, cells were lysed in 0.1% triton-X-100.
556 Lysed cells were serially diluted and plated on *Salmonella-Shigella* (SS) or LB agar to obtain
557 colony-forming units (CFU). Percent invasion was determined using the following formula
558 (60, 61):

559 **Percent invasion= [CFU at 2 h]/ [CFU of pre-inoculum] X 100**

560 Fold proliferation was calculated as CFU at 16hr divided by CFU at 2hr.

561 **Fold Proliferation= [CFU at 16h] / [CFU at 2h]**

562 **Immunofluorescence confocal microscopic studies**

At the specified time points post infection with mCherry-tagged STM, or GFP-tagged OS or with both mCherry-STM and GFP-OS, cells were fixed with 3.5% paraformaldehyde for 15 min. Primary antibody staining was performed with specific primary antibody in the presence of a permeabilizing agent, 0.01% saponin (Sigma) dissolved in 2.5% BSA containing PBS at 4°C for overnight or for 6hr at room temperature (RT). Following this, cells were washed with PBS stained with appropriate secondary antibody tagged with fluorochrome for 1 hr at RT. This was followed by DAPI staining and mounting of the coverslip onto a clean glass slide using the mounting media containing the anti-fade agent. The coverslip sides were sealed with a transparent nail paint. All immunofluorescence images were obtained using Zeiss Multiphoton 880 and were analyzed using ZEN black 2012 software.

Growth Curve analysis

For *in vitro* growth curve experiments a single colony of STM and OS was inoculated in 5mL of LB broth singly or in co-culture and grown overnight at 37ºC in anaerobic jar. In another set, STM was inoculated in 5mL of LB in presence of OS supernatant. Overnight-grown stationary phase bacteria were sub-cultured at a ratio of 1: 100 in freshly prepared LB in presence or absence of OS supernatant and kept at 37ºC. At different time intervals, aliquots were taken for measurement of [OD]600nm by TECAN 96 well microplate reader and were plated for CFU enumeration.

Biofilm-inducing growth media and conditions

LB medium lacking NaCl and containing 1% casein enzyme hydrolysate (Hi-Media, India) and 0.5% yeast extract (Hi-Media, India)) was used as biofilm media as per previous literature (38). Overnight grown culture was subcultured in 2 ml biofilm medium at the dilution of 1:100 in a flat-bottom 24-well plate (Tarsons, India) and incubated at 28˚C for 72 h without shaking.

Biofilm inoculation with OS culture supernatant

20 µl of STM overnight culture and indicated volume (1% v/v or as indicated) of the OS culture supernatants were added to 2 ml of biofilm media and incubated under biofilm-promoting conditions(38). For co-culture experiments, the overnight cultures of the STM and OS or STM and PFA-fixed OS were added in a 1:1 ratio to 2 ml of biofilm media and incubated under biofilm-inducing conditions.

Crystal Violet Staining

Post 72 h of biofilm induction, the media was discarded, and the plates were thoroughly washed in water. The plates were dried, and 2 ml of 1% Crystal Violet (CV) was added to each well and incubated for 15 min. Post 15 min incubation, the CV stain was removed, and the plate was thoroughly rinsed in water to remove excess stain. The stained biofilm was destained with 70% ethanol, and the intensity of the colour of the destained solution was quantified at OD_{595} in the Tecan plate reader (Infinite Pro 200) (38).

Glass bead assay

1 mm glass beads were added onto the pellicle to assess the strength of the pellicle at the air-liquid interface. The initial weight of the glass beads was noted. The glass beads were added until the pellicle collapsed, and the final weight was noted down and plotted.

Gut Permeability Assay

The infected mice cohorts were orally administered with FITC Dextran (25mg/kg,FD-4-100MG, Sigma) 4h before euthanization. The blood plasma was collected post-euthanization by cardiac puncture followed by centrifugation. The blood plasma was evaluated for mean fluorescence via plate reader (TECAN) and flow cytometry(CytoFlex, Beckman).

MTT Assay

Post-16h treatment of pre-seeded Caco-2 cells with 10µg/ml of bacteriocin, MTT staining solution (0.5mg/ml) was added to each well followed by incubation at 37ºC CO_2incubator for 4h. 50µl of DMSO was added per well for solubilizing the formazan crystals. Absorbance was measured at 570nm using a plate reader (TECAN).

Transmission electron microscopy

Overnight STM or LM-grown cultures (in the presence or absence of OS supernatant or bacteriocin) were subcultured into fresh media (1:10) ratio and incubated at 37ºC for 6 hours under shaking conditions. These samples were centrifugated at 1000rpm for 10 min to obtain the bacterial pellet. The bacterial pellet was subjected to PBS wash twice via centrifugation at 1000 rpm for 10 min.5 µl of the finally resuspended cell suspension was added on a glow-discharged copper-grid, air dried, stained with 1% uranyl acetate for 30 s, and visualized under a transmission electron microscope (JEM-100 CX II; JEOL).

Supernatant Treatment

The supernatant was treated with 7.5 mM concentrations of EDTA and incubated at 65 ℃ for 1 h. 10 µl of proteinase-K (NEB, stock 20 mg/ml) was added to the 200 µl supernatant and incubated at 37 ℃ for 1 h. The proteinase was inactivated with 0.5 mM PMSF and incubated at 28 ℃ for 1 h. The supernatant was subjected to heating at 37˚C (60 min), 65˚C (15 min) or 95˚C (15 min) and immediately frozen at − 20˚C (38). Post-treatment, the supernatants were used to inoculate the biofilm to test the nature of the biofilm inhibitory molecules.

Supernatant concentration and molecular weight-based separation

4 ml of the supernatants were transferred to the 3k MWCO or 10k MWCO Amicon ultra filter centrifugal device (Amicon® Ultra-4 centrifugal filter device, 3k MWCO, UFC800324;

Amicon® Ultra-4 Centrifugal filter Unit, 10k MWCO, UFC801024) and centrifuged at 4000 g for 30 min in a swing bucket rotor(38). The concentrated solute from the bottom of the filter device and the flowthrough were collected and subjected to biofilm inoculation.

Size Exclusion Chromatography

The bacterial supernatant was concentrated to 0.5ml using 3k MWCO-Amicon-Ultra-4-centrifugal unit and loaded onto the Superdex 200pg size exclusion column (XK16/60, 124mL; Cytiva, USA), pre-equilibrated Tris-Cl buffer (pH-8) containing 100mM NaCl and 20mM Tris-Cl. The sample was eluted with the same buffer at a flow rate of 0.8mL/min, and 1mL fractions were collected. The fractions corresponding to the elution peaks were analyzed for biofilm inhibition activity and subjected to mass spectrometry.

LC/MS analysis of the supernatant fractions

The concentrated gel filtration fractions of supernatants were subjected to in-solution trypsin digestion for LC Q-TOF MS analysis. Briefly, 100 µg of total protein was resuspended in 100 µl of 7-8M of urea buffer. To this, 5 µl 200mM DTT was added and incubated at room temperature for 1 hr, followed by alkylation with 20µl of 200 mM iodoacetamide and incubation at room temperature for 1h in the dark. This was followed by the addition of 1mM of Calcium chloride and incubation at RT for 10 min. For protein digestion, trypsin solution was added to the sample to a final trypsin to protein ratio of 1:30 (w/w) and incubated at 37˚C for 16 h, with frequent shaking. The reaction was stopped by adding 0.1% formic acid to adjust the pH to 3-4. The digested protein samples were desalted using a reverse phase C-18 column (Acclaim prep EASY-Spray (C18-RP)) using mobile phase solvent A-2% acetonitrile and solvent B- 80% acetonitrile. The sample injection volume was 10µl. All the samples were analyzed using Thermo Scientific SII for Xcalibur method. The MS scan was acquired using

Orbitrap detector with 60000 resolution in the positive polarity and scan range (*m/z*) 350-2000. The ion source type was NSI with static voltage; positive ion (V)- 2200V and negative ion (V)- 600 along with temperature settings at 275ºC. This was followed by $ddMS^2$ IT HCD with 30% fragmentation HCD collision energy using ion trap detector. The raw data was analyzed using Proteome Discoverer 2.5 against the *O. splanchnicus* proteome available in UniProt (Proteome ID: UP000006657).

Purification of bacteriocin

O. splanchnicus culture supernatant was concentrated within the range of >3kDa and <10kDa using the Amicon Ultra-4 Centrifugal filter units of 10MWCO and 3MWCO. The concentrated cell-free supernatant containing the bacteriocin (~7kDa) was precipitated by ammonium sulphate (80% to 98%). The precipitate was collected by centrifugation at 12000rpm for 30 min and dissolved in 1X PBS. The dissolved precipitate was again filtrated using the 3KDa cutoff Amicon centrifugal filter units. This concentrated fraction was further subjected to Fast Performance Liquid Chromatography using Superdex 75 Increase 10/300 GL- 24ml volume (GE Healthcare) column. The column was equilibrated with 1X Phosphate Buffered Saline buffer and 0.5ml of concentrated sample (23.6 mg/ml) was injected into the column. Based on the increase in Absorbance units at 280nm from baseline, 0.3ml fractions were collected at a retention volume of 13.3ml to 21.8ml (Fig. S9). The fractions were analyzed by 20% SDS-PAGE electrophoresis and stained with Coomassie staining solution.

***In vitro* swim motility assay**

2 µl ($2*10^6$ CFU/ml) of treated or untreated stationary phase bacterial samples were spotted on the 0.3% agar (LB-STM, BHI-LM) plates supplemented with 0.5% yeast extract, 1% casein

enzyme hydrolysate, 0.5% NaCl, and 0.5% glucose. The plates were incubated at 37˚C and images were taken every 6 h (STM) or 24h (LM) using the camera of Biorad illuminator.

Statistical analysis

Data were analyzed and graphed using the GraphPad Prism 8 software (San Diego, CA). Statistical significance was determined by Student's t-test or One-way ANOVA followed by Dunnett's Multiple Comparisons test to obtain p values. ANOVA was used during comparison among three or more groups whereas Student's t-test was used to compare the difference between two groups. Mann Whitney t-test was used as a non-parametric counterpart of Student t-test when variances differed. The log-rank test also known as Mantel-Cox test is used to compare the survival percentages of the mice groups. Adjusted p-values below 0.05 are considered statistically significant (****$p<0.0001$, *** $p < 0.001$, ** $p<0.01$, * $p<0.05$). The results are expressed as mean ± SD or SEM of three independent experiments.

Acknowledgements

We thank Nikhita Kirthivasan for her support during the commencement of the project.
We also thank our Divisional Mass Spectrometry facility, TEM facility, Departmental Confocal Facility, Divisional Flowcytometry Facility and Central Animal Facility at IISc.

Funding

This work was supported by the DAE SRC fellowship (DAE00195) and DBT-IISc partnership umbrella program for advanced research in biological sciences and Bioengineering to DC.
Infrastructure support from ICMR (Centre for Advanced Study in Molecular Medicine), DST (FIST), UGC (special assistance) and TATA fellowship is highly acknowledged.
DH sincerely acknowledges the CSIR- SPM fellowship for her financial support.
DM and RV are supported by MHRD-GATE and CSIR fellowships respectively.
The funders had no role in study design, data collection and analysis, decision to publish, or preparation of the manuscript.

Author Contribution

Conceptualization: DH, DC

Methodology: DH, DM, RV, VD (Gel Filtration Chromatography), DD (Fast Performance Liquid Chromatography)

Investigation: DH, DM, RV, VD (Gel Filtration Chromatography), DD (Size exclusion chromatography for bacteriocin purification), RSR (Scoring of haemoxylin and eosin-stained samples)
Visualization: DH, DM, RV
Formal analysis: DH
Funding acquisition: DC
Project administration: DH, DC
Supervision: DC, UT (Proteomics), TH (Size Exclusion Chromatography), MG (Size Exclusion Chromatography)
Writing – original draft: DH
Writing – review & editing: DH, DM, RV, RSR, VD, DD, TH, MG, UT, DC

Competing interests Authors declare that they have no competing interests.

Data and materials availability

All data are available in the main text or the supplementary materials.
The article has been submitted to the preprint server (62).

REFERENCES

1. Spadoni I, Zagato E, Bertocchi A, Paolinelli R, Hot E, Di Sabatino A, et al. A gut-vascular barrier controls the systemic dissemination of bacteria. Science (New York, NY). 2015;350(6262):830-4.
2. Brescia P, Rescigno M. The gut vascular barrier: a new player in the gut–liver–brain axis. Trends in Molecular Medicine. 2021;27(9):844-55.
3. Ghosh S, Whitley CS, Haribabu B, Jala VR. Regulation of Intestinal Barrier Function by Microbial Metabolites. Cellular and Molecular Gastroenterology and Hepatology. 2021;11(5):1463-82.
4. Zhao Y, Chen F, Wu W, Sun M, Bilotta AJ, Yao S, et al. GPR43 mediates microbiota metabolite SCFA regulation of antimicrobial peptide expression in intestinal epithelial cells via activation of mTOR and STAT3. Mucosal immunology. 2018;11(3):752-62.
5. Schulthess J, Pandey S, Capitani M, Rue-Albrecht KC, Arnold I, Franchini F, et al. The short chain fatty acid butyrate imprints an antimicrobial program in macrophages. Immunity. 2019;50(2):432-45. e7.
6. Hajra D, Kirthivasan N, Chakravortty D. Symbiotic Synergy from Sponges to Humans: Microflora-Host Harmony Is Crucial for Ensuring Survival and Shielding against Invading Pathogens. ACS infectious diseases. 2024;10(2):317-36.
7. Hajra D, Rajmani RS, Chaudhary AD, Gupta SK, Chakravortty D. Salmonella-induced SIRT1 and SIRT3 are crucial for maintaining the metabolic switch in bacteria and host for successful pathogenesis. eLife Sciences Publications, Ltd; 2024.
8. Hajra D, Rajmani RS, Chaudhary AD, Gupta SK, Chakravortty D. Salmonella-induced SIRT1 and SIRT3 are crucial for maintaining the metabolic switch in bacteria and host for successful pathogenesis. bioRxiv. 2024:2022.11.21.517246.
9. Garcia-del Portillo F, Foster JW, Finlay BB. Role of acid tolerance response genes in Salmonella typhimurium virulence. Infection and immunity. 1993;61(10):4489-92.
10. Haraga A, Ohlson MB, Miller SI. Salmonellae interplay with host cells. Nat Rev Microbiol. 2008;6(1):53-66.
11. Hensel M. Evolution of pathogenicity islands of Salmonella enterica. International journal of medical microbiology : IJMM. 2004;294(2-3):95-102.

12. Hajra D. Understanding the mechanism of host deacetylase SIRT1 and SIRT3 in the modulation of Salmonella pathogenesis. 2024.
13. Wang J, Lang T, Shen J, Dai J, Tian L, Wang X. Core Gut Bacteria Analysis of Healthy Mice. Frontiers in microbiology. 2019;10:887.
14. Hiippala K, Barreto G, Burrello C, Diaz-Basabe A, Suutarinen M, Kainulainen V, et al. Novel Odoribacter splanchnicus Strain and Its Outer Membrane Vesicles Exert Immunoregulatory Effects in vitro. Frontiers in microbiology. 2020;11:575455.
15. Xing C, Wang M, Ajibade AA, Tan P, Fu C, Chen L, et al. Microbiota regulate innate immune signaling and protective immunity against cancer. Cell host & microbe. 2021;29(6):959-74.e7.
16. Balakrishnan A, Schnare M, Chakravortty D. Of men not mice: bactericidal/permeability-increasing protein expressed in human macrophages acts as a phagocytic receptor and modulates entry and replication of Gram-negative bacteria. Frontiers in immunology. 2016;7:455.
17. Chatterjee R, Chowdhury AR, Nair AV, Hajra D, Kar A, Datey A, et al. Salmonella Typhimurium PgtE is an essential arsenal to defend against the host resident antimicrobial peptides. Microbiological research. 2023;271:127351.
18. McGuckin MA, Lindén SK, Sutton P, Florin TH. Mucin dynamics and enteric pathogens. Nature reviews Microbiology. 2011;9(4):265-78.
19. Estimates of the global, regional, and national morbidity, mortality, and aetiologies of lower respiratory infections in 195 countries, 1990-2016: a systematic analysis for the Global Burden of Disease Study 2016. The Lancet Infectious diseases. 2018;18(11):1191-210.
20. Davis CW, Dickey BF. Regulated airway goblet cell mucin secretion. Annual review of physiology. 2008;70:487-512.
21. Enss ML, Cornberg M, Wagner S, Gebert A, Henrichs M, Eisenblätter R, et al. Proinflammatory cytokines trigger MUC gene expression and mucin release in the intestinal cancer cell line LS180. Inflammation research : official journal of the European Histamine Research Society [et al]. 2000;49(4):162-9.
22. Hill RR, Cowley HM, Andremont A. Influence of colonizing micro-flora on the mucin histochemistry of the neonatal mouse colon. The Histochemical journal. 1990;22(2):102-5.
23. Cash HL, Whitham CV, Behrendt CL, Hooper LV. Symbiotic bacteria direct expression of an intestinal bactericidal lectin. Science (New York, NY). 2006;313(5790):1126-30.
24. Goubier A, Dubois B, Gheit H, Joubert G, Villard-Truc F, Asselin-Paturel C, et al. Plasmacytoid Dendritic Cells Mediate Oral Tolerance. Immunity. 2008;29(3):464-75.
25. Müller-Redetzky HC, Suttorp N, Witzenrath M. Dynamics of pulmonary endothelial barrier function in acute inflammation: mechanisms and therapeutic perspectives. Cell and tissue research. 2014;355(3):657-73.
26. Daneman R, Rescigno M. The gut immune barrier and the blood-brain barrier: are they so different? Immunity. 2009;31(5):722-35.
27. Yuan SY, Rigor RR. Integrated Systems Physiology: From Molecule to Function to Disease. Regulation of Endothelial Barrier Function. San Rafael (CA): Morgan & Claypool Life Sciences

Copyright © 2011 by Morgan & Claypool Life Sciences.; 2010.
28. Wang Y, Rattner A, Zhou Y, Williams J, Smallwood PM, Nathans J. Norrin/Frizzled4 signaling in retinal vascular development and blood brain barrier plasticity. Cell. 2012;151(6):1332-44.
29. Liebner S, Corada M, Bangsow T, Babbage J, Taddei A, Czupalla CJ, et al. Wnt/beta-catenin signaling controls development of the blood-brain barrier. The Journal of cell biology. 2008;183(3):409-17.
30. Simmons DL, Satterthwaite AB, Tenen DG, Seed B. Molecular cloning of a cDNA encoding CD34, a sialomucin of human hematopoietic stem cells. Journal of immunology (Baltimore, Md : 1950). 1992;148(1):267-71.
31. Pusztaszeri MP, Seelentag W, Bosman FT. Immunohistochemical expression of endothelial markers CD31, CD34, von Willebrand factor, and Fli-1 in normal human tissues. The journal of histochemistry and cytochemistry : official journal of the Histochemistry Society. 2006;54(4):385-95.

32. Oehlers SH, Cronan MR, Scott NR, Thomas MI, Okuda KS, Walton EM, et al. Interception of host angiogenic signalling limits mycobacterial growth. Nature. 2015;517(7536):612-5.
33. Iwase T, Uehara Y, Shinji H, Tajima A, Seo H, Takada K, et al. Staphylococcus epidermidis Esp inhibits Staphylococcus aureus biofilm formation and nasal colonization. Nature. 2010;465(7296):346-9.
34. Lee J, Jayaraman A, Wood TK. Indole is an inter-species biofilm signal mediated by SdiA. BMC microbiology. 2007;7(1):1-15.
35. Fux CA, Costerton JW, Stewart PS, Stoodley P. Survival strategies of infectious biofilms. Trends in microbiology. 2005;13(1):34-40.
36. Costerton JW, Stewart PS, Greenberg EP. Bacterial biofilms: a common cause of persistent infections. Science (New York, NY). 1999;284(5418):1318-22.
37. Hajra D, Nair AV, Chakravortty D. An elegant nano-injection machinery for sabotaging the host: Role of Type III secretion system in virulence of different human and animal pathogenic bacteria. Physics of life reviews. 2021;38:25-54.
38. Chandra K, Nair AV, Chatterjee R, Muralidhara P, Singh A, Kamanna S, et al. Absence of proline-peptide transporter YjiY in Salmonella Typhimurium leads to secretion of factors which inhibits intra-species biofilm formation. Microbiological research. 2023;273:127411.
39. Jennings ME, Quick LN, Ubol N, Shrom S, Dollahon N, Wilson JW. Characterization of Salmonella type III secretion hyper-activity which results in biofilm-like cell aggregation. PloS one. 2012;7(3):e33080.
40. Ducarmon QR, Zwittink RD, Hornung BVH, van Schaik W, Young VB, Kuijper EJ. Gut Microbiota and Colonization Resistance against Bacterial Enteric Infection. Microbiology and molecular biology reviews : MMBR. 2019;83(3).
41. Caballero-Flores G, Pickard JM, Núñez G. Microbiota-mediated colonization resistance: mechanisms and regulation. Nature Reviews Microbiology. 2023;21(6):347-60.
42. Qin J, Li R, Raes J, Arumugam M, Burgdorf KS, Manichanh C, et al. A human gut microbial gene catalogue established by metagenomic sequencing. Nature. 2010;464(7285):59-65.
43. Gewolb IH, Schwalbe RS, Taciak VL, Harrison TS, Panigrahi P. Stool microflora in extremely low birthweight infants. Archives of disease in childhood Fetal and neonatal edition. 1999;80(3):F167-73.
44. Chakraborty P, Bajeli S, Kaushal D, Radotra BD, Kumar A. Biofilm formation in the lung contributes to virulence and drug tolerance of Mycobacterium tuberculosis. Nature communications. 2021;12(1):1606.
45. Yamamoto K, Tsujimura Y, Ato M. Catheter-associated Mycobacterium intracellulare biofilm infection in C3HeB/FeJ mice. Sci Rep. 2023;13(1):17148.
46. Heilbronner S, Krismer B, Brötz-Oesterhelt H, Peschel A. The microbiome-shaping roles of bacteriocins. Nature reviews Microbiology. 2021;19(11):726-39.
47. Cotter PD, Ross RP, Hill C. Bacteriocins - a viable alternative to antibiotics? Nature reviews Microbiology. 2013;11(2):95-105.
48. Watson KG, Holden DW. Dynamics of growth and dissemination of Salmonella in vivo. Cellular microbiology. 2010;12(10):1389-97.
49. Eberl C, Weiss AS, Jochum LM, Durai Raj AC, Ring D, Hussain S, et al. E. coli enhance colonization resistance against Salmonella Typhimurium by competing for galactitol, a context-dependent limiting carbon source. Cell host & microbe. 2021;29(11):1680-92.e7.
50. Litvak Y, Mon KKZ, Nguyen H, Chanthavixay G, Liou M, Velazquez EM, et al. Commensal Enterobacteriaceae Protect against Salmonella Colonization through Oxygen Competition. Cell host & microbe. 2019;25(1):128-39.e5.
51. Oliveira RA, Ng KM, Correia MB, Cabral V, Shi H, Sonnenburg JL, et al. Klebsiella michiganensis transmission enhances resistance to Enterobacteriaceae gut invasion by nutrition competition. Nat Microbiol. 2020;5(4):630-41.

851 52. Kommineni S, Bretl DJ, Lam V, Chakraborty R, Hayward M, Simpson P, et al. Bacteriocin
852 production augments niche competition by enterococci in the mammalian gastrointestinal tract.
853 Nature. 2015;526(7575):719-22.
854 53. Kommineni S, Kristich CJ, Salzman NH. Harnessing bacteriocin biology as targeted therapy in
855 the GI tract. Gut Microbes. 2016;7(6):512-7.
856 54. Lawrence GW, McCarthy N, Walsh CJ, Kunyoshi TM, Lawton EM, O'Connor PM, et al. Effect of
857 a bacteriocin-producing Streptococcus salivarius on the pathogen Fusobacterium nucleatum in a
858 model of the human distal colon. Gut Microbes. 2022;14(1):2100203.
859 55. Heeney DD, Zhai Z, Bendiks Z, Barouei J, Martinic A, Slupsky C, et al. Lactobacillus plantarum
860 bacteriocin is associated with intestinal and systemic improvements in diet-induced obese mice and
861 maintains epithelial barrier integrity in vitro. Gut Microbes. 2019;10(3):382-97.
862 56. Kuniyoshi TM, O'Connor PM, Lawton E, Thapa D, Mesa-Pereira B, Abulu S, et al. An oxidation
863 resistant pediocin PA-1 derivative and penocin A display effective anti-Listeria activity in a model
864 human gut environment. Gut Microbes. 2022;14(1):2004071.
865 57. Gogoi M, Chandra K, Sarikhani M, Ramani R, Sundaresan NR, Chakravortty D. Salmonella
866 escapes adaptive immune response via SIRT2 mediated modulation of innate immune response in
867 dendritic cells. PLoS pathogens. 2018;14(11):e1007437.
868 58. Schaefer JS, Montufar-Solis D, Nakra N, Vigneswaran N, Klein JR. Small intestine inflammation
869 in Roquin-mutant and Roquin-deficient mice. PloS one. 2013;8(2):e56436.
870 59. Erben U, Loddenkemper C, Doerfel K, Spieckermann S, Haller D, Heimesaat MM, et al. A
871 guide to histomorphological evaluation of intestinal inflammation in mouse models. International
872 journal of clinical and experimental pathology. 2014;7(8):4557-76.
873 60. Hajra D, Nair AV, Roy Chowdhury A, Mukherjee S, Chatterjee R, Chakravortty D. Salmonella
874 Typhimurium U32 peptidase, YdcP, promotes bacterial survival by conferring protection against in
875 vitro and in vivo oxidative stress. Microbial pathogenesis. 2022;173(Pt B):105862.
876 61. Roy Chowdhury A, Hajra D, Mukherjee D, Nair AV, Chakravortty D. Functional OmpA of
877 Salmonella Typhimurium provides protection from lysosomal degradation and inhibits autophagic
878 processes in macrophages. The Journal of infectious diseases. 2024.
879 62. Hajra D, Mukherjee D, Vij R, Rajmani RS, Dadireddy V, Das D, et al.Odoribacter splanchnicus
880 mitigates Salmonella-induced gut inflammation and its associated pathogenesis via its secreted
881 bacteriocin. bioRxiv. 2024:2024.08.23.609322.

882
883

884 **MAIN FIGURES AND LEGENDS**

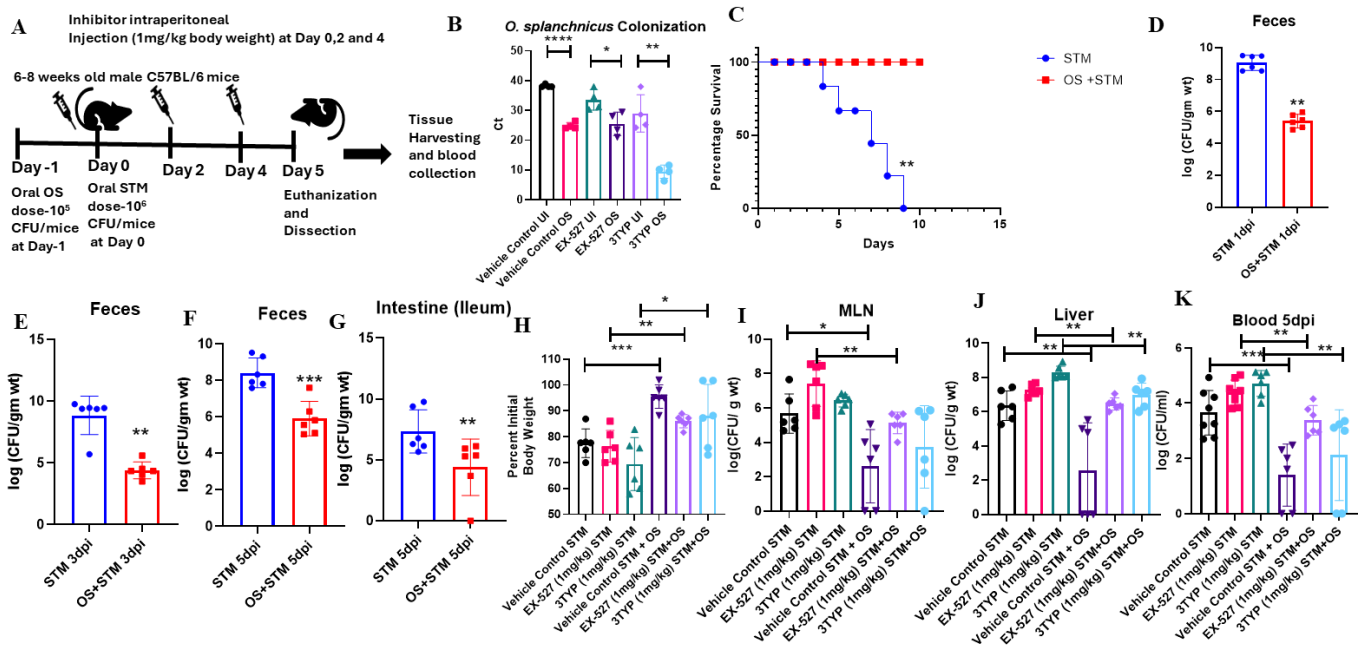

885

886 **Figure 1. *Odoribacter splanchnicus* colonization protects mice from *Salmonella***
887 **colonization and dissemination**

888 **A**-Schematic representation showing animal experimental strategy of infection.

889 **B**-OS colonization validation via qPCR quantification of *O. splanchnicus* 16S rRNA from fecal
890 samples of mice at 6th day post-OS colonization in the presence or absence of SIRT1 (EX-527)
891 or SIRT3 (3TYP) inhibitor treatment (1mg/kg of mice body weight).

892 **C**-Survival percentage of non-colonized-STM-infected mice versus OS-colonized-STM-
893 infected mice cohorts. Data is representative of N=2, n=5 where N denotes number of
894 biological replicates and n denotes the number of mice per group. Mantel Cox or the log-rank
895 test was used to determine the p values.

896 **D-G**- STM organ loads in feces at 1st day post-infection (D), 3rd day post-infection (E), 5th
897 post-infection (F) and in ileal tissues (contents and wall) at 5th day post-infection (G) in OS
898 colonized and non-colonized mice cohorts. Data is representative of N=1, n=6 where N

899 denotes number of biological replicates and n denotes the number of mice per group. Mann
900 Whitney Test was performed to obtain p-values.

901 **H**-Percent of initial weight (at Day 0) exhibited by OS colonized and non-colonized mice upon
902 STM infection at 5th day post-infection in the presence or absence of SIRT1 (EX-527) or SIRT3
903 (3TYP) inhibitor treatment (1mg/kg of mice body weight). Data is representative of N=3,n=6
904 where N denotes number of biological replicates and n denotes the number of mice per group.

905 **I-K**- STM organ loads in MLN (I), liver (J) and blood (K) at 5th post-infection in OS colonized
906 and non-colonized mice cohorts in untreated, and SIRT1 (EX-527) or SIRT3 (3TYP) inhibitor
907 treatment (at 1mg/kg mice body weight concentration). Data is representative of N=3, n=6
908 where N denotes number of biological replicates and n denotes the number of mice per group.
909 Mann Whitney Test was performed to obtain p-values.

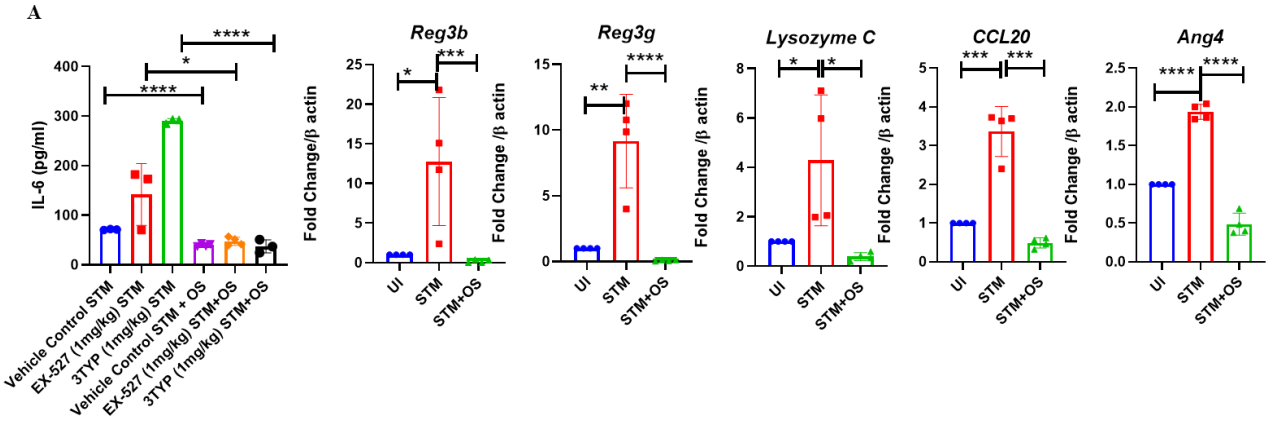

910

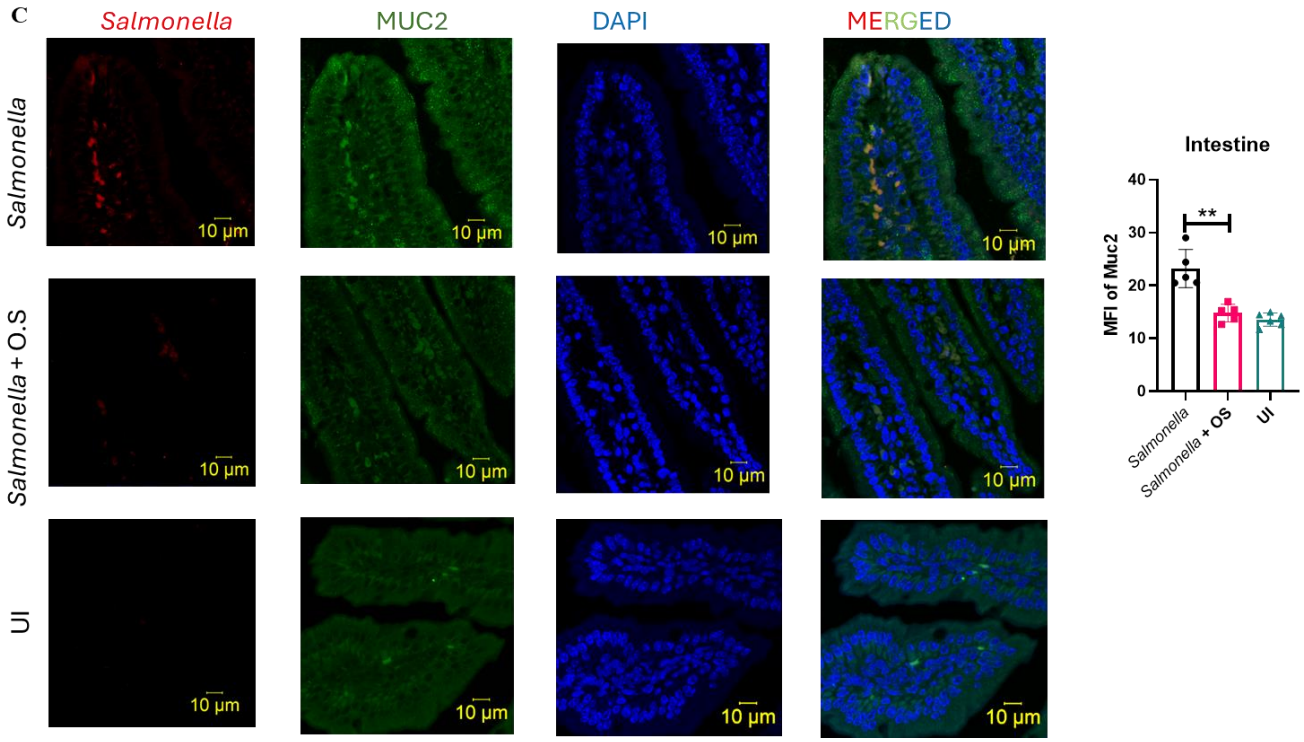
C
Salmonella
MUC2
DAPI
MERGED
Salmonella
Salmonella + O.S
UI
10 µm
Intestine
MFI of Muc2
40
30
20
10
0
**
Salmonella
Salmonella + OS
UI

911

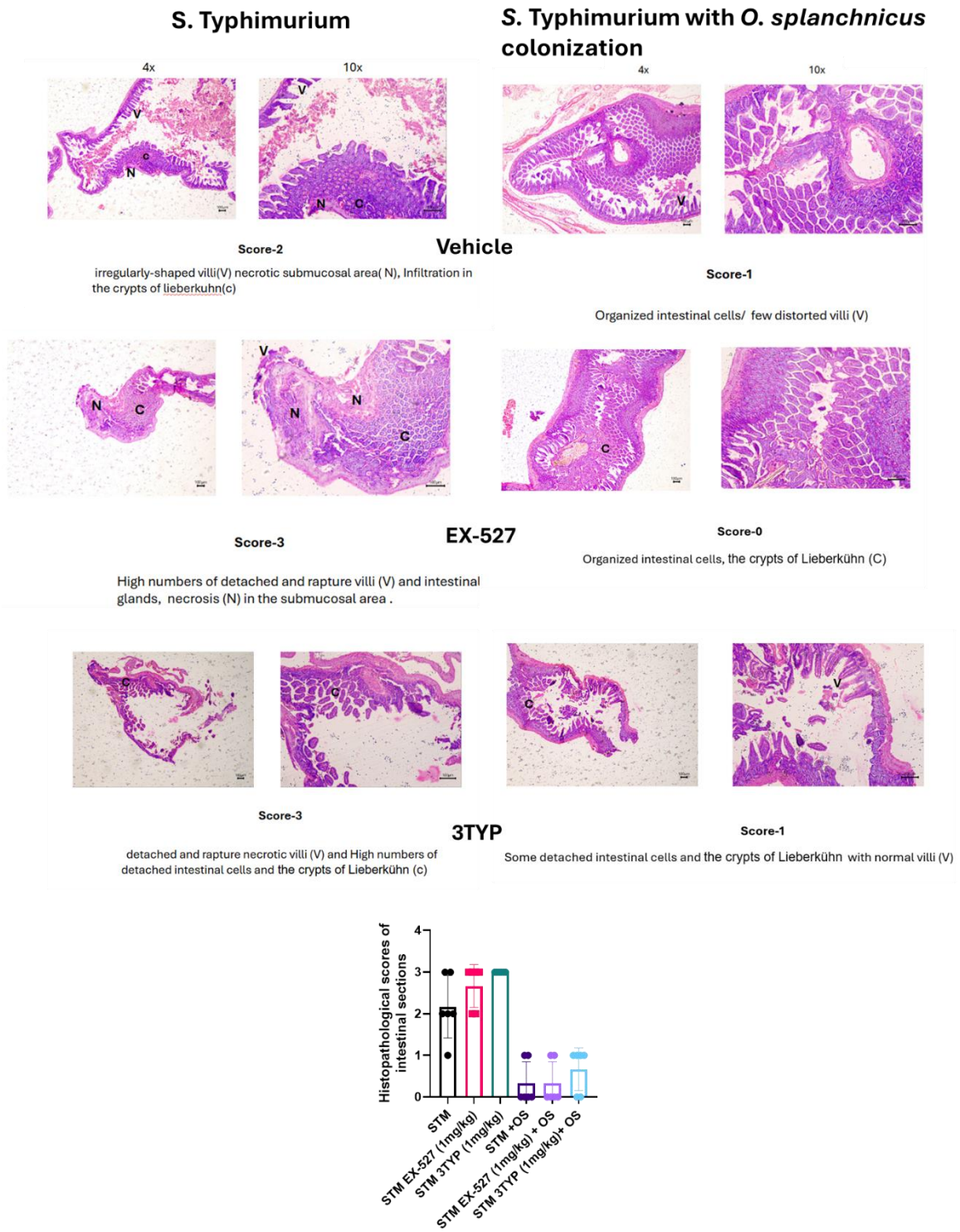

Figure 2. *O. splanchnicus* reduces *Salmonella* induced inflammation and intestinal damage

916 **A**-Estimation of serum IL-6 production via ELISA upon STM infection in OS non-colonized
917 and colonized mice cohorts in presence or absence of SIRT1 or SIRT3 inhibitor treatment at
918 5th day post-*Salmonella* infection. Unpaired t-test is performed to obtain the p-values. Data is
919 representative of N=3, n=3.

920 **B**-Quantitative gene expression data of several antimicrobial peptides (AMPs) precursor genes
921 in uninfected and STM-infected mice intestinal tissues harvested at 5th dpi from OS colonized
922 or non-colonized cohorts. Unpaired t-test is performed to obtain the p-values. Data is
923 representative of N=3, n=4.

924 **C**- Immunostaining representing Muc2 protein expression in intestinal ileal tissues of OS non-
925 colonized and colonized mice cohorts upon STM infection. Unpaired t-test is performed to
926 obtain the p-values. Data is representative of N=3, n=5.

927 **D**-Haematoxylin-eosin-stained intestinal sections harvested from STM-infected OS non-
928 colonized or colonized mice cohorts at 5th dpi. 0-represents normal pathology, 1- represents-
929 mild pathology, 2-3-represents severe pathology.

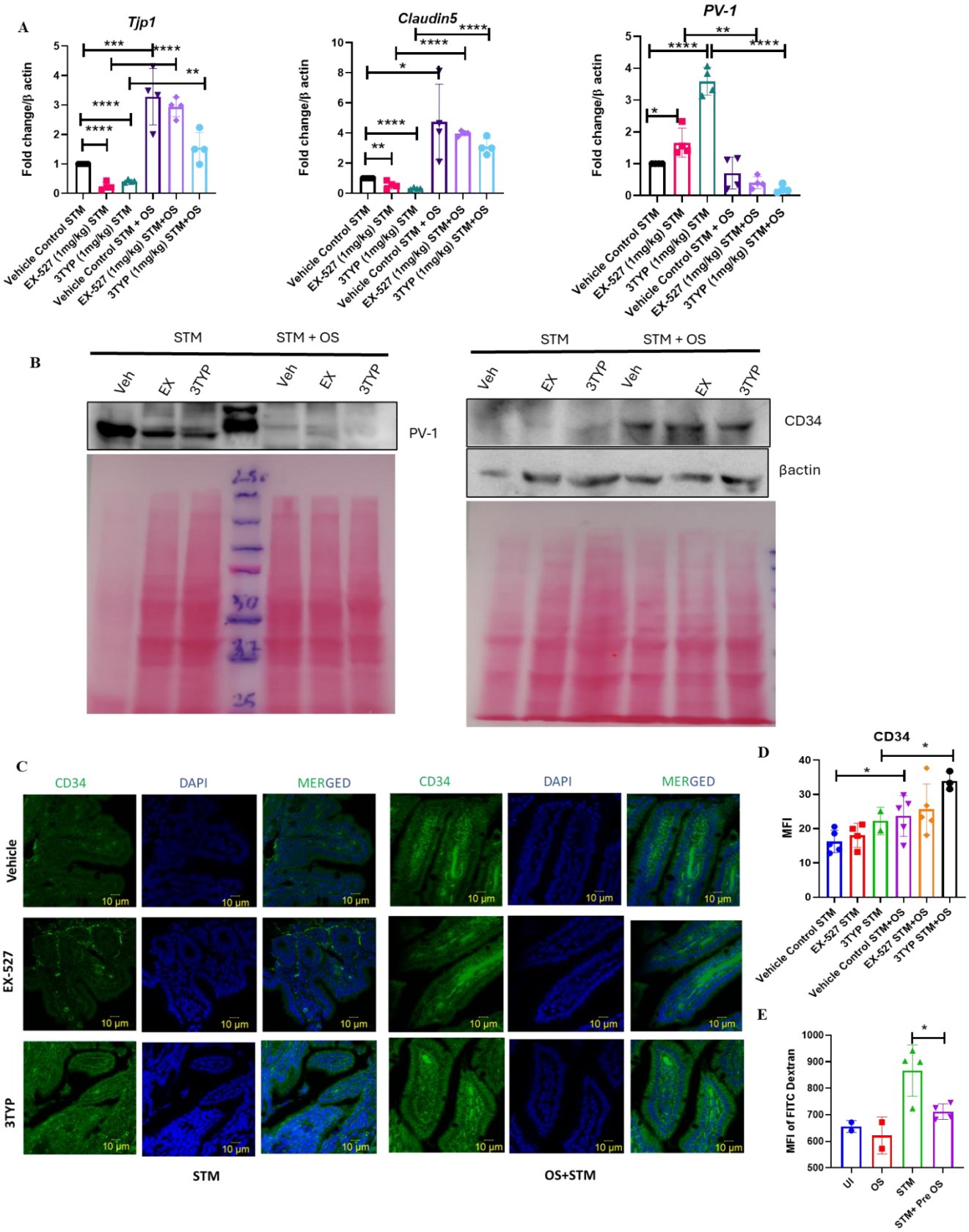
A
Tjp1
Claudin5
PV-1
Fold change/β actin
Vehicle Control STM
EX-527 (1mg/kg) STM
3TYP (1mg/kg) STM
Vehicle Control STM + OS
EX-527 (1mg/kg) STM+OS
3TYP (1mg/kg) STM+OS
B
STM
STM + OS
Veh
EX
3TYP
PV-1
CD34
βactin
C
CD34
DAPI
MERGED
Vehicle
EX-527
3TYP
10 µm
STM
OS+STM
D
CD34
MFI
Vehicle Control STM
EX-527 STM
3TYP STM
Vehicle Control STM+OS
EX-527 STM+OS
3TYP STM+OS
E
MFI of FITC Dextran
UI
OS
STM
STM+ Pre OS

930

931 **Fig 3. *Odoribacter splanchnicus* gut colonization prevents *Salmonella*-induced GVB**
932 **damage by promoting tight junction gene expression.**

933 **A**-Quantitative gene expression studies of tight junction protein complexes (*Tjp1*, *Claudin5*)
934 and PV-1 gene (marker of GVB damage) in STM-infected mice intestinal (ileal) tissue in
935 presence or absence of OS gut colonization at 5th day post-infection. Un-paired t-test was used
936 to obtain the p-values. Data is representative of N=3, n=4.

937 **B**-Immunoblotting depicting expression of PV-1 and CD34 protein in intestinal (ileal) tissues
938 of OS non-colonized and colonized mice cohorts upon STM infection at 5th day post-infection.

939 **C**-Immunofluorescence images representing CD34 (endothelial marker of vasculature) protein
940 expression in intestinal ileal tissues of OS non-colonized and colonized mice cohorts upon
941 STM infection at 5th day post-infection.

942 **D**-Quantitative representation of the Median Fluorescence Intensity (MFI) of CD34 protein
943 expression in intestinal (ileal) immunofluorescence images shown in (C). Data is representative
944 of N=2, n>50. Un-paired t-test was used to obtain the p-values.

945 **E**- Estimation of FITC fluorescence in mice plasma via gut permeability assay in infected mice
946 cohorts upon oral administration of FITC Dextran (25mg/kg) 4h before euthanization at 5th day
947 post *Salmonella* infection. Un-paired t-test was used to obtain the p-values. Data is
948 representative of N=2, n>2.

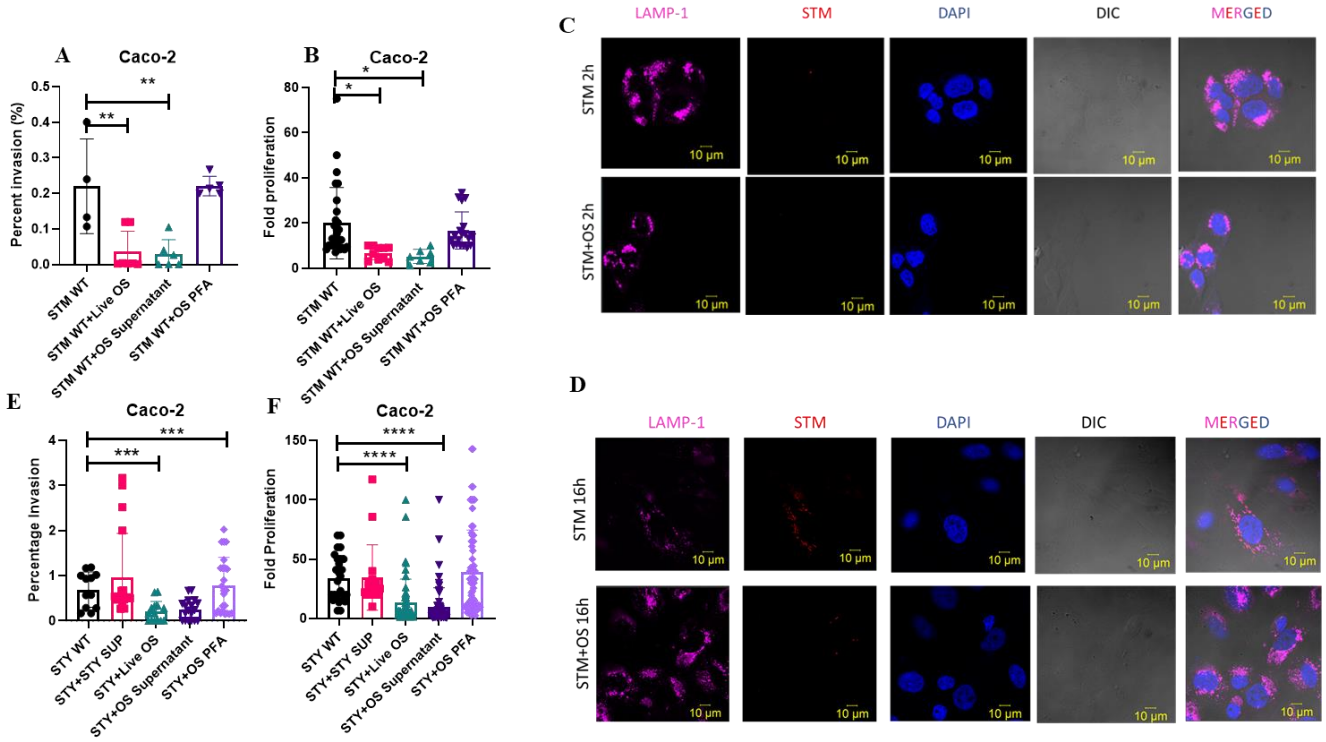
A
Caco-2
Percent invasion (%)
STM WT
STM WT+Live OS
STM WT+OS Supernatant
STM WT+OS PFA
B
Caco-2
Fold proliferation
C
LAMP-1
STM
DAPI
DIC
MERGED
STM 2h
STM+OS 2h
10 µm
D
STM 16h
STM+OS 16h
E
Caco-2
Percentage Invasion
STY WT
STY+STY SUP
STY+Live OS
STY+OS Supernatant
STY+OS PFA
F
Caco-2
Fold Proliferation

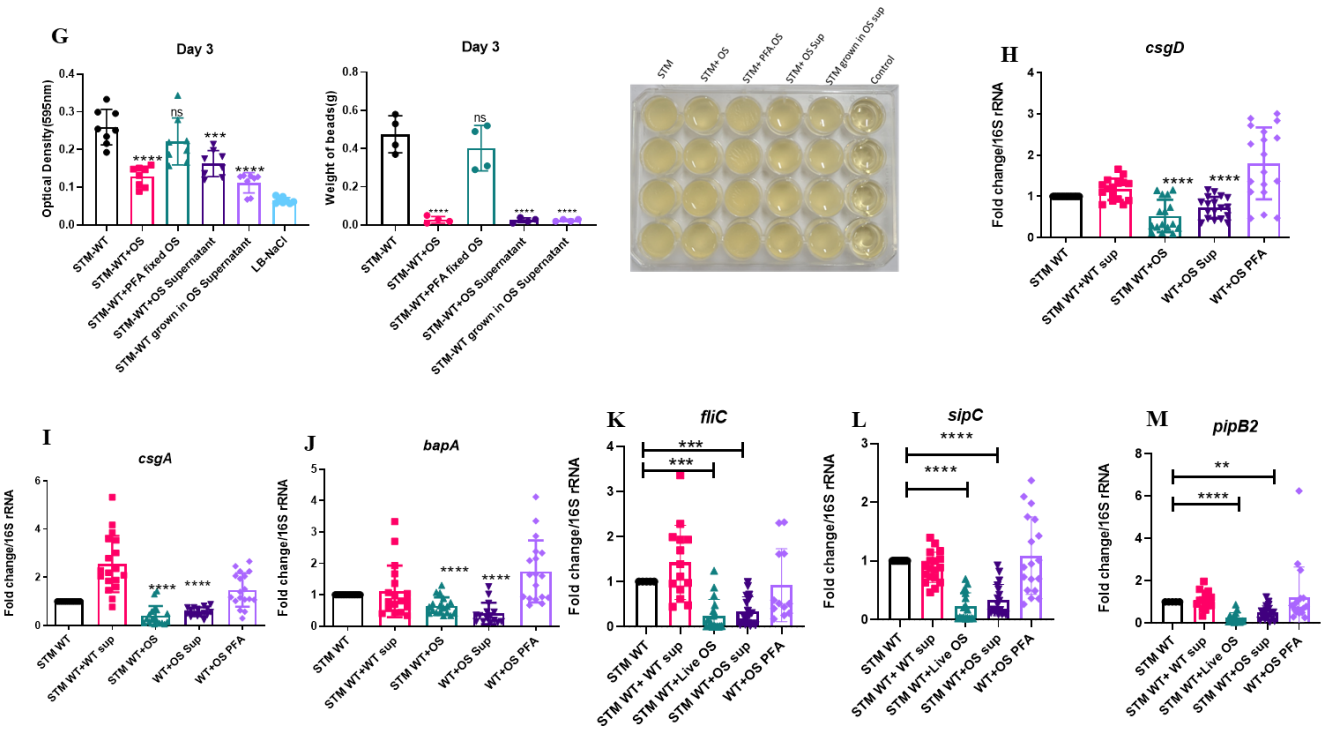
G
Day 3
Optical Density(595nm)
STM-WT
STM-WT+OS
STM-WT+PFA fixed OS
STM-WT+OS Supernatant
STM-WT grown in OS Supernatant
LB-NaCl
Day 3
Weight of beads(g)
STM
STM+OS
STM+PFA OS
STM+OS Sup
STM grown in OS sup
Control
H
csgD
Fold change/16S rRNA
STM WT
STM WT+WT sup
STM WT+OS
WT+OS Sup
WT+OS PFA
I
csgA
J
bapA
K
fliC
L
sipC
M
pipB2

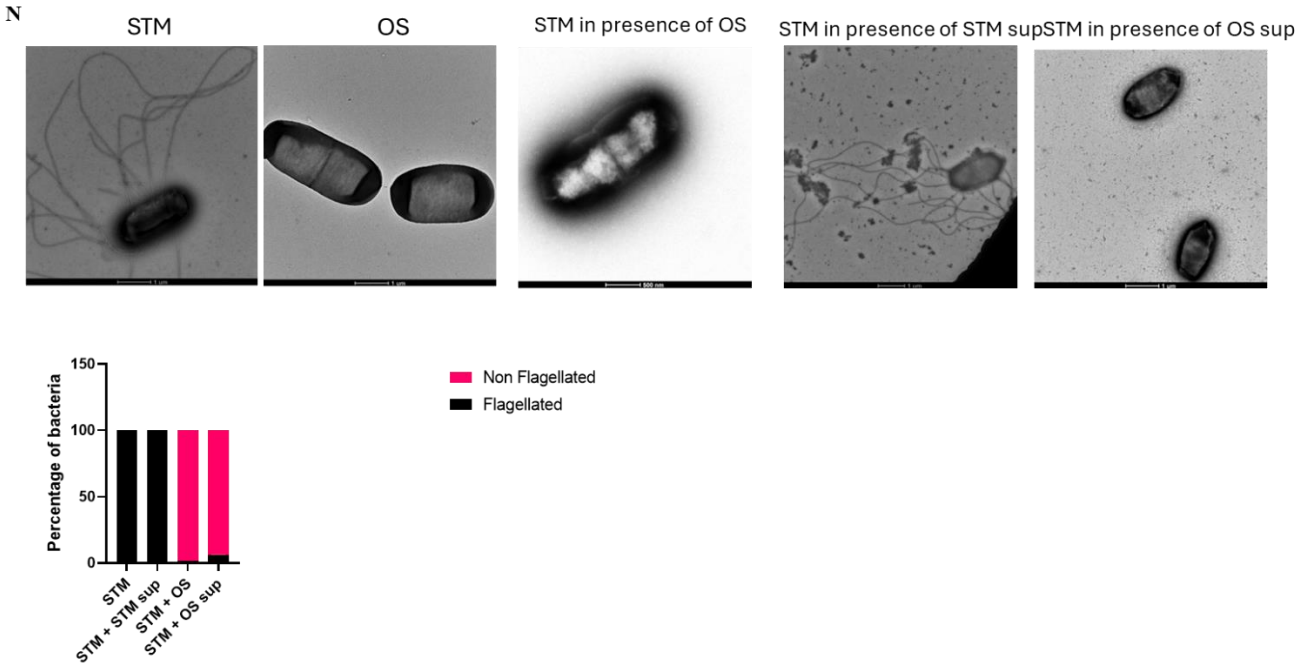

Fig 4. *O. splanchnicus* exhibits its inhibitory effect on *Salmonella* biofilm formation and inhibits invasion and intracellular replication in human intestinal cells

A-Percent invasion of STM in human Caco-2 human intestinal cells in presence or absence of live OS, OS culture supernatant, PFA-fixed-OS. Data is representative of N=3, n=4. One-way ANOVA was used to determine the p-values.

B-Intracellular proliferation of STM Caco-2 cells in presence or absence of live OS, OS culture supernatant, PFA-fixed-OS. Data is representative of N=3, n=4. One-way ANOVA was used to determine the p-values.

C- Representative immunofluorescence images depicting STM invasion into Caco-2 cells in the presence or absence of OS at 2hr post-infection. Data is representative of N=3, n=100.

966 **D**- Representative immunofluorescence images depicting STM invasion into Caco-2 cells in
967 presence or absence of OS at 2hr post-infection. Data is representative of N=3, n=100.

968 **E**-Percent invasion of STY in Caco-2 human cells in presence or absence of OS, OS culture
969 supernatant, PFA-fixed OS. Data is representative of N=3, n≥9. One-way ANOVA was used to
970 determine the p-values.

971 **F**-Intracellular proliferation of STY in Caco-2 cells in presence or absence of live OS, OS
972 culture supernatant, PFA-fixed-OS. Data is representative of N=3, n≥9. One-way ANOVA was
973 used to determine the p-values.

974 **G**- Biofilm assay showing the biofilm formation ability of STM-WT or STM-WT grown in OS
975 supernatant after 72h of inoculation in presence or absence of live OS, OS culture supernatant,
976 PFA-fixed-OS. Data is representative of N=4, n=4.One-way ANOVA was used to determine
977 the p-values. Image of the STM biofilm-formed plate in the above stated conditions has been
978 shown.

979 **H-M-** RT-qPCR mediated gene expression of STM biofilm regulatory genes (*csgD*) (H), *csgA*
980 (I), *bapA* (J), along with flagellar gene (*fliC*) (K), SPI-1 (*sipC*) (L) and SPI-2 (*pipB2*) (M)
981 genes in presence or absence of live OS or its spent media or PFA-fixed-OS. Data is
982 representative of N=4, n=4. One-way ANOVA was used to determine the p-values.

983 **N-** Transmission Electron Microscopic (TEM) images of STM in presence or absence of
984 *Salmonella* WT supernatant, OS and its supernatant to assess the possession of flagella. The
985 quantification plot exhibits the percentage of bacterial flagellated or non-flagellated cells
986 (number of cells quantified n≥ 100)

987

988

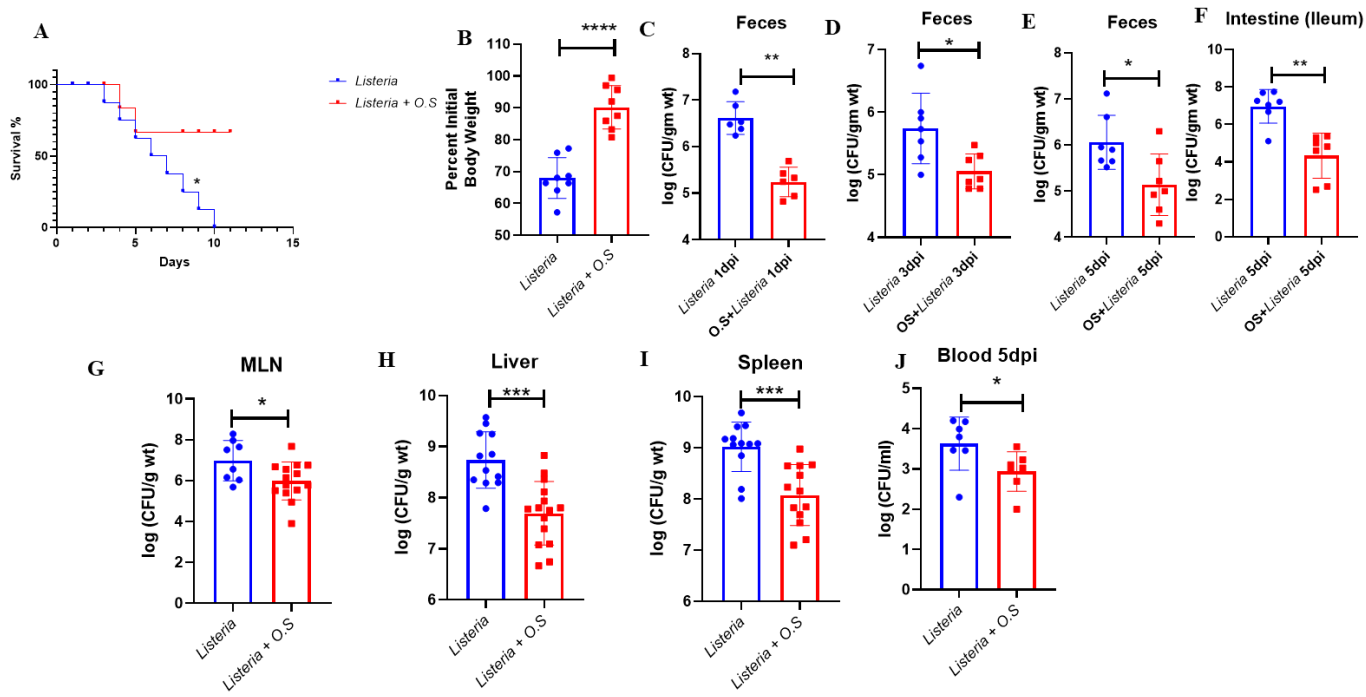

Fig 5. *Odoribacter splanchnicus* exerts its protective role against *Listeria monocytogenes* in mice

A- Survival percentage of non-colonized LM-infected mice versus OS-colonized *Listeria*-infected mice cohorts. Data is represantative of N=2, n=8, where N denotes number of biological replicates and n denotes the number of mice per group. Mantel Cox or the log-rank test was used to determine the p values.

B-Percent of initial weight (at Day 0) exhibited by OS colonized and non-colonized mice upon LM infection at 5th dpi. Data is representative of N=2,n=8, where N denotes number of biological replicates and n denotes the number of mice per group. Mann Whitney Test was performed to obtain p-values.

C-F- LM organ loads in feces at 1st day post-infection (C), 3rd day post-infection (D), 5th post-infection (E) and in ileal tissues (contents and wall) at 5th day post-infection (F) in OS pre-colonized and non-colonized mice cohorts. Data is representative of N=1, n=7 where N

1003 denotes number of biological replicates and n denotes the number of mice per group. Mann
1004 Whitney Test was performed to obtain p-values.

1005 **G-J**- LM organ loads in Mesenteric lymph Node (MLN) (G), liver (H), spleen (I) and blood
1006 (J) at 5th dp. in OS colonized and non-colonized mice cohorts Data is representative of N=2,
1007 n=8, where N denotes number of biological replicates and n denotes the number of mice per
1008 group. Mann Whitney Test was performed to obtain p-values.

1009

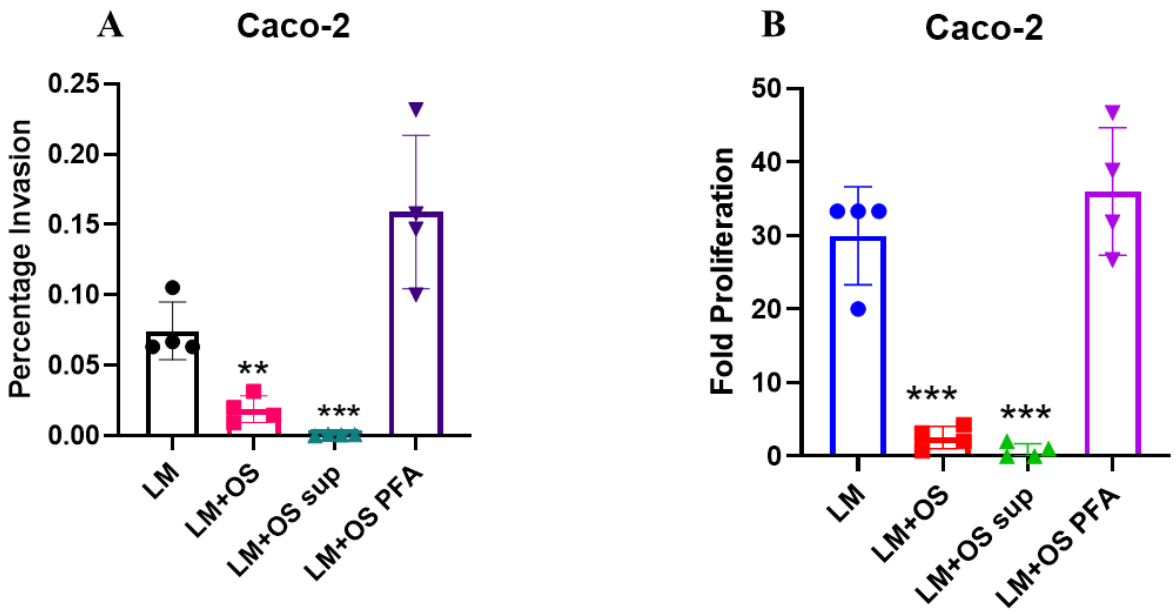

1010

1011 **Fig. 6 *Odoribacter splanchnicus* and its culture supernatant restricts *Listeria***
1012 ***monocytogenes* pathogenesis in human intestinal cells**

1013 **A**- Percent invasion of LM in Caco-2 cells in presence or absence of live OS, OS sup, PFA-
1014 fixed-OS. Data is representative of N=3, n=4. One-way ANOVA and Multiple Comparison test
1015 is used to obtain the p-values.

1016 **B**-Intracellular fold proliferation of LM in Caco-2 cells in the presence or absence of live OS,

1017 OS sup, PFA-fixed-OS. Data is representative of N=3, n=4. One-way ANOVA and Multiple

1018 Comparison test is used to obtain the p-values.

1019

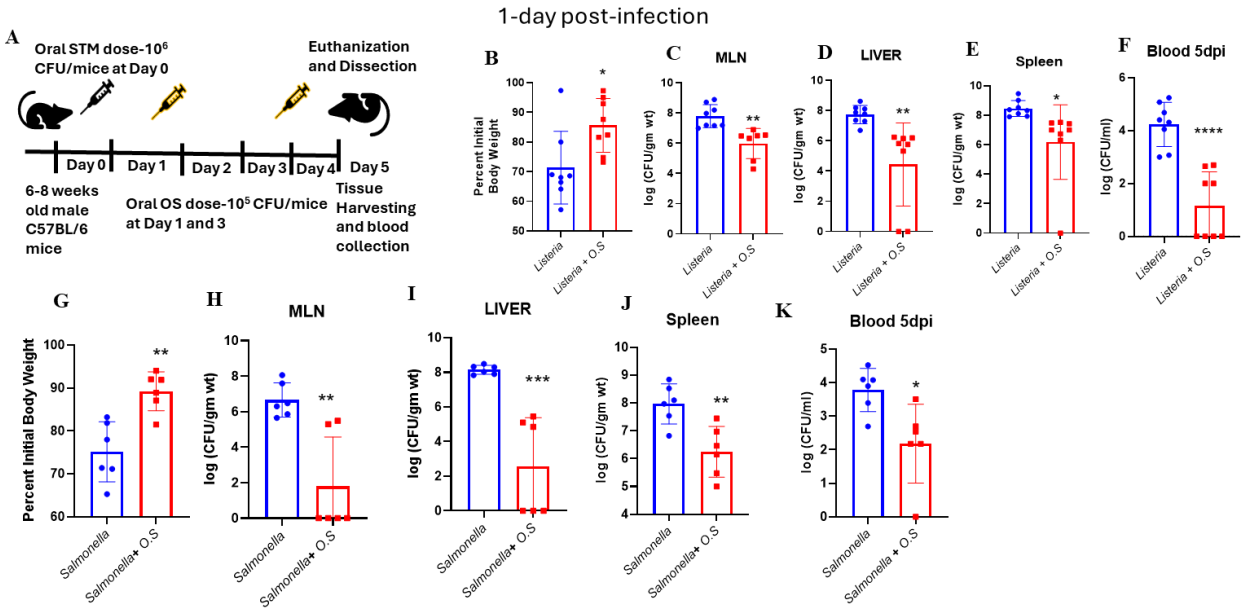

1020

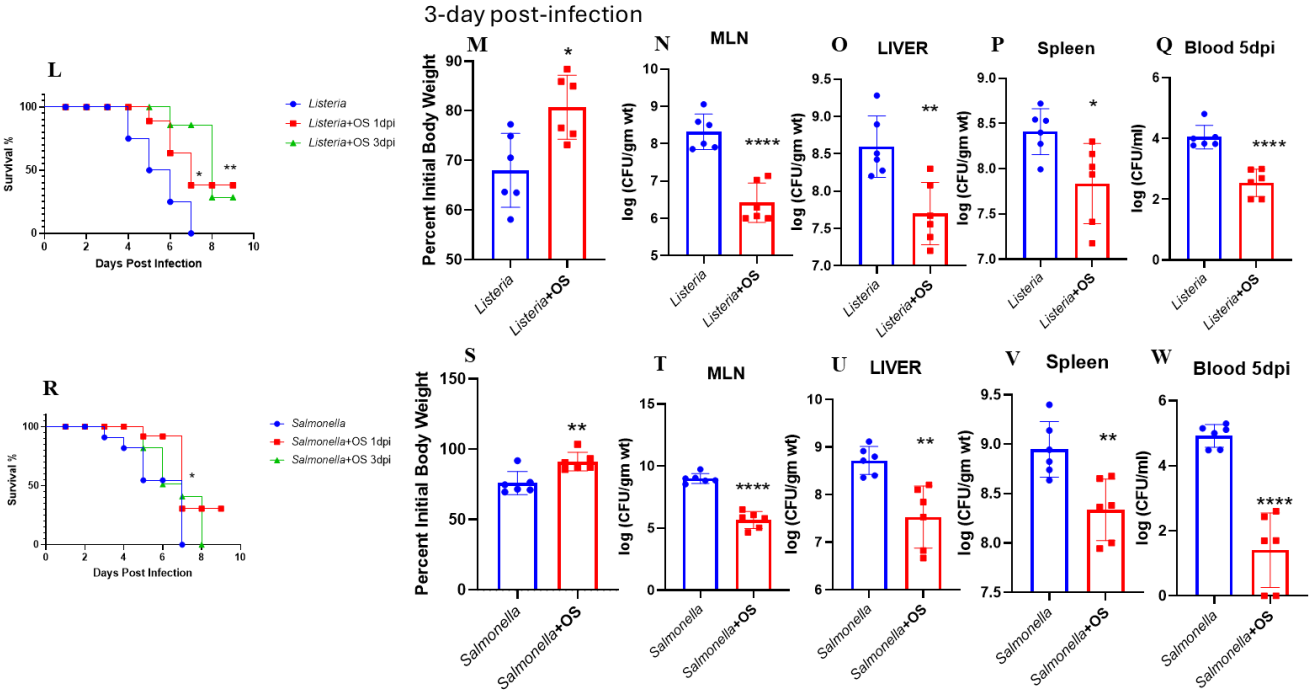

1021

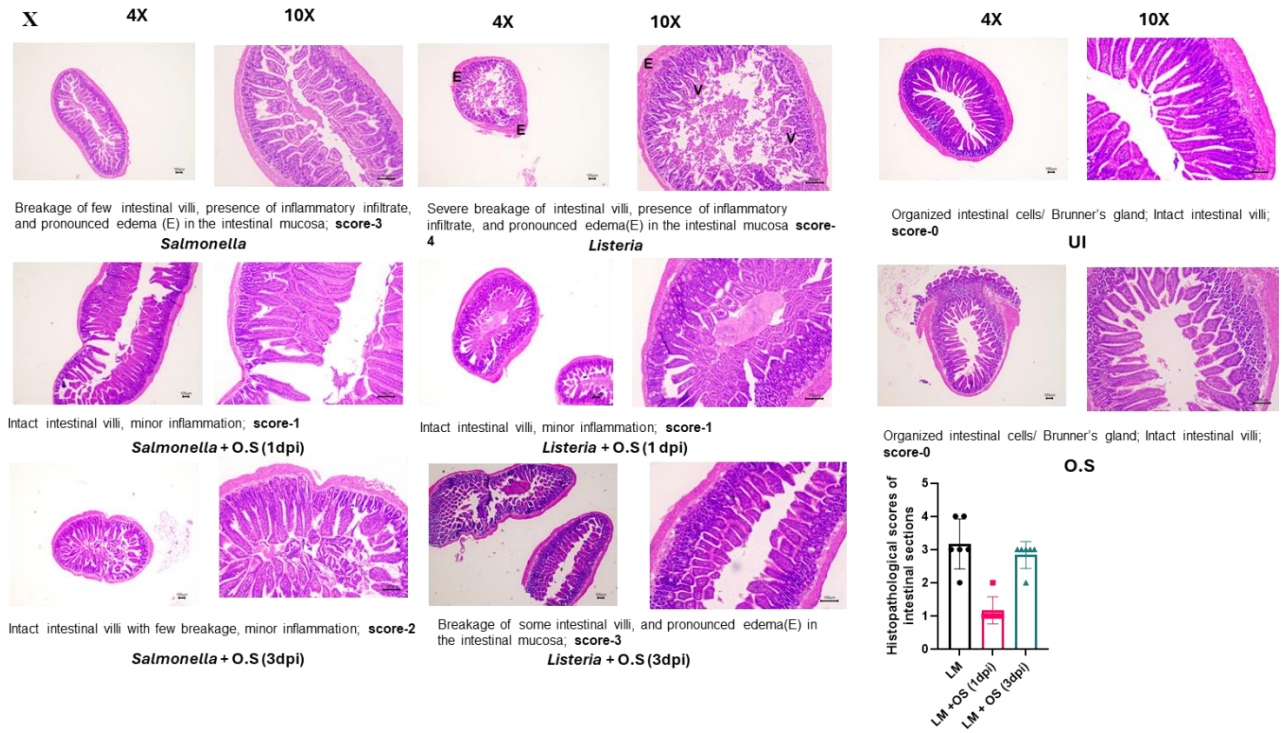

1022

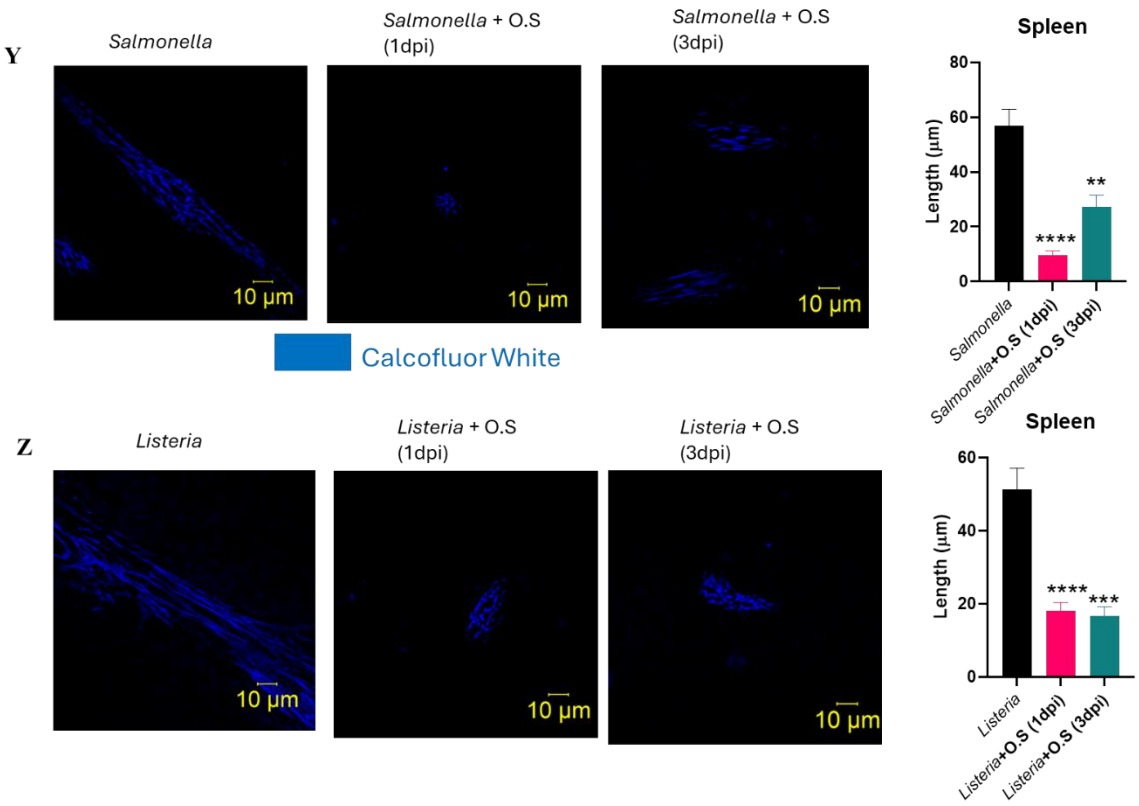

1023

1024 **Fig. 7 *O. splanchnicus* even confers protection against foodborne pathogens when**

1025 **administered post-pathogenic challenge**

1026 **A-** Schematic representation showing the animal experimental strategy of infection.

1027 **B-** Percent of initial weight (at Day 0) exhibited by OS colonized (1-dpi) and non-colonized
1028 mice upon LM infection at 5th dpi. Data is representative of N=2,n=8, where N denotes number
1029 of biological replicates and n denotes the number of mice per group. Mann Whitney Test was
1030 performed to obtain p-values.

1031 **C-F**- LM organ loads in MLN (C), liver (D), spleen (E) and blood (F) at 5th dpi upon OS
1032 administration at 1-dpi. Data is representative of N=2, n=8, where N denotes number of
1033 biological replicates and n denotes the number of mice per group. Mann Whitney Test was
1034 performed to obtain p-values.

1035 **G**- Percent of initial weight (at Day 0) exhibited by OS colonized (1-dpi) and non-colonized
1036 mice upon STM infection at 5th dpi. Data is representative of N=2,n=8, where N denotes
1037 number of biological replicates and n denotes the number of mice per group. Mann Whitney
1038 Test was performed to obtain p-values.

1039 **H-K**- STM organ loads in MLN (H), liver (I), spleen (J) and blood (K) at 5th-dpi upon OS
1040 administration at 1-dpi. Data is representative of N=2, n=8, where N denotes number of
1041 biological replicates and n denotes the number of mice per group. Mann-Whitney Test was
1042 performed to obtain p-values.

1043 **L**- Survival percentage of non-colonized LM-infected mice versus OS-colonized (1 dpi or 3
1044 dpi) *Listeria*-infected mice cohorts. Data is representative of N=2, n=8, where N denotes
1045 number of biological replicates and n denotes the number of mice per group. Mantel Cox or
1046 the log-rank test was used to determine the p values.

1047 **M**- Percent weight loss exhibited by OS colonized (3-dpi) and non-colonized mice upon LM
1048 infection at 5th-day post-infection. Data is representative of N=2,n=8, where N denotes number

1049 of biological replicates and n denotes the number of mice per group.Mann-Whitney Test was
1050 performed to obtain p-values.

1051

1052 **N-Q**- LM organ loads in MLN (N), liver (O), spleen (P) and blood (Q) at 5th-dpi upon OS
1053 administration at 3-dpi. Data is representative of N=2, n=8, , where N denotes number of
1054 biological replicates and n denotes the number of mice per group. Mann-Whitney Test was
1055 performed to obtain p-values.

1056 **R**- Survival percentage of non-colonized *Salmonella*-infected mice versus OS-colonized (1 dpi
1057 or 3 dpi) *Listeria*-infected mice cohorts. Data is represantative of N=2, n=8, where N denotes
1058 number of biological replicates and n denotes the number of mice per group. Mantel Cox or
1059 the log-rank test was used to determine the p values.

1060 **S**- Percent weight loss exhibited by OS-colonized (3-dpi) and non-colonized mice upon STM
1061 infection at 5th-day post-infection. Data is representative of N=2,n=8, where N denotes number
1062 of biological replicates and n denotes the number of mice per group. Mann-Whitney Test was
1063 performed to obtain p-values.

1064 **T-W**-STM organ loads in MLN (T), liver (U), spleen (V), and blood (W) at 5th-dpi upon OS
1065 administration at 3-dpi. Data is representative of N=2, n=8, where N denotes number of
1066 biological replicates and n denotes the number of mice per group. Mann-Whitney Test was
1067 performed to obtain p-values.

1068 **X-** Haematoxylin-eosin-stained intestinal sections harvested at 5th-dpi from Uninfected (UI) or
1069 *Salmonella* or *Listeria*-infected mice cohorts having non-administered or administered OS (at
1070 1st or 3rd dpi). 0-represents normal pathology, 1- represents- mild pathology, 2-3-represents
1071 severe pathology.

1072 **Y**- Representative Calcofluor white (CW) staining of STM-infected mice spleen tissues at 5th-
1073 day post-infection with or without OS administration at 1st or 3rd dpi depicting the
1074 quantification of the length of the fibril architecture of CW-stained sections. One-way ANOVA
1075 and multiple comparison test were used to obtain the p-values.

1076 **Z**- Representative CW staining of LM-infected mice spleen tissues at 5th-dpi with or without
1077 OS administration at 1st or 3rd dpi depicting the quantification of the length of the fibril
1078 architecture of CW-stained sections. One-way ANOVA and multiple comparison test were used
1079 to obtain the p-values.

1080

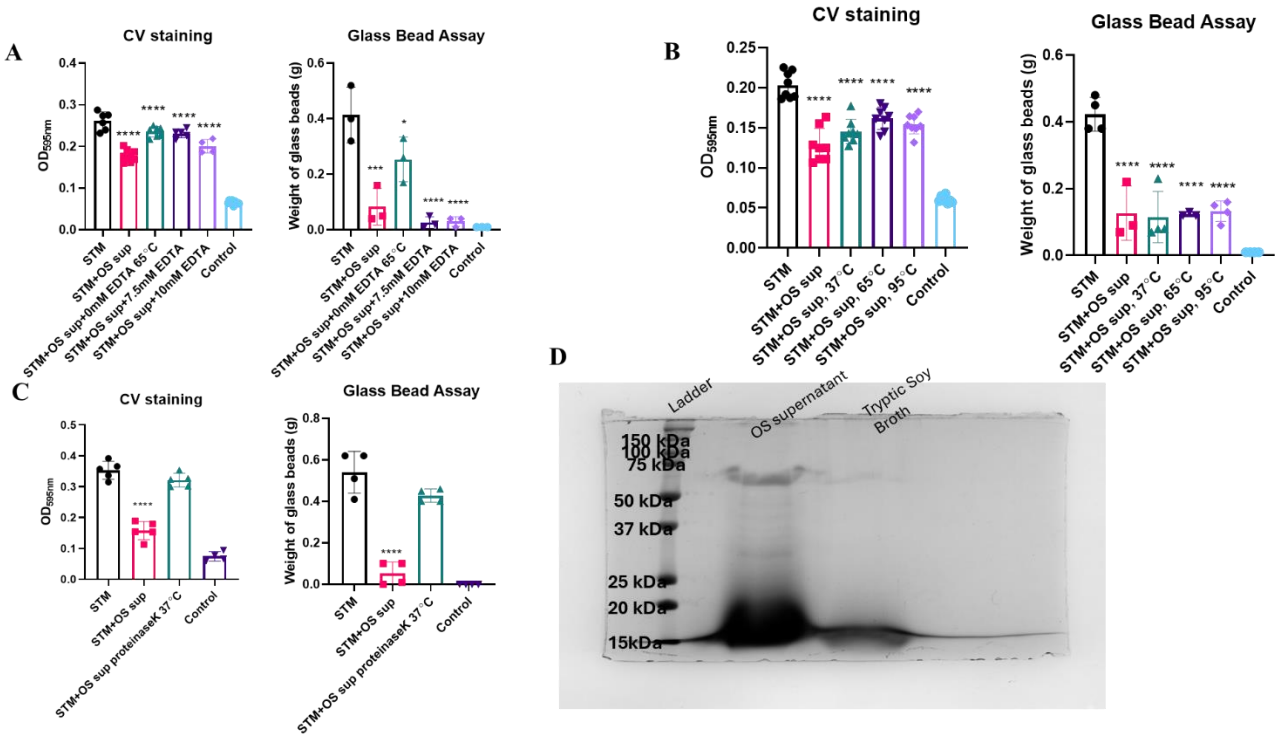

1081

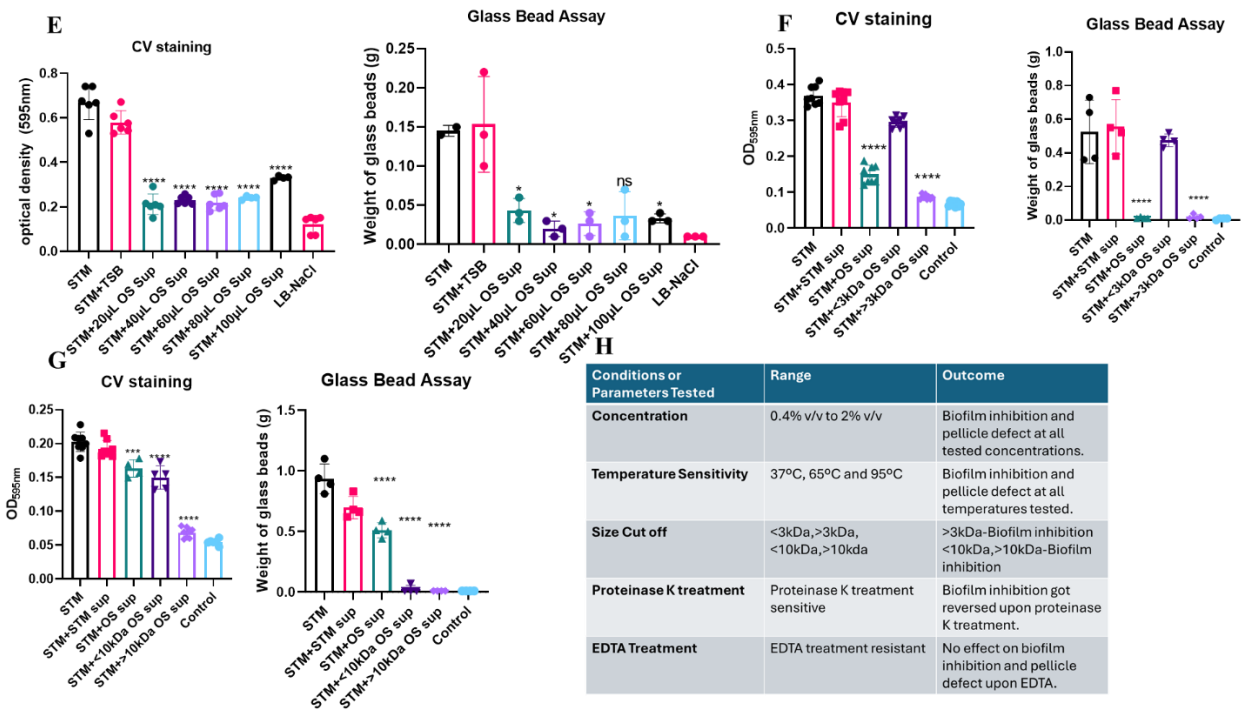

Conditions or Parameters Tested	Range	Outcome
Concentration	0.4% v/v to 2% v/v	Biofilm inhibition and pellicle defect at all tested concentrations.
Temperature Sensitivity	37°C, 65°C and 95°C	Biofilm inhibition and pellicle defect at all temperatures tested.
Size Cut off	<3kDa,>3kDa, <10kDa,>10kda	>3kDa-Biofilm inhibition <10kDa,>10kDa-Biofilm inhibition
Proteinase K treatment	Proteinase K treatment sensitive	Biofilm inhibition got reversed upon proteinase K treatment.
EDTA Treatment	EDTA treatment resistant	No effect on biofilm inhibition and pellicle defect upon EDTA.

Fig. 8- Characterization of the nature of inhibitory active molecule within *O. splanchnicus* culture supernatant

A- Biofilm assay showing the biofilm formation ability of STM after 72h of inoculation in presence of OS culture supernatant upon EDTA treatment. Data is representative of N=4, n=4. One-way ANOVA is used to obtain the p-values.

B- Biofilm assay showing the biofilm formation ability of STM after 72h of inoculation in presence of OS culture supernatant at high temperature conditions. Data is representative of N=4, n=4. One-way ANOVA is used to obtain the p-values.

C- Biofilm assay showing the biofilm formation ability of STM after 72h of inoculation in presence of OS culture supernatant under Proteinase K treatment. Data is representative of N=4, n=4. One-way ANOVA is used to obtain the p-values.

D- Coomassie-stained SDS-PAGE demonstrating the size range of the differential protein bands present in OS supernatant as opposed to the tryptic soy broth media control.

E- Biofilm assay showing the biofilm formation ability of STM after 72h of inoculation in presence of varying concentration OS culture supernatant. Data is representative of N=4, n=4. One-way ANOVA is used to obtain the p-values.

F- Biofilm assay showing the biofilm formation ability of STM after 72h of inoculation in presence of OS culture supernatant fractions fractionated using 3kDa Amicon filter. Data is representative of N=4, n=4. One-way ANOVA is used to obtain the p-values.

G- Biofilm assay showing the biofilm formation ability of STM after 72h of inoculation in presence of OS culture supernatant fractions fractionated using 10kDa Amicon filter. Data is representative of N=4, n=4. One-way ANOVA is used to obtain the p-values.

H- Summary table demonstrating the conditions tested for active molecule characterization and their effective outcome.

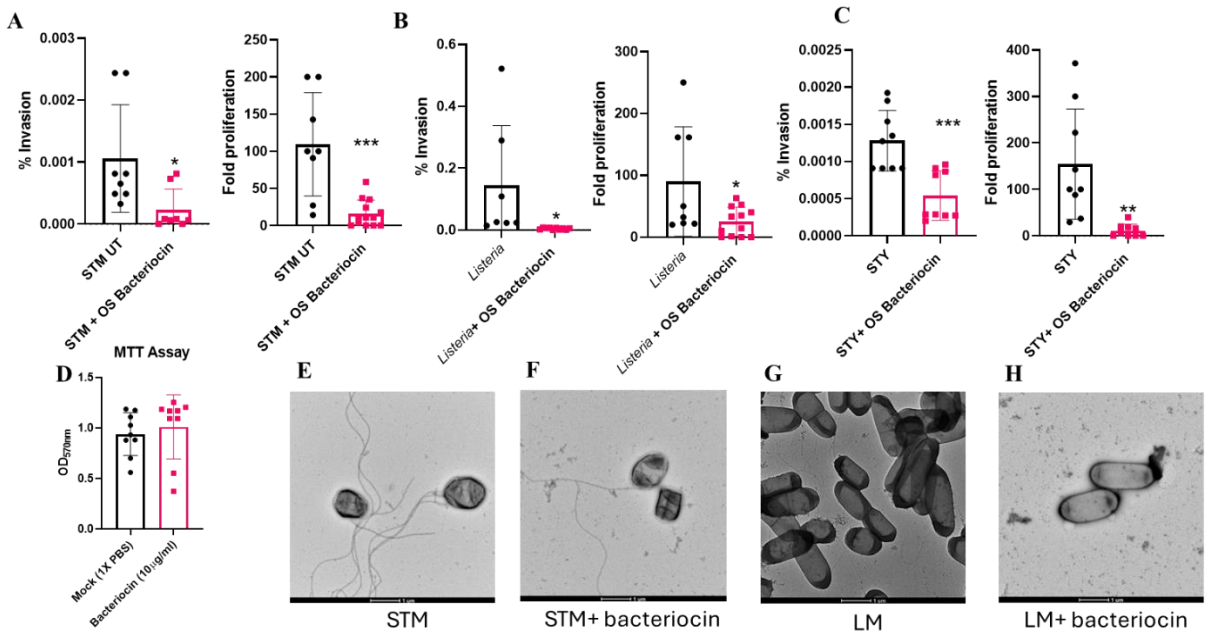

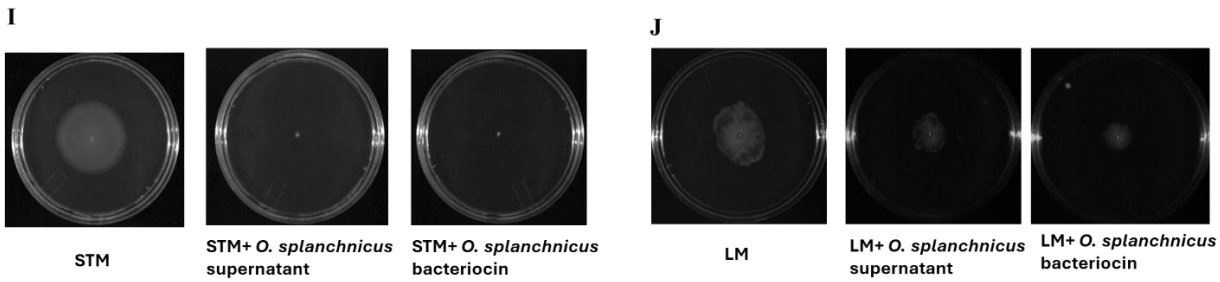

Fig. 9- *O. splanchnicus* bacteriocin restricts both *Salmonella* and *Listeria* pathogenesis *in vitro*

A- Percent invasion and intracellular fold proliferation of STM in Caco-2 cells under OS bacteriocin (10µg/ml) treatment. Data is representative of N=2, n=3. Unpaired t-test is used to obtain the p-values.

B- Percent invasion and intracellular fold proliferation of LM in Caco-2 cells under OS bacteriocin (10µg/ml) treatment. Data is representative of N=2, n=3. Unpaired t-test is used to obtain the p-values.

C- Percent invasion and intracellular fold proliferation of STY in Caco-2 cells under OS bacteriocin (10µg/ml) treatment. Data is representative of N=2, n=3. Unpaired t-test is used to obtain the p-values.

D-MTT assay evaluating the viability of Caco-2 cells upon 16h of mock or bacteriocin (10µg/ml) treatment. Data is representative of N=2, n=4.

E-F-TEM images of STM under untreated (D) or bacteriocin (10µg/ml) (E) treatment to assess the possession of flagella.

G-H- TEM images of LM under untreated (D) or bacteriocin (10µg/ml) (E) treatment to assess the possession of flagella.

I- Swimming motility assay of STM under OS supernatant or bacteriocin treatment.

1128 **J-** Swimming motility assay of LM under OS supernatant or bacteriocin treatment.

1129

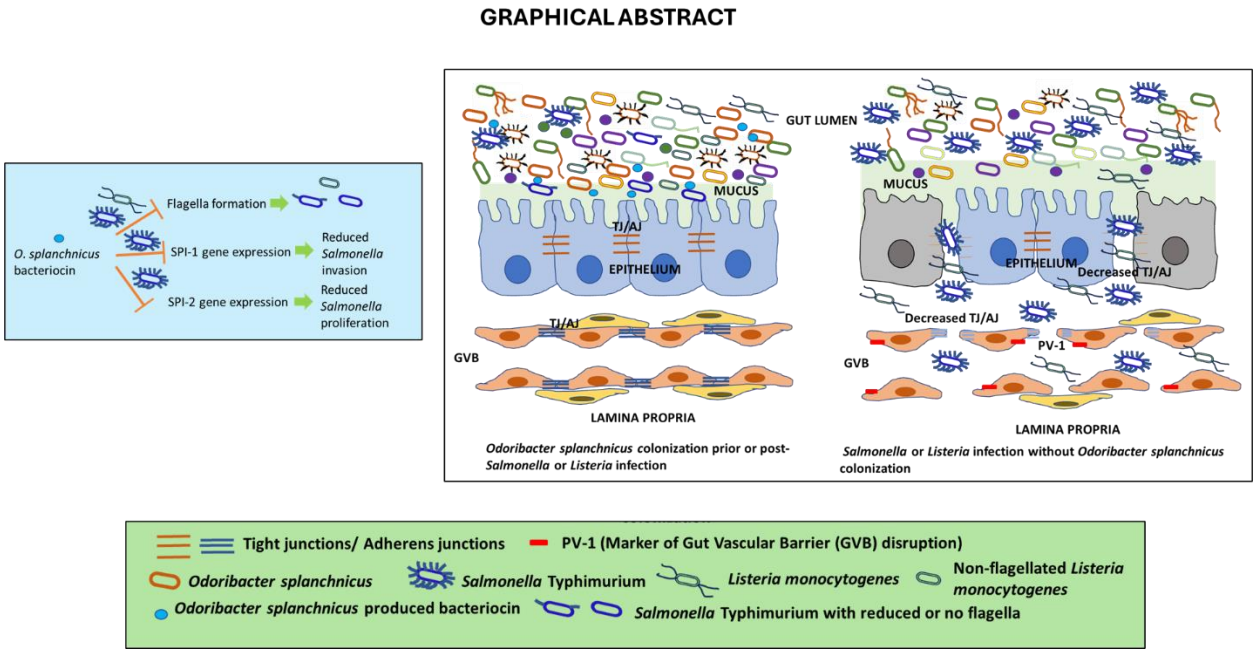

1130

1131

1132

1133 **SUPPLEMENTARY FIGURES AND LEGENDS**

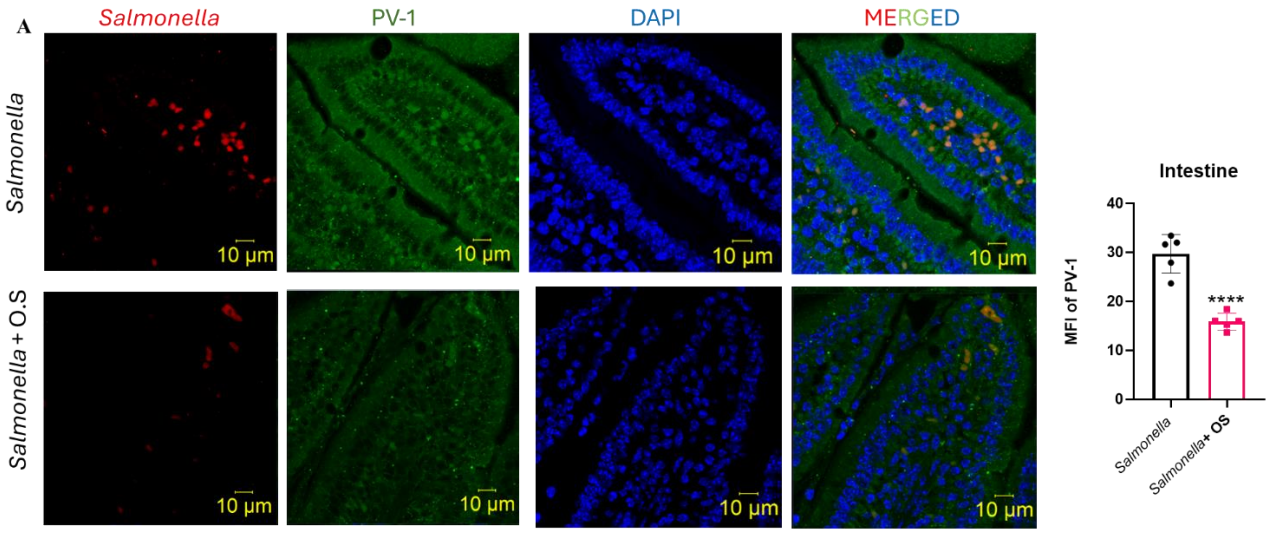

1134

1135

1136

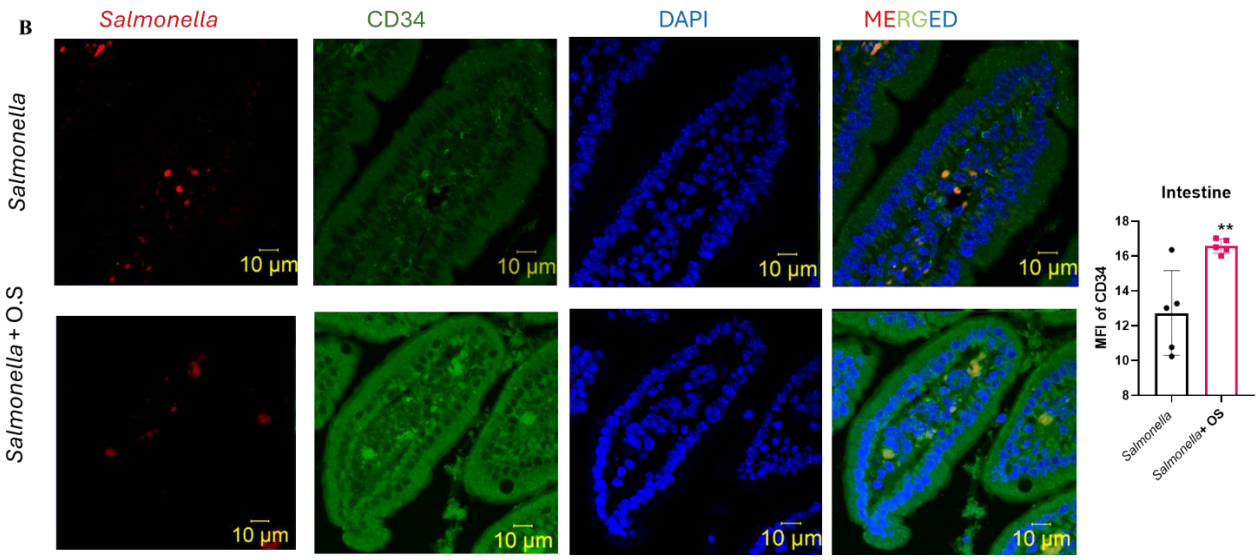
B
Salmonella
CD34
DAPI
MERGED
Salmonella
Salmonella + O.S
10 µm
Intestine
MFI of CD34
18
16
14
12
10
8
**
Salmonella
Salmonella+ OS

1137

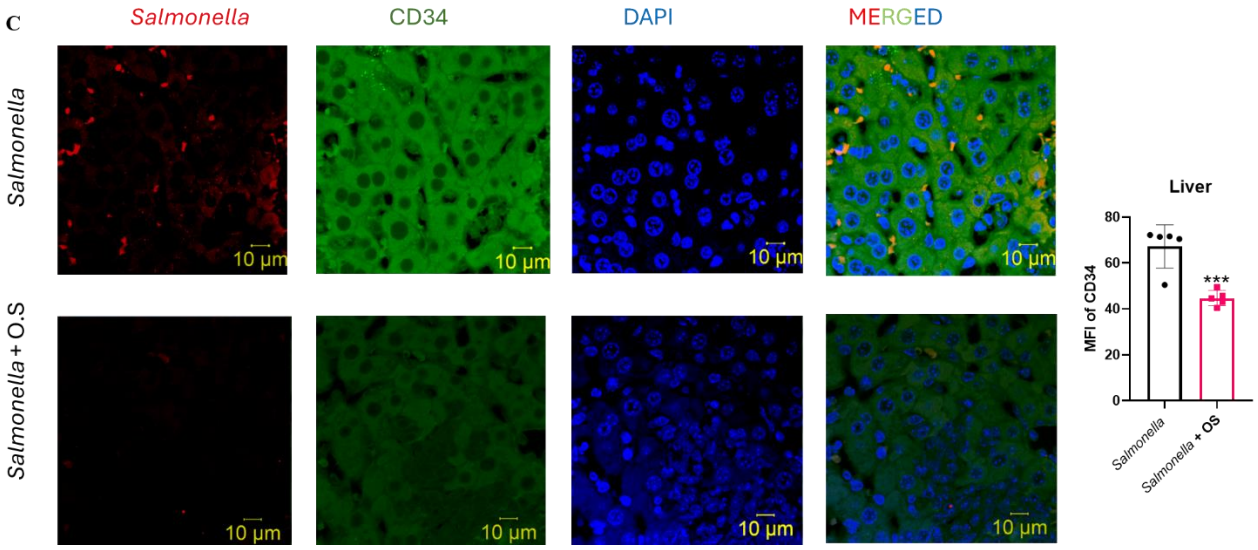
C
Salmonella
CD34
DAPI
MERGED
Salmonella
Salmonella + O.S
10 µm
Liver
MFI of CD34
80
60
40
20
0
***
Salmonella
Salmonella + OS

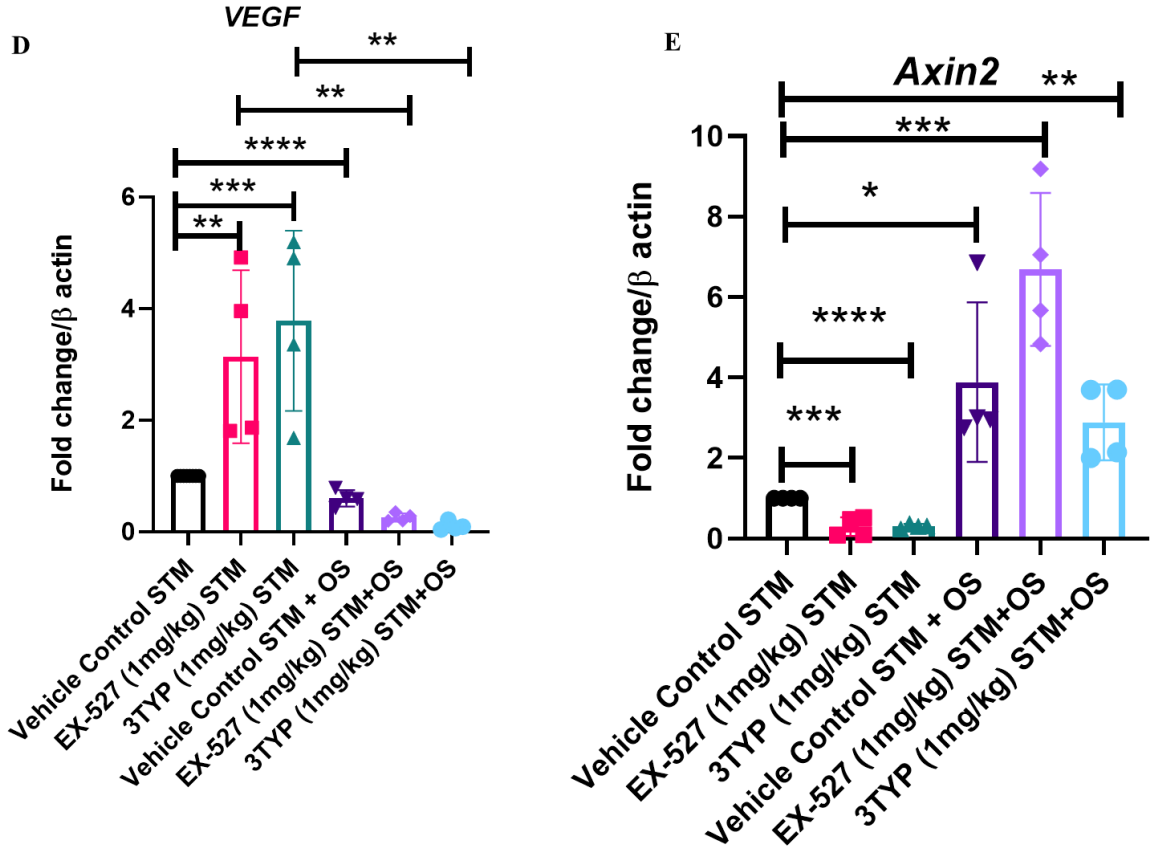

Fig S1. *O. splanchnicus* gut colonization prevents *Salmonella* dissemination by restricting intestinal GVB damage and angiogenesis

A-Immunofluorescence image demonstrating PV-1 protein expression in intestinal (ileal) tissues of OS non-colonized and colonized mice cohorts upon STM infection. Data is representative of N=2, n=5 (tissue samples). Un-paired t-test was used to obtain the p-values.

B-C Immunofluorescence image representing CD34 (an endothelial marker of vasculature) protein expression in intestinal (ileal) (B) and liver (C) tissues of OS non-colonized and

1148 colonized mice cohorts upon STM infection. Data is representative of N=2, n=5 (tissue
1149 samples). Un-paired t-test was used to obtain the p-values.

1150 **D**- qPCR mediated gene expression of pro-angiogenic marker *Vegf* in STM-infected mice liver
1151 tissues in presence or absence of OS pre-colonization. Data is representative of N=2, n=4. Un-
1152 paired t-test was used to obtain the p-values.

1153 **E**- qPCR mediated gene expression of *Axin2* in STM-infected mice intestinal tissues in the
1154 presence or absence of OS pre-colonization. Data is representative of N=2, n=4. Un-paired t-
1155 test was used to obtain the p-values.

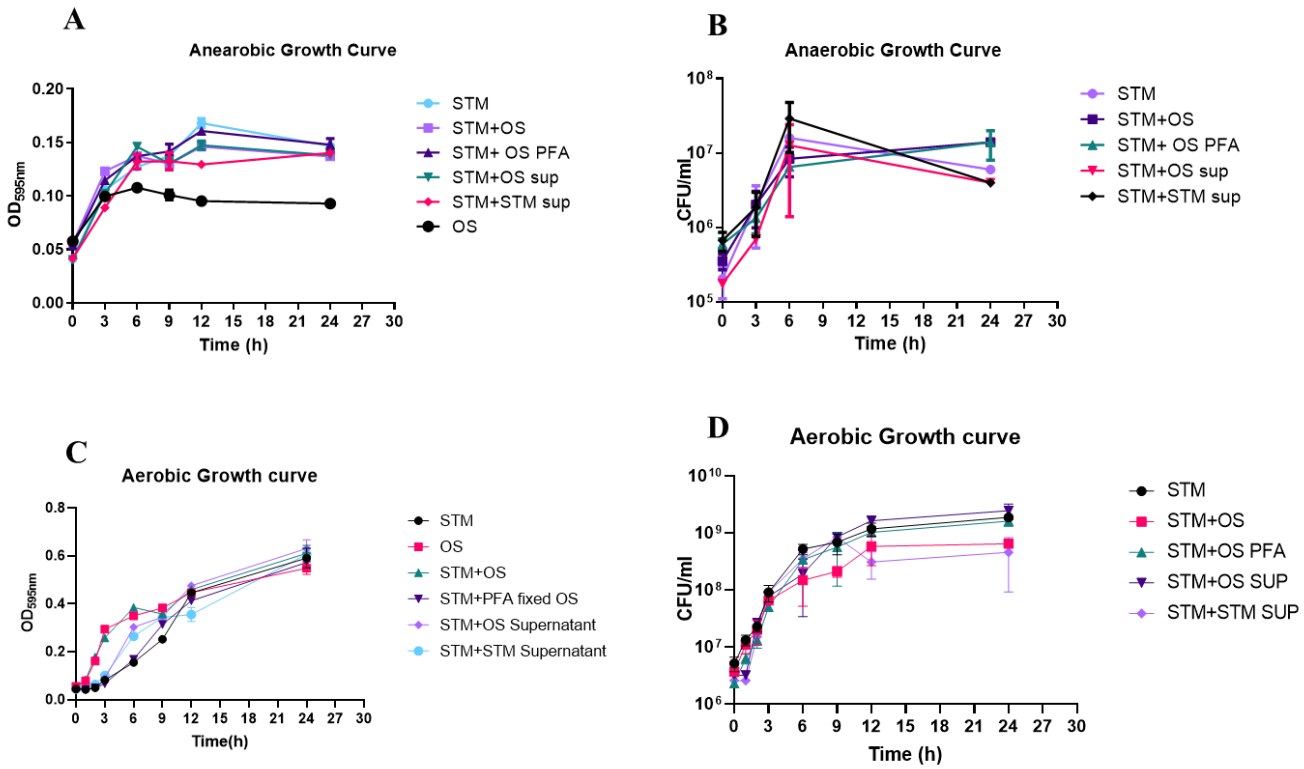

1156

1157 **Fig. S2 In vitro growth kinetics of *Salmonella* Typhimurium in presence of live or dead**
1158 ***O. splanchnicus* or its culture supernatant**

1159 **A-B** Growth kinetics of STM-WT, OS, STM-WT in presence of OS, STM-WT in presence of
1160 STM or OS culture supernatant and STM-WT in presence of PFA-fixed OS in LB under
1161 anaerobic growth conditions.

1162 **C-D**- Growth kinetics of STM-WT, OS, STM-WT in presence of OS, STM-WT in presence of
1163 STM or OS culture supernatant, STM-WT supernatant, and STM-WT in presence of PFA-fixed
1164 OS in LB under aerobic growth conditions.

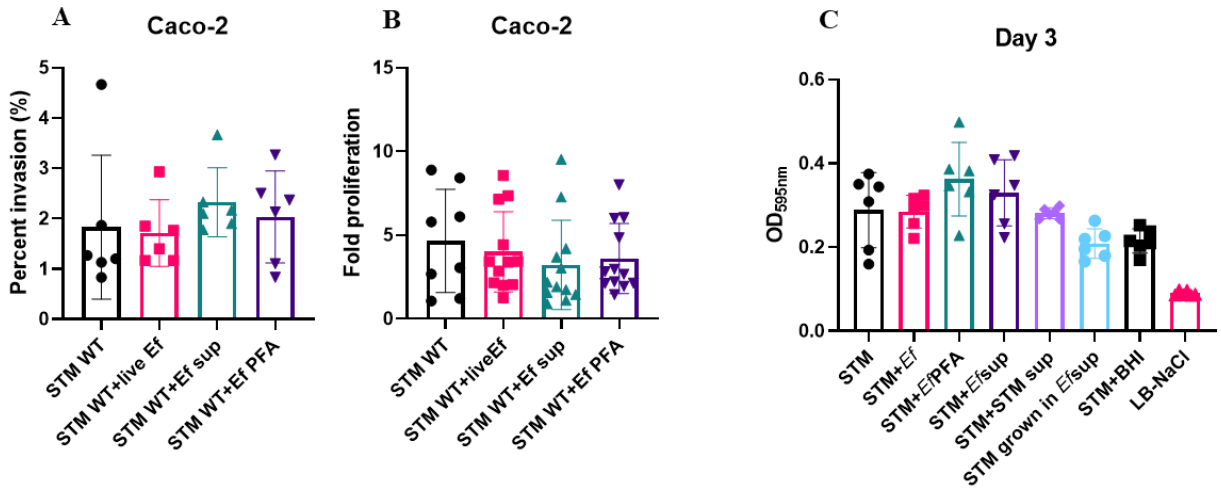

1165

1166 **Fig S3. Unlike *O. splanchnicus, E. faecalis* fail to exert any inhibitory effect on *Salmonella***
1167 ***in vitro* biofilm formation or *Salmonella* invasion and intracellular replication in human**
1168 **intestinal cells**

1169 **A**-Percent invasion of STM in Caco-2 cells in presence or absence of live *E. faecalis* (Ef), Ef
1170 culture supernatant, PFA-fixed-Ef. Data is representative of N=3, n=3. One-way ANOVA is
1171 used to obtain the p-values.

1172 **B**-Intracellular proliferation of STM in Caco-2 cells in presence or absence of live Ef, Ef culture
1173 supernatant, PFA-fixed-Ef. Data is representative of N=3, n=3. One-way ANOVA is used to
1174 obtain the p-values.

1175 **C**- Biofilm assay depicting the biofilm formation ability of STM-WT or STM-WT grown in Ef
1176 supernatant after 72h of inoculation in presence or absence of live Ef, Ef or STM culture
1177 supernatant, PFA-fixed. Crystal-violet staining was performed to assess the biofilm formation

1178 on the solid-liquid interphase and the $[OD]_{595}$ absorbance reading was recorded. Data is

1179 representative of N=3, n=3. One-way Anova is used to obtain the p-values.

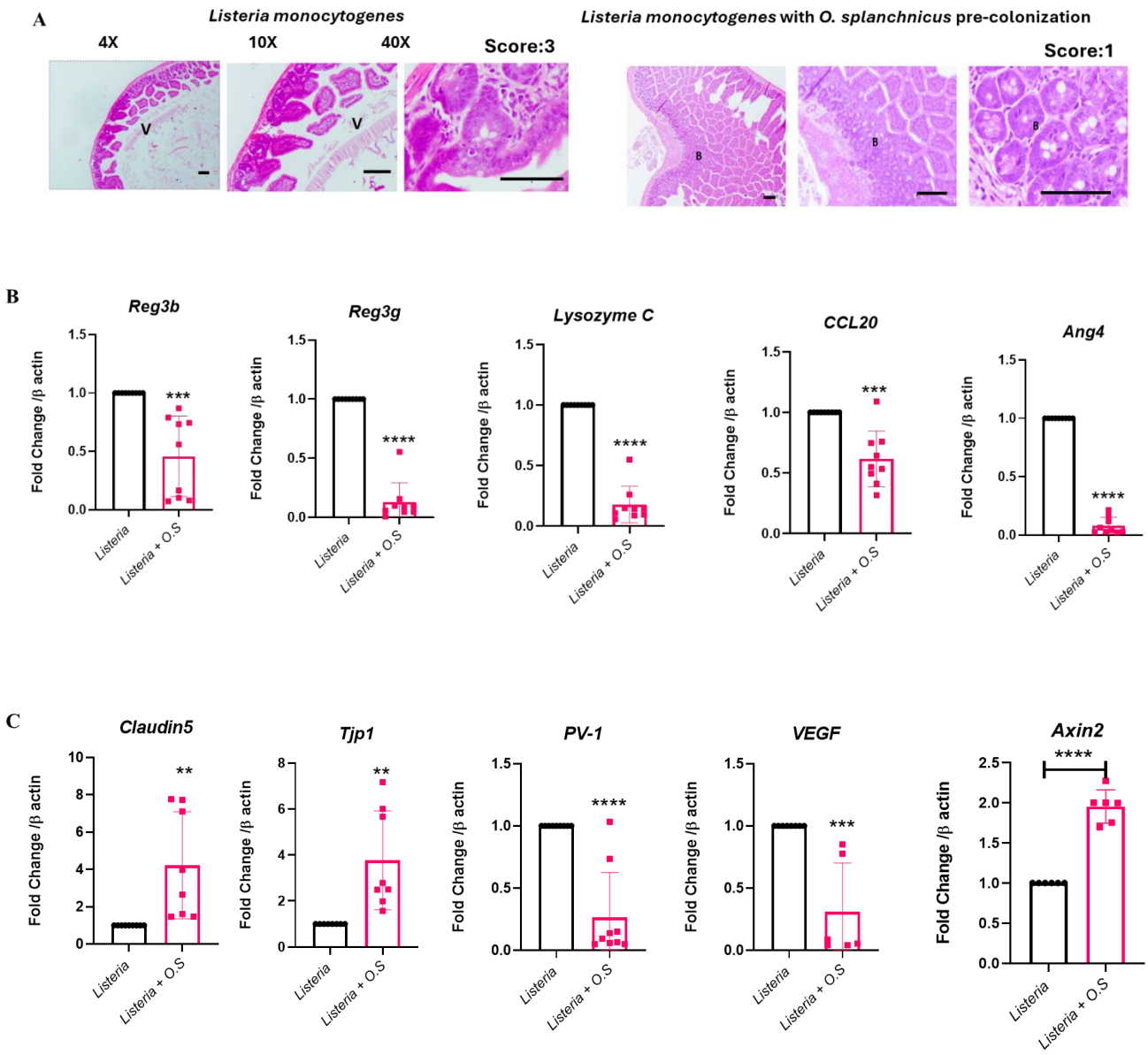

1180

1181

1182

1183

1184

1185

1186

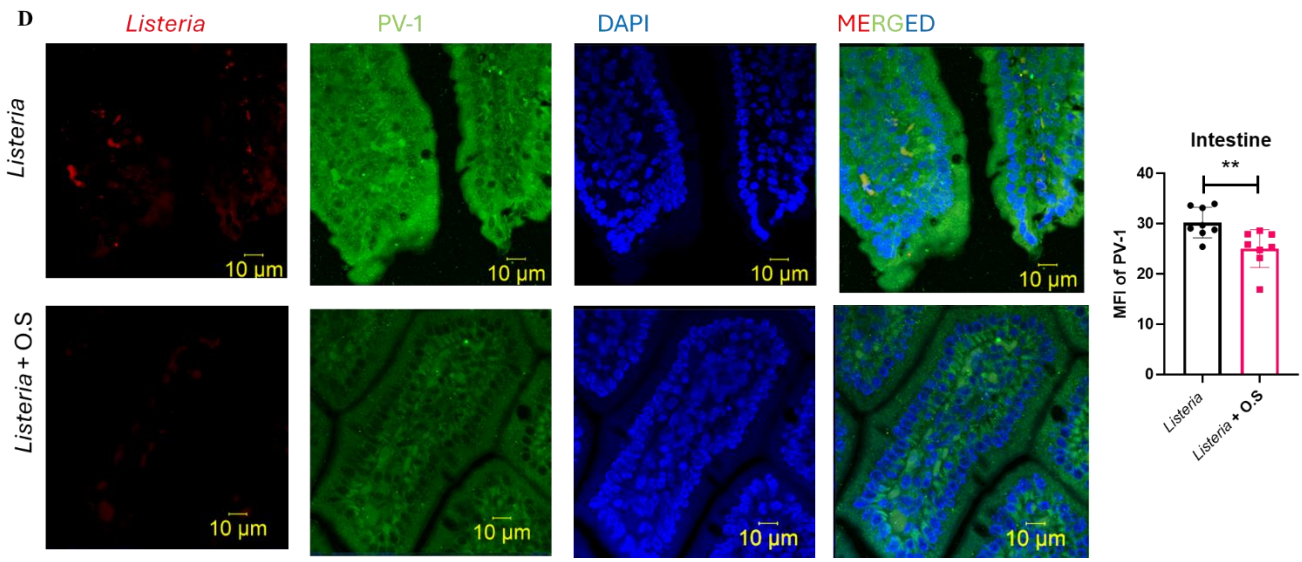

1187

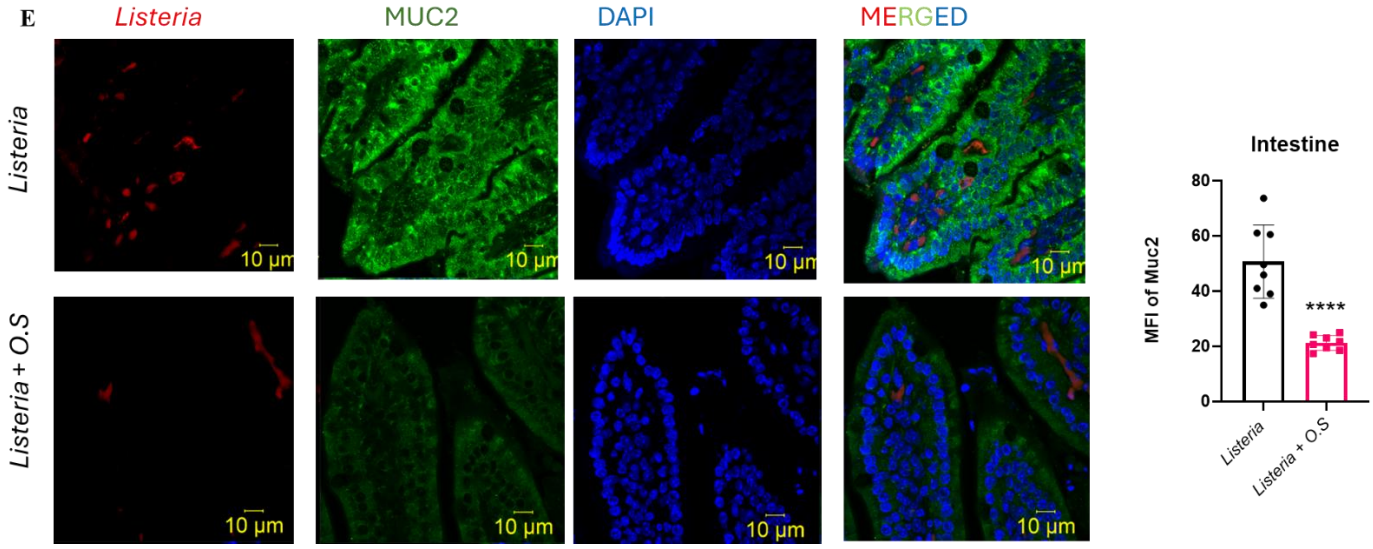

1188

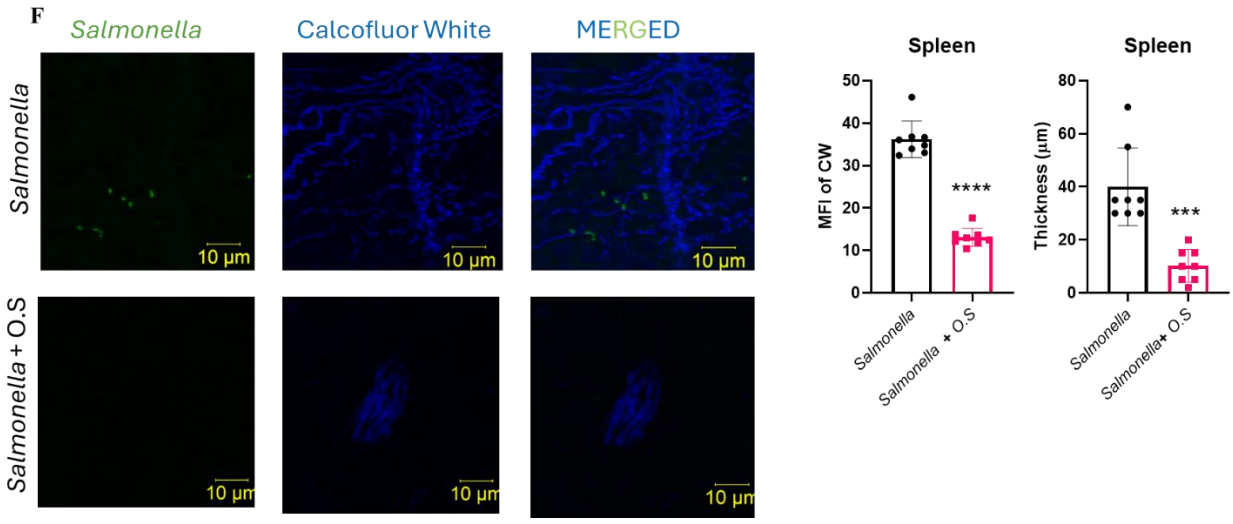

1189

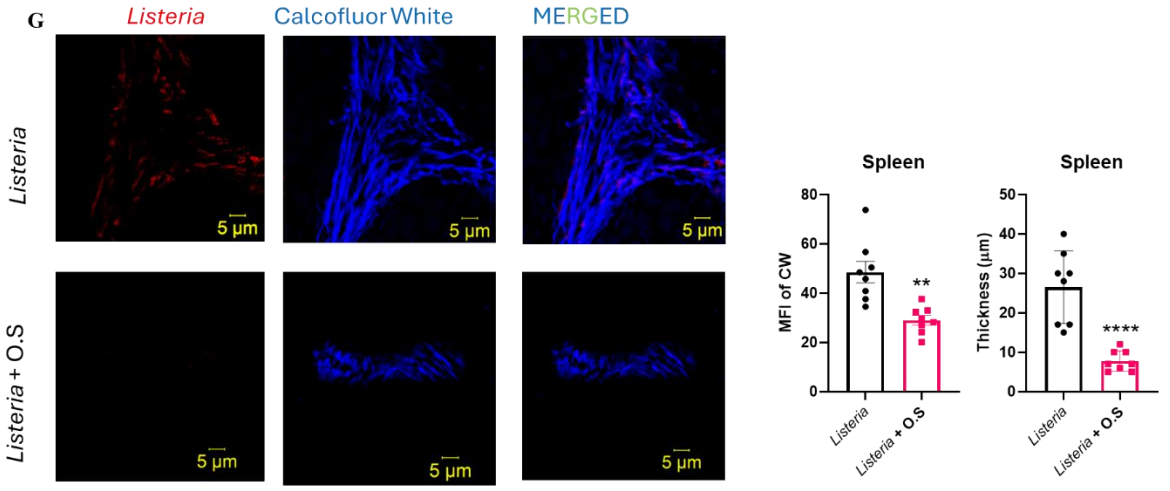
G
Listeria
Calcofluor White
MERGED
Listeria
Listeria + O.S
5 µm
Spleen
MFI of CW
**
Listeria
Listeria + O.S
Spleen
Thickness (µm)
****
Listeria
Listeria + O.S

1190

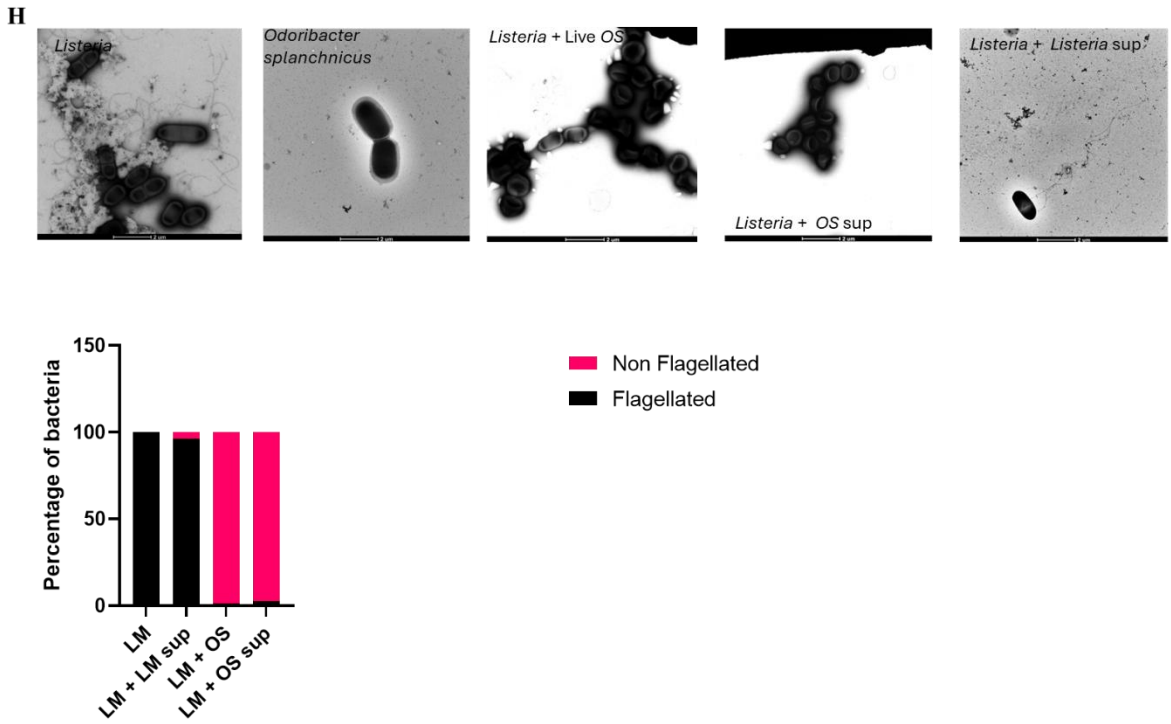
H
Listeria
Odoribacter splanchnicus
Listeria + Live OS
Listeria + OS sup
Listeria + Listeria sup
Percentage of bacteria
Non Flagellated
Flagellated
LM
LM + LM sup
LM + OS
LM + OS sup

1191

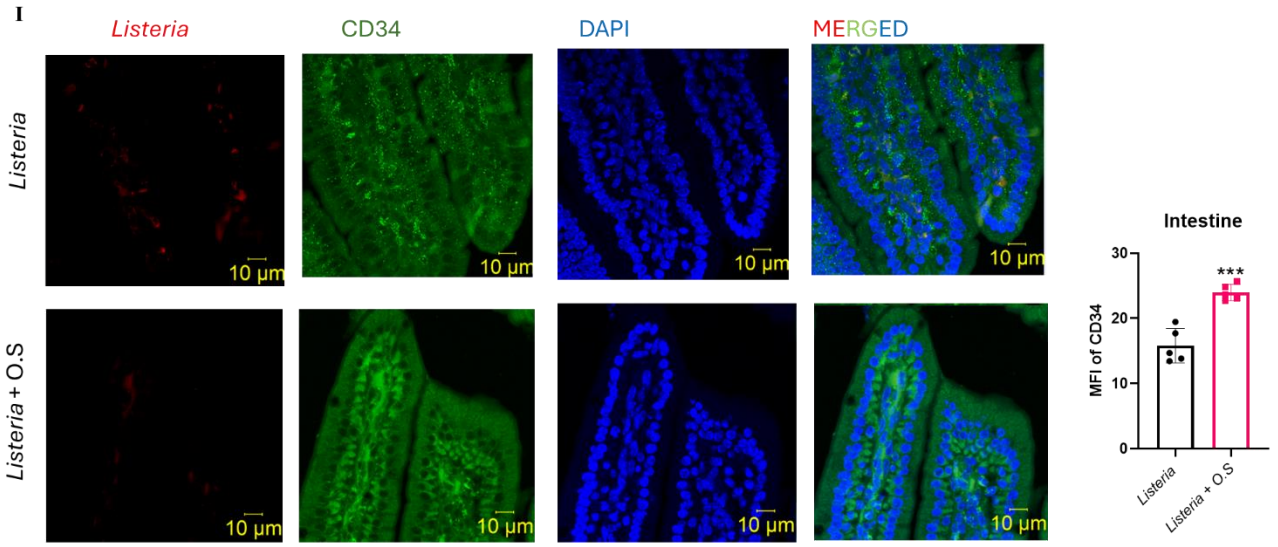

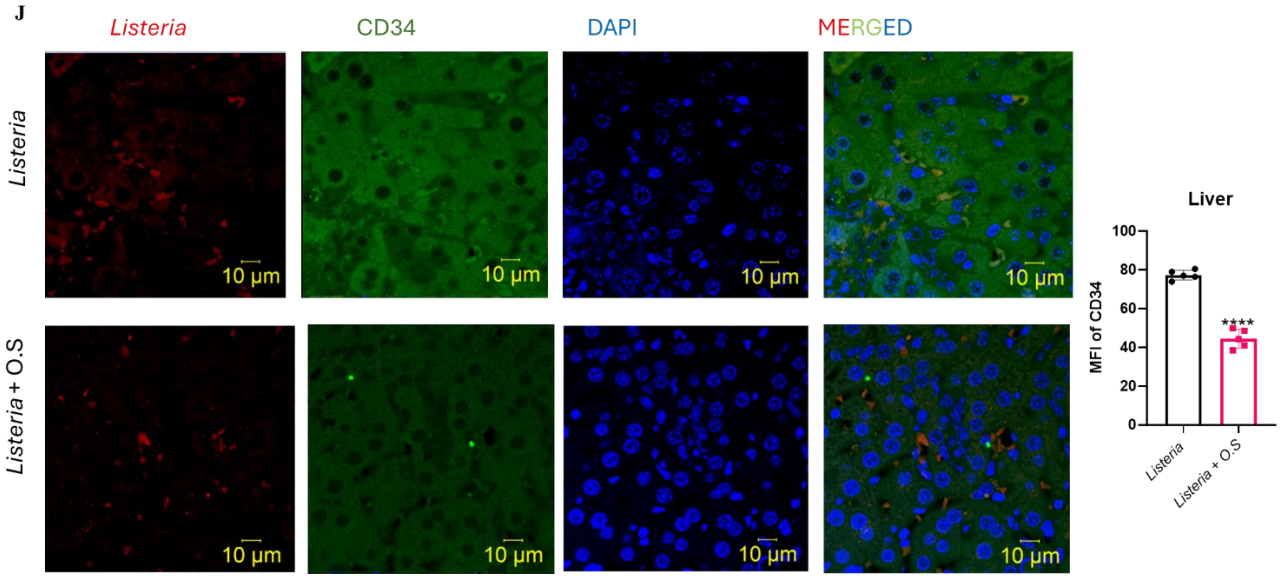

Fig. S4. *Odoribacter splanchnicus* gut colonization protects mice against *Listeria monocytogenes* pathogenesis similar to *Salmonella* infection

A-Haematoxylin-eosin-stained intestinal sections harvested from OS non-colonized or colonized mice cohorts at 5th-day-post-LM-infection. 0-represents normal pathology, 1-represents- mild pathology, 2-3-represents severe pathology.

1201 **B**-Quantitative gene expression data of several antimicrobial peptides (AMPs) precursor genes
1202 in LM-infected mice intestinal tissues harvested at 5th day post-infection from OS colonized or
1203 non-colonized cohorts. Unpaired Student's t-test is performed to obtain the p-values. Data is
1204 representative of N=2, n=9.

1205 **C**- Quantitative gene expression study of tight junction protein genes *Tjp1*, *Claudin5*, GVB
1206 damage marker *PV-1*, angiogenesis marker-*Vegf,* and *Axin2* in LM- infected mice intestinal
1207 tissues harvested at 5th-dpi from OS colonized or non-colonized cohorts. Unpaired Student's
1208 t-test is performed to obtain the p-values. Data is representative of N=2, n=5.

1209 **D-E**- Immunofluorescence images representing PV-1 protein expression (D) and Muc2 (E) in
1210 intestinal (ileal) tissues of OS-non-colonized and colonized mice cohorts at 5th day post LM
1211 infection. Data is representative of N=2, n=8 (tissue samples). Un-paired t-test was used to
1212 obtain the p-values.

1213 **F**- Representative Calcofluor white (CW) staining of STM-infected mice spleen tissues at 5th-
1214 dpi. Data is representative of N=2, n=8 (tissue samples). Un-paired t-test was used to obtain
1215 the p-values.

1216 **G**- Representative CW staining of LM-infected mice spleen tissues at 5th-dpi. Data is
1217 representative of N=2, n=8 (tissue samples). Un-paired t-test was used to obtain the p-values.

1218 **H**- Transmission Electron Microscopic (TEM) images of LM in presence or absence of LM
1219 supernatant, OS and its supernatant to assess the possession of flagella. The quantification plot
1220 exhibits the percentage of bacterial flagellated or non-flagellated cells (number of cells
1221 quantified n$\geq$ 100)

1222 **I-J**- Immunofluorescence images representing CD34 (an endothelial marker of vasculature)
1223 protein expression in intestinal (N) and liver (O) tissues of OS non-colonized and colonized

mice cohorts upon LM infection. Data is representative of N=2, n=5 (tissue samples). Unpaired t-test was used to obtain the p-values.

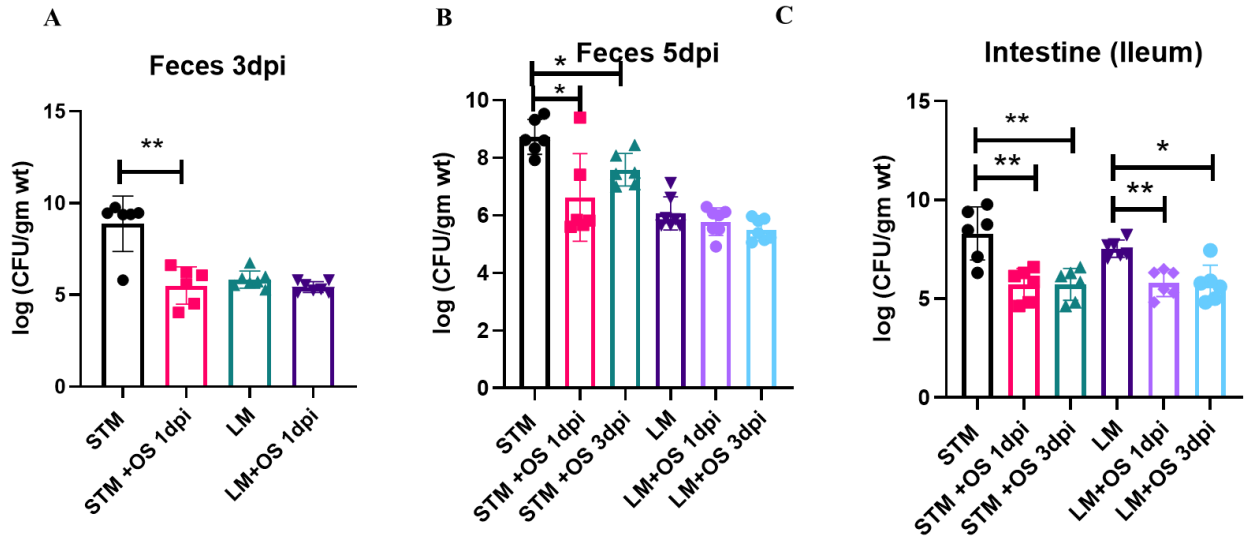

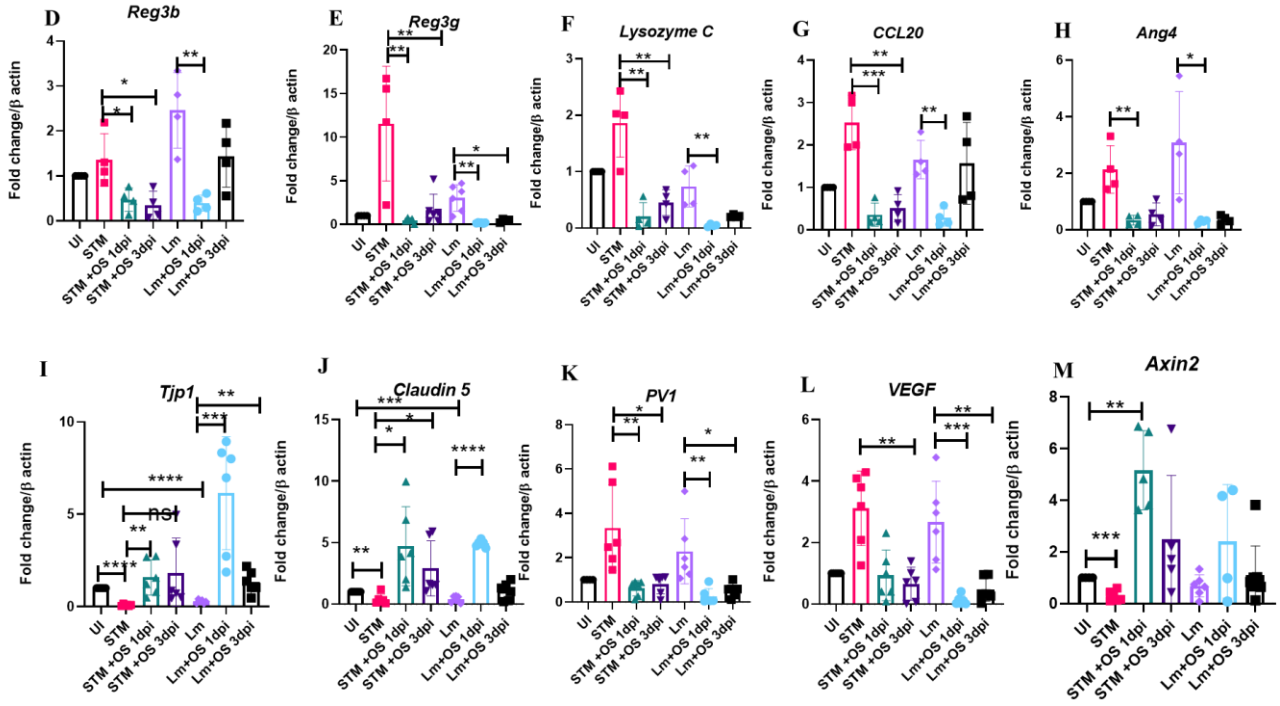

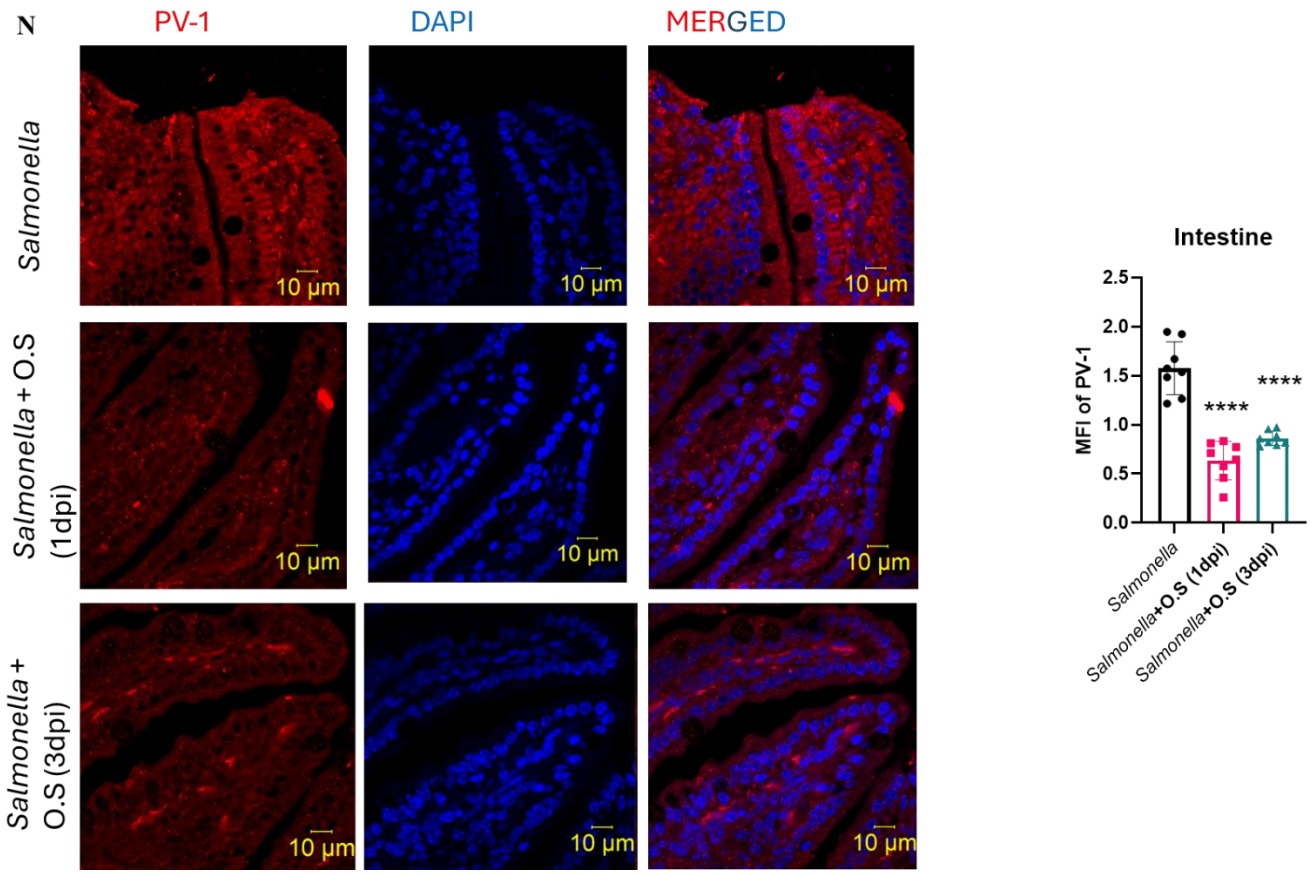
N
PV-1
DAPI
MERGED
Salmonella
Salmonella + O.S (1dpi)
Salmonella + O.S (3dpi)
10 µm
Intestine
MFI of PV-1
2.5
2.0
1.5
1.0
0.5
0.0
****
****
Salmonella
Salmonella+O.S (1dpi)
Salmonella+O.S (3dpi)

1230

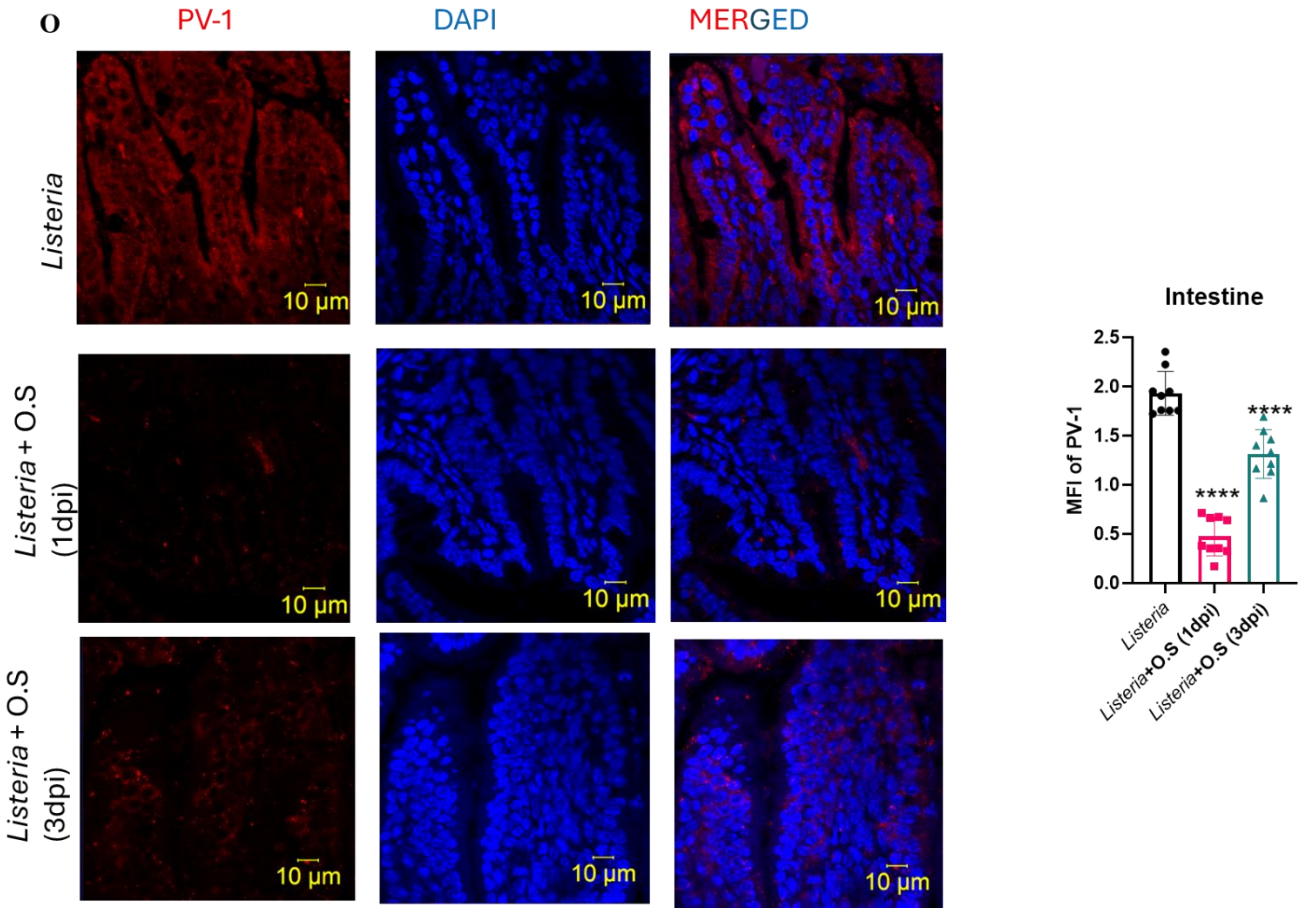
O
PV-1
DAPI
MERGED
Listeria
Listeria + O.S (1dpi)
Listeria + O.S (3dpi)
10 µm
Intestine
MFI of PV-1
2.5
2.0
1.5
1.0
0.5
0.0
****
****
Listeria
Listeria+O.S (1dpi)
Listeria+O.S (3dpi)

1231

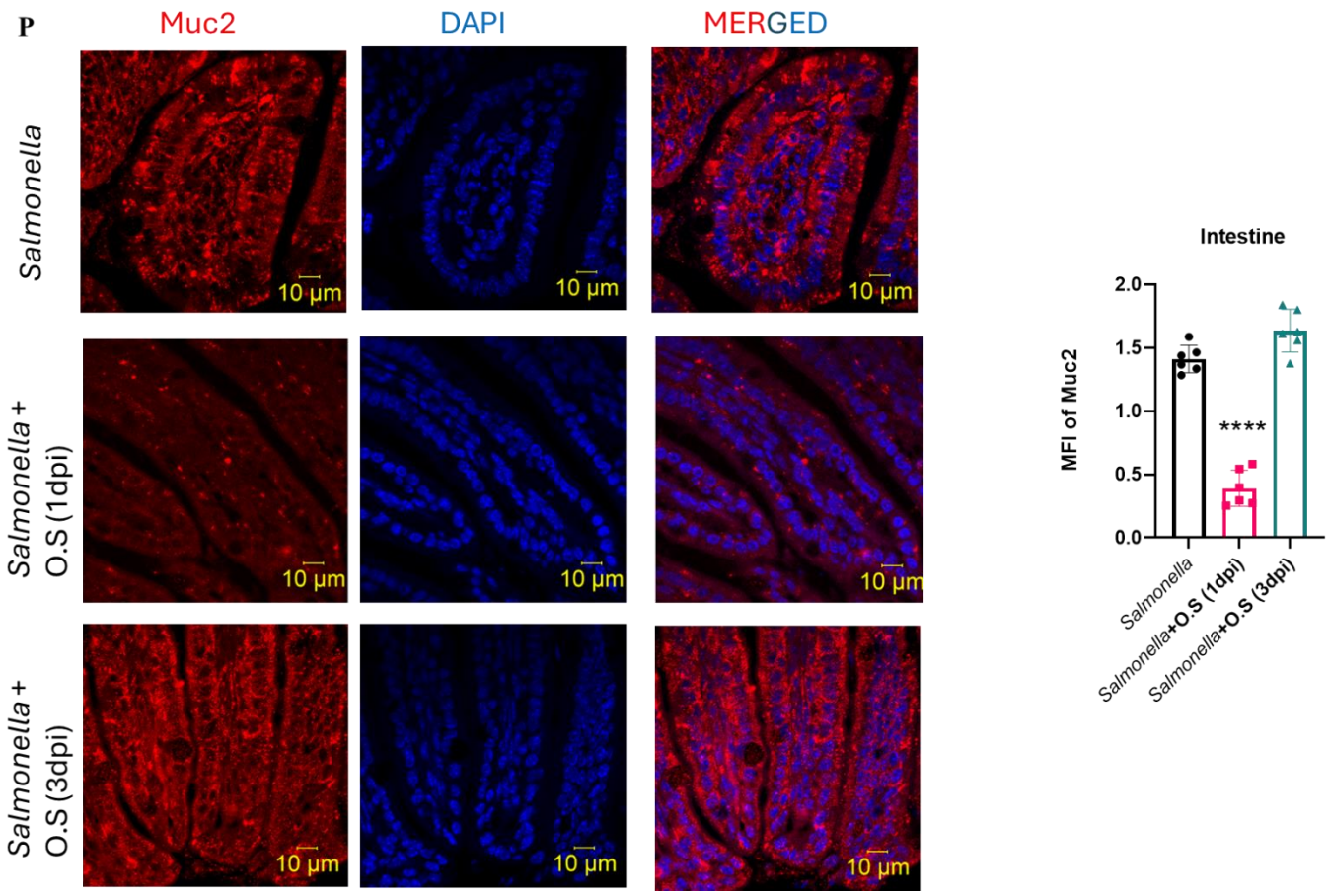
P
Muc2
DAPI
MERGED
Salmonella
Salmonella + O.S (1dpi)
Salmonella + O.S (3dpi)
10 µm
Intestine
MFI of Muc2
2.0
1.5
1.0
0.5
0.0
****
Salmonella
Salmonella+O.S (1dpi)
Salmonella+O.S (3dpi)

1232

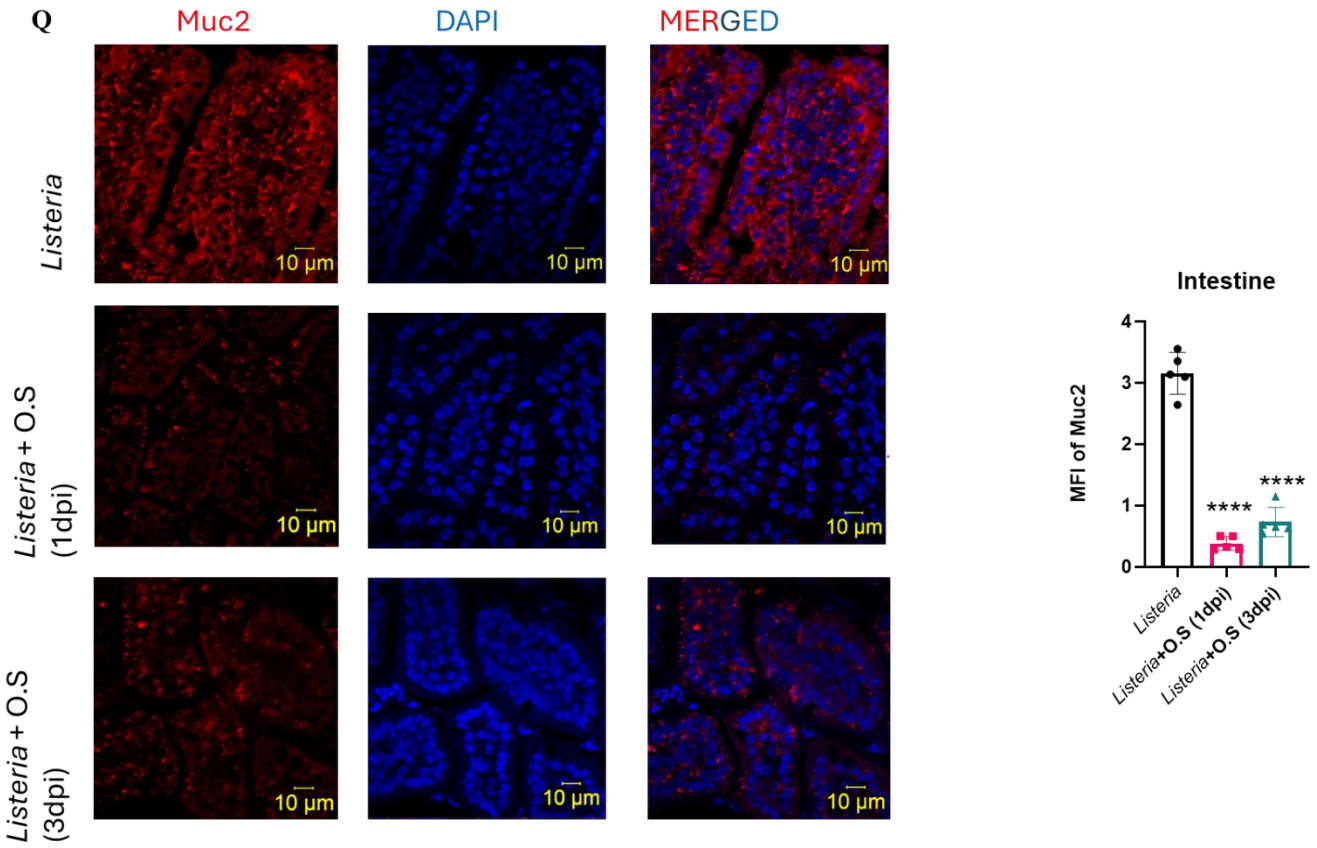
Q
Muc2
DAPI
MERGED
Listeria
Listeria + O.S (1dpi)
Listeria + O.S (3dpi)
10 µm
Intestine
MFI of Muc2
4
3
2
1
0
****
****
Listeria
Listeria+O.S (1dpi)
Listeria+O.S (3dpi)

1233

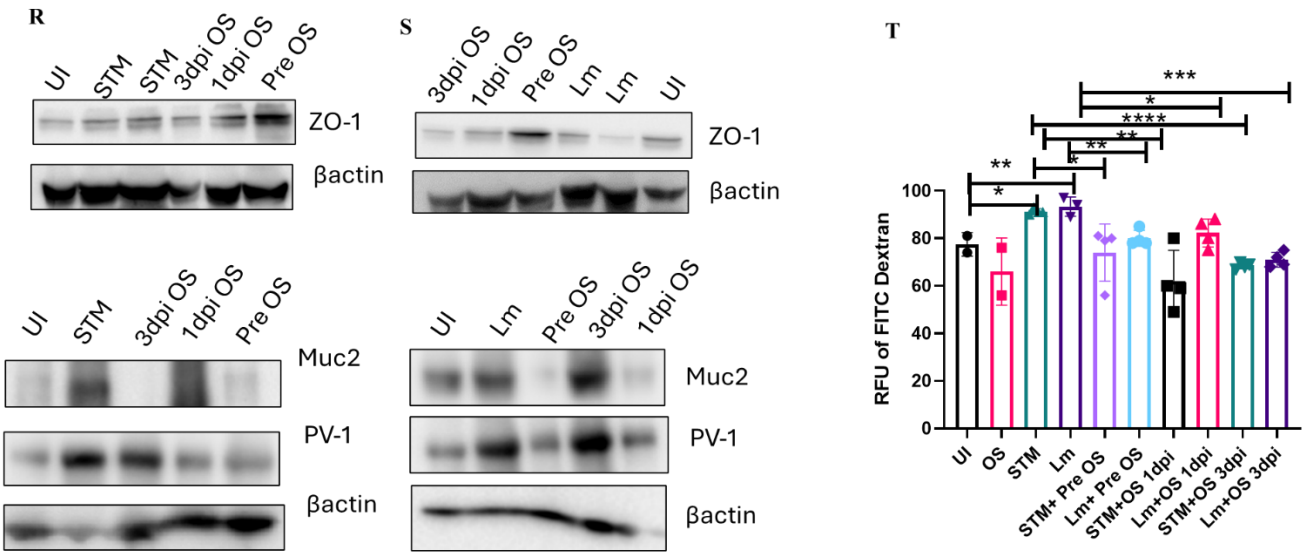

Fig. S5 ***Odoribacter splanchnicus*** **administration post-establishment of infection protected mice against** ***Listeria monocytogenes*** **and** ***Salmonella*** **Typhimurium**

A-C- STM and LM organ loads in feces at 3rd day post-infection (A), 5th post-infection (B) and in ileal tissues (contents and wall) at 5th day post-infection (C) upon OS administration at 1-dpi or 3-dpi. Data is representative of N=1, n=6 where N denotes number of biological replicates and n denotes the number of mice per group. Mann-Whitney Test was performed to obtain p-values.

D-H-Quantitative gene expression data of several antimicrobial peptides (AMPs) precursor genes in LM and STM-infected mice intestinal tissues harvested at 5th dpi upon OS colonization at 1-dpi or 3-dpi. Unpaired Student's t-test is performed to obtain the p-values. Data is representative of N=2, n=4.

I-M- Quantitative gene expression study of tight junction protein genes *Tjp1*, *Claudin5*, GVB damage marker *PV-1*, angiogenesis marker-*Vegf,* and *Axin2* in LM and STM-infected mice intestinal tissues harvested at 5th-dpi upon OS colonization at 1-dpi or 3-dpi. Unpaired Student's t-test is performed to obtain the p-values. Data is representative of N=2, n=6.

1250 **N-O**- Intestinal (ileal) immunofluorescence images representing PV-1 protein expression in
1251 *Salmonella* (N) or *Listeria* (O)-infected mice harvested on 5th-dpi with or without OS
1252 administration at 1-dpi or 3-dpi. Unpaired Student's t-test is performed to obtain the p-values.
1253 Data is representative of N=2, n=8 (or 9).

1254 **P-Q**- Intestinal (ileal) immunofluorescence images representing Muc2 protein expression in
1255 *Salmonella* (M) or *Listeria* (N)-infected mice harvested on the 5th dpi with or without OS
1256 administration at 1-dpi or 3-dpi. Unpaired Student's t-test is performed to obtain the p-values.
1257 Data is representative of N=2, n=6 (or 5).

1258 **R-S**- Immunoblotting representing the protein expression profile of Muc2, ZO-1, and PV-1 in
1259 *Salmonella* (O) or *Listeria* (P)-infected mice intestinal tissue harvested on 5th-dpi with or
1260 without OS pre-or post-colonization (1-dpi or 3-dpi).

1261 **T**- Estimation of FITC fluorescence in mice plasma via gut permeability assay in *Salmonella*
1262 or *Listeria*-infected mice cohorts with or without OS pre-or post-colonization (1dpi or 3dpi)
1263 upon oral administration of FITC Dextran (25mg/kg) 4h before euthanization at 5th-dpi.
1264 Unpaired Student's t-test is performed to obtain the p-values. Data is representative of N=2,
1265 n=4 (UI and OS, n=2).

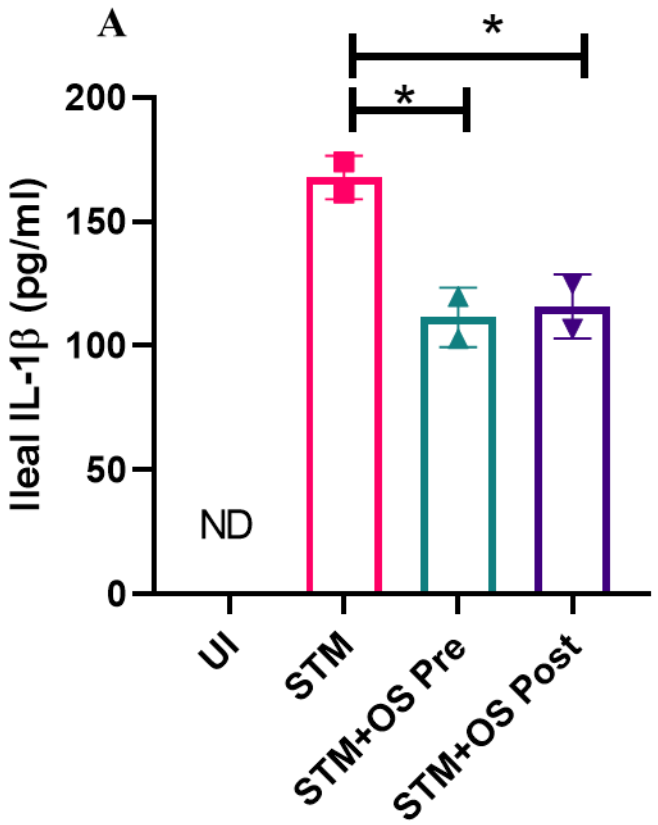

1266

1267 **Fig. S6 *Odoribacter splanchnicus* alleviates *Salmonella*-induced intestinal inflammation in**

1268 **mice both during pre and post-treatment**

1269 **A**- Estimation of IL-1β in the ileal sections of UI or *Salmonell*a-infected mice tissues harvested

1270 at 5th dpi with or without OS pre-or post-colonization (1dpi). Unpaired Student's t-test is

1271 performed to obtain the p-values. Data is representative of N=2, n=4 (UI and OS, n=2).

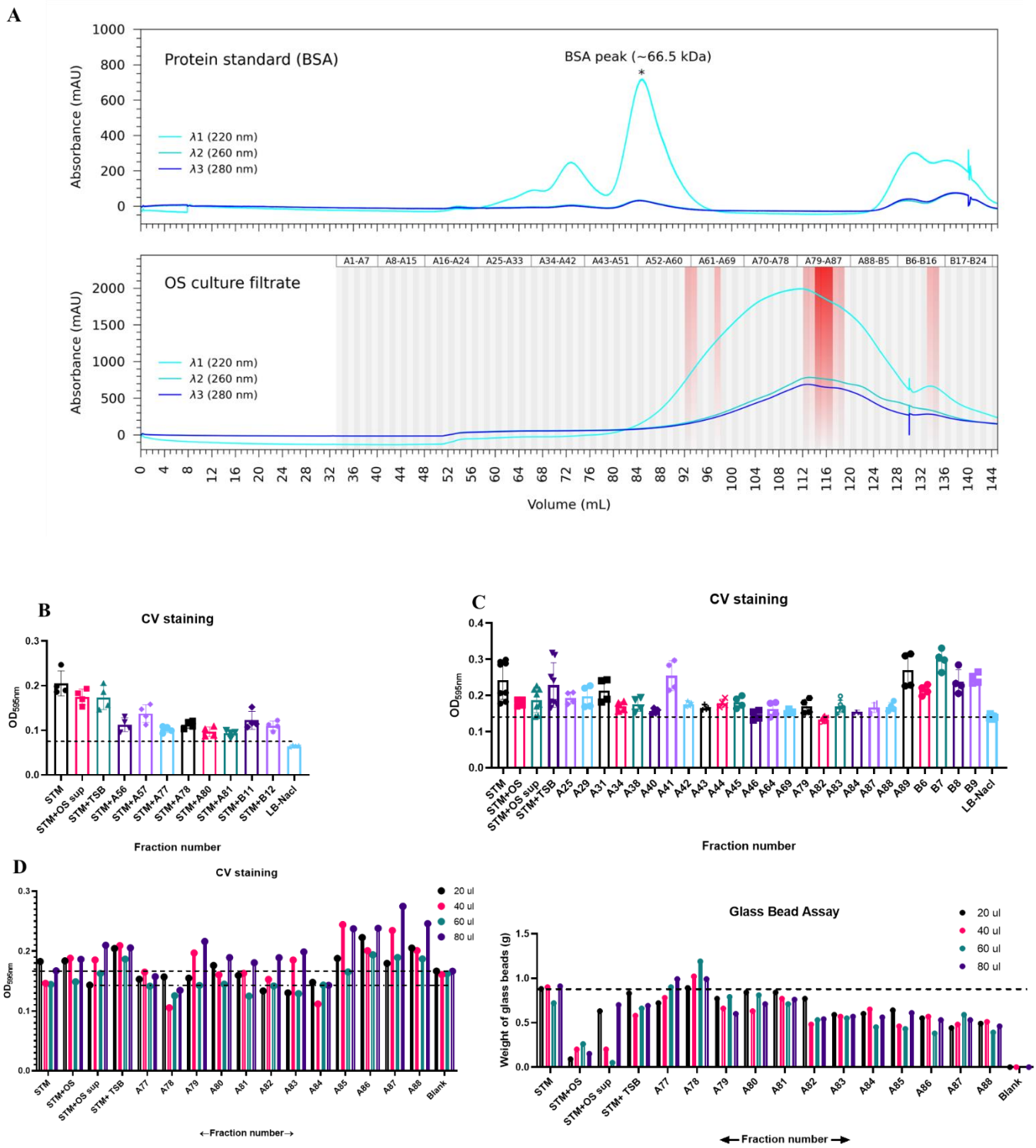
A
Protein standard (BSA)
BSA peak (~66.5 kDa)
Absorbance (mAU)
λ1 (220 nm)
λ2 (260 nm)
λ3 (280 nm)
OS culture filtrate
A1-A7
A8-A15
A16-A24
A25-A33
A34-A42
A43-A51
A52-A60
A61-A69
A70-A78
A79-A87
A88-B5
B6-B16
B17-B24
Volume (mL)
B
CV staining
Fraction number
C
CV staining
Fraction number
D
CV staining
20 ul
40 ul
60 ul
80 ul
←Fraction number→
Glass Bead Assay
Weight of glass beads (g)
Fraction number

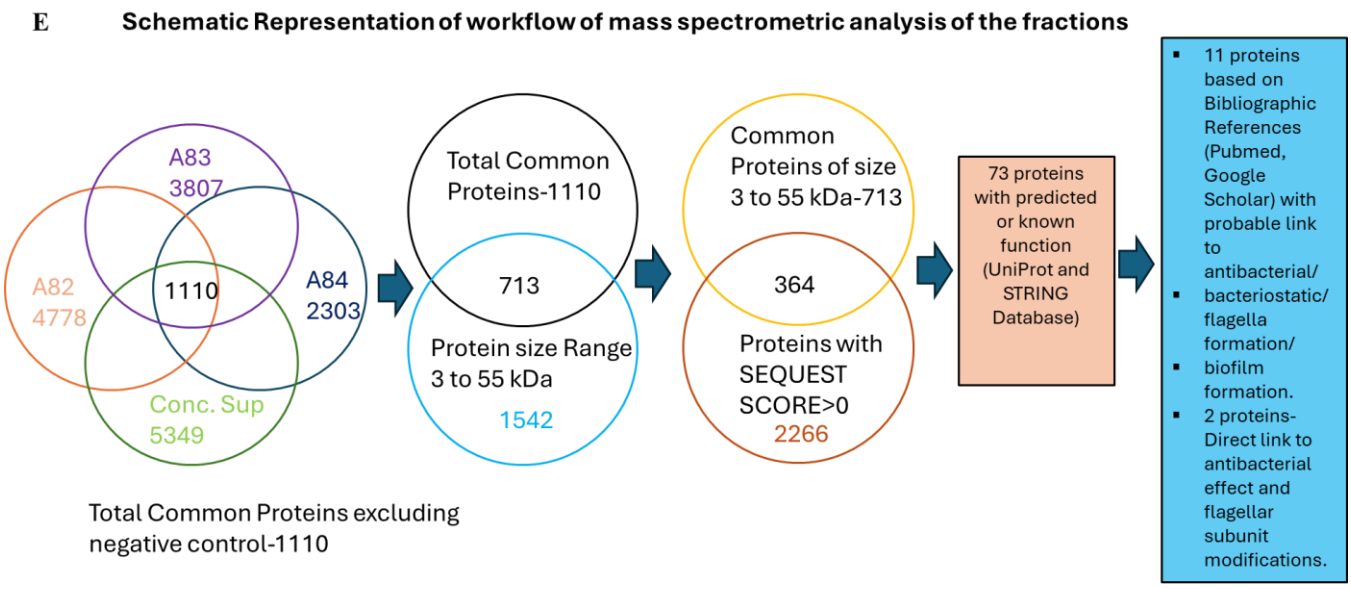

Fig. S7 Characterization of the inhibitory active molecule within *O. splanchnicus* culture supernatant

A-Gel filtration chromatogram of protein standards and the OS culture supernatant. Red shaded region shows the fractions with biofilm inhibitory activity. The dark shaded region indicates the fractions with the highest inhibitory activity.

B-C- Biofilm assay showing the biofilm formation ability of STM after 72h of inoculation in presence of OS supernatant gel filtration fractions. Data is representative of N=2, n=2. One-way ANOVA is used to obtain the p-values.

D- Biofilm assay showing the biofilm formation ability of STM after 72h of inoculation in presence of varying concentration of OS supernatant biofilm inhibitory gel filtration fractions. Data is representative of N=2, n=1.

E-Schematic representation of the workflow of mass spectrometric analysis of the gel filtration fractions (A82, A83, A84 and Concentrated supernatant).

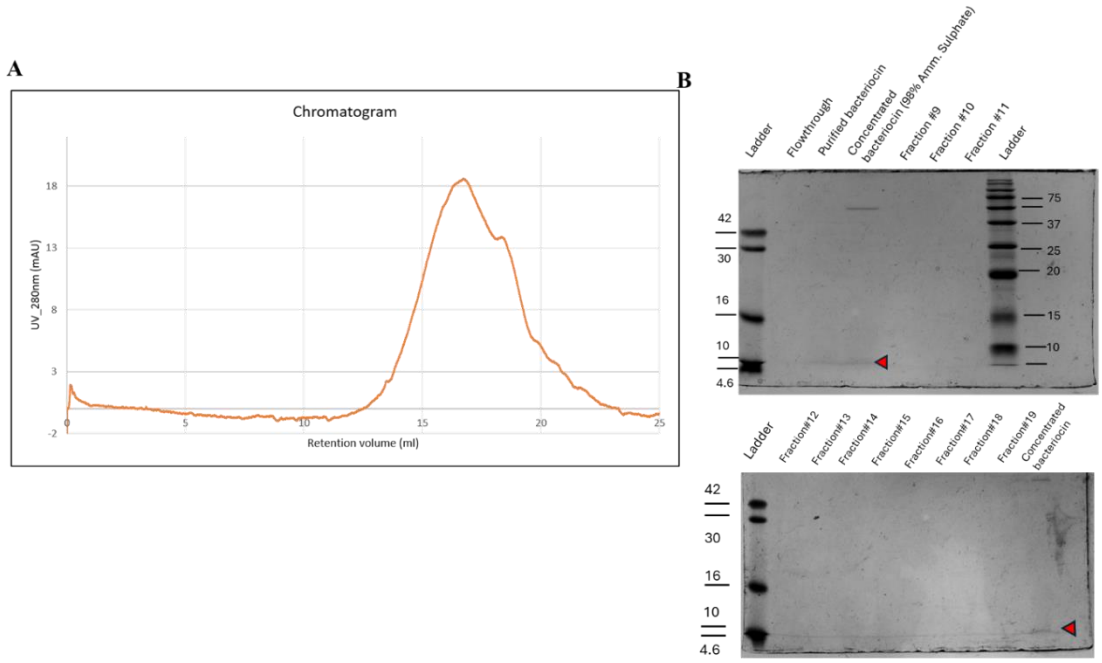

Fig. S8 Purification procedure of *O. splanchnicus* produced bacteriocin via ammonium sulphate precipitation method followed by Fast Performance Liquid Chromatography

A-Size exclusion chromatogram of OS-produced bacteriocin fractions post 95-98% ammonium sulphate precipitation.

B- Coomassie-stained SDS PAGE showing the purified and concentrated OS bacteriocin.

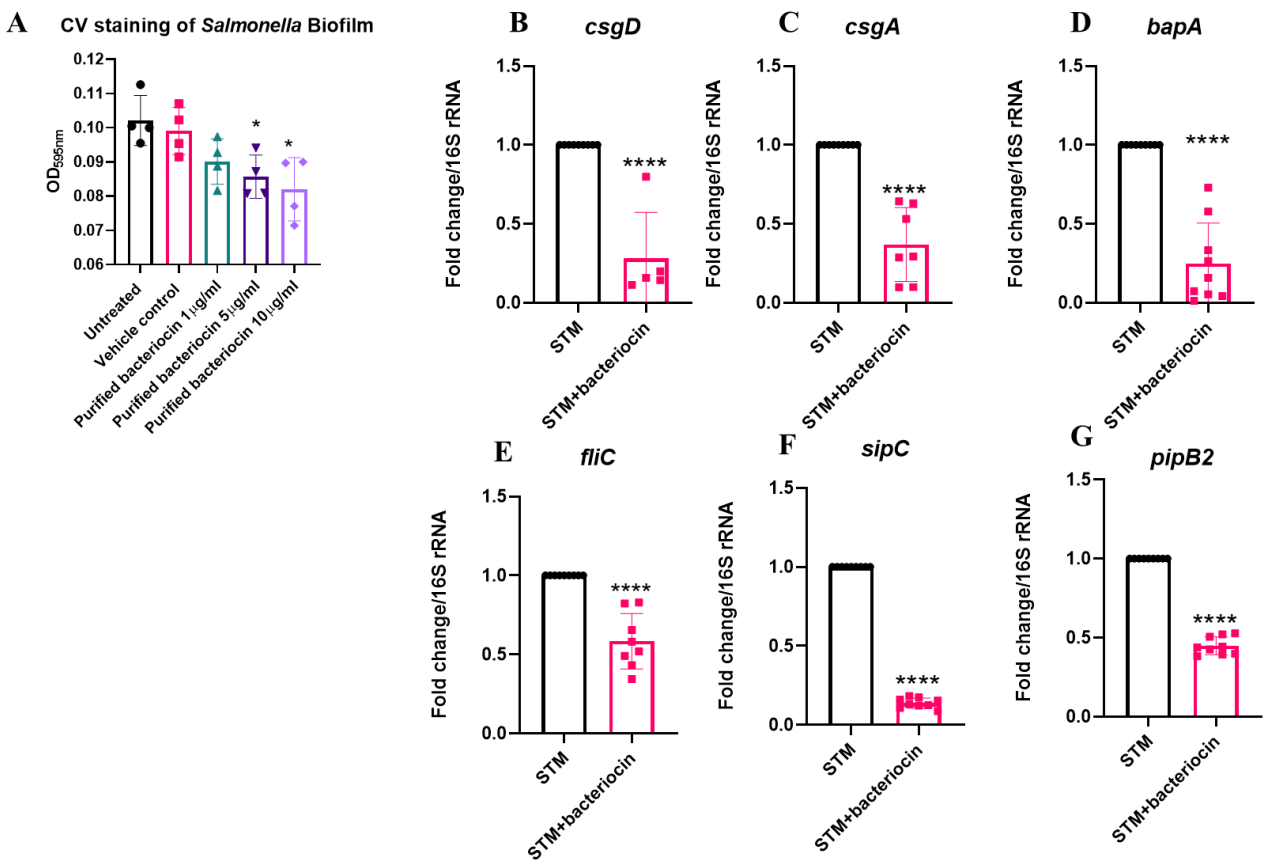

1295

1296 **Fig. S9 *O. splanchnicus* bacteriocin attenuates *Salmonella* pathogenesis *in vitro***

1297 **A**- Biofilm assay showing the biofilm formation ability of STM after 72h of inoculation under

1298 varying concentration of OS bacteriocin. Data is representative of N=2, n=2. Unpaired t-test is

1299 used to obtain the p-values.

1300 **B-G**- RT-qPCR mediated gene expression of STM biofilm regulatory genes *csgD* (B),

1301 *csgA*(C), *bap* (D), along with flagellar gene *fliC*(E), SPI-1-*sipC* (F) and SPI-2-*pipB2*(G) in

1302 presence or absence of OS bacteriocin treatment. Data is representative of N=2, n≥5. Unpaired

1303 Student's t-test was used to obtain the p-values.

1304

1305

1306

Table S1- Selected List of 11 proteins from Mass Spectrometric Analysis based on bibliographic search

Accession ID	Protein Name and	Referenced Function
A0A412WBT8	Immunity protein Imm5 domain-containing protein	Uncharacterized
F9Z8G5	Peptidase	Modulate biofilm formation and host defense.
R6F650	Carboxyl-terminal protease	Critical for post-translational processing and associated with regulation of gene expression, stress response, maintenance of cell envelope integrity and bacterial virulence.
A0A412TJE3	ATP-dependent Clp protease proteolytic subunit	Influence virulence and infectivity of pathogenic bacteria. ClpP enhance biofilm formation in *Enterococcus faecalis*.
F9Z604	Peptidase C39 bacteriocin processing	The cysteine peptidase cleave the double glycine leader peptides from the precursors of bacteriocin
A0A412TJV3	UDP-2,4-diacetamido-2,4, 6-trideoxy-beta-L-altropyranose hydrolase	It catalyzes the third step in the biosynthesis of pseudaminic acid. Pseudaminic acid is a sialic-like sugar that modifies flagellin.
A0A412WSU3	Bacteriocin	Antimicrobial peptides that can kill or inhibit closely related or unrelated bacterial strains.
A0A413I832	Serine Protease	Extracellular proteases regulate biofilm formation and growth of competitors.
A0A412W3J2	Glutamate dehydrogenase	Involved in bacterial response to stress adaptation and virulence.
A0A412WSS0	Bacteriocin	Antimicrobial peptides that can kill or inhibit closely related or unrelated bacterial strains.
F9ZBU9	Peptidylprolyl isomerase	Promote biofilm formation in *Mycobacterium tuberculosis*.

Table S2-List of primers

Primer Name	Sequence (5'---3')
O. splanchnicus 16S rRNA FP	ATGTAATGATGAGCACTCTAACGG
O. splanchnicus 16S rRNA RP	GGCTTTTGAGATTGGCATCC
PV-1 FP	CGAACTGGAGGCGCGTAA
PV-1 RP	GCAGCGACTTGGCCTTGAC
Claudin5 FP	CCCAGTTAAGGCACGGGTAG
Claudin5 RP	GGCACCGTCGGATCATAGAA
βactin FP	CAGCAAGCAGGAGTACGATG
βactin RP	GCAGCTCAGTAACAGTCCG
Vegf FP	GCAGCGACAAGGCAGACTAT

Vegf RP	AACCTCCTCAAACCGTTGGC
Tjp1 FP	TCTTGCAAAGTATCCCTTCTGT
Tjp1 RP	CAGAAATCGTGCTGATGTGCC
Reg3b FP	GCTTGTCAAGAGCTTCTGGATTTC
Reg3b RP	TGTCCCTTGTCCATGATGCTC
Reg3g FP	CGCTGAAGCTTCCTTCCTGT
Reg3g RP	GGGTTCATAGCCCAGTGTCG
Lysozyme C FP	GGTCTACAATCGTTGTGAGTTG
Lysozyme C RP	TGAGCTAAACACACCCAGTCA
CCL 20 FP	GCAACTACGACTGTTGCCTC
CCL20 RP	TTCTTGACTCTTAGGCTGAGGA
Ang4 FP	TGGTTGTGATTCCTCCAACTCT
Ang4 RP	TGTTGACATCTTTGCAAGGCG
fliC FP	CTAAACAAACTGGGTGGCGC
fliC RP	GCACCCAGGTCAGAACGTAA
bapA FP	ACGGTGACTACGCCTAAAAC
bapA RP	CTTCCGCCTCAGTCACTTTT
csgD FP	ACGATTATCCCTACCGTGAA
csgD RP	GCGGACTCGGTGCTGTTGTA
Salmonella 16S rRNA FP	GTGAGGTAACGGCTCACCAA
Salmonella 16S rRNA RP	TAACCGCAACACCTTCCTCC
sipC FP	GCAGTACGCCGCTACTCAGG
sipC RP	AGCGCGAATATTGCCTGCGA
pipB2 FP	TGGCGCCAATTTACAACACGC

pipB2 RP	CTCGCCTTTCGCAGGTTTGC
csgA FP	TCGCAGCAATCGTAGTT
csgA RP	CGGAACCGTACTGATAA

Table S3-List of Antibodies

Antibody Name	**Catalogue Number**	**Source**
PV-1	**A15906-20ul (Abclonal)**	**Rabbit**
CD34	**A19015-20ul (Abclonal)**	**Rabbit**
Muc2	**A4767 (Abclonal)**	**Rabbit**
ZO-1	**R26.4C DHSB, CRL 1597**	**Mouse**
β actin	**A3854 (Sigma), Clone AC-15**	**Mouse**